

## CALCAREOUS NANNOFOSSIL BIOSTRATIGRAPHY OF UPPER CALLOVIAN-LOWER BERRIASIAN SUCCESSIONS FROM THE SOUTHERN ALPS, NORTH ITALY

CRISTINA EMANUELA CASELLATO

Received: February 25, 2010; accepted: October 4, 2010

**Key words:** Calcareous nannofossils, biostratigraphy, magnetostratigraphy, Tethys, Late Jurassic, Southern Alps.

**Abstract.** Calcareous nannofossil biostratigraphy was investigated in uppermost Callovian-lower Berriasian sections from Southern Alps, previously detected through magnetostratigraphy, in order to achieve an integrated stratigraphic framework valid at low latitudes. Nannofossil investigations were carried out on smear slides and ultra-thin sections, revealing generally scarce to common abundances and poor-moderate preservation of nannofloras. An exhaustive taxonomic revision was performed to unambiguously separate forms which are transitional between two species and better delineate rapidly evolving groups. Four new species have been described: *Zeugrhabdotus fluxus*, *Nannoconus puer*, *Nannoconus erbae*, *Hexalithus geometricus*. Particular attention was paid to taxonomical aspects of primitive nannoconids, appearing and evolving across the early-late Tithonian transition and the Tithonian/Berriasian boundary intervals; the revision was also verified at DSDP Site 534A from Atlantic Ocean.

Forty-eight nannofossil bioevents were detected and the results help to increase potential stratigraphic resolution in this interval. Thirty-seven nannofossil bioevents in the upper Kimmeridgian-lower Berriasian interval have been directly correlated to magnetostratigraphy (CM22-CM17) revealing a systematically older stratigraphic occurrence of these taxa than previously reported.

A revised and partly new Tethyan calcareous nannofossil zonation scheme is here proposed for the uppermost Callovian-lower Berriasian interval. It consists of seven bio-zones and eight subzones based on thirty-one bioevents, thirteen of them related to dissolution resistant taxa assuring highest reproducibility even in sections with high diagenetic overprint. The proposed biostratigraphic scheme gives higher resolution than previous zonations, especially for the Callovian-Kimmeridgian interval, where no biozonation was available for the Tethyan Realm.

**Riassunto.** L'analisi della biostratigrafia a nannofossili calcarei condotta su sezioni provenienti dalle Alpi Meridionali, di cui è disponibile la magnetostratigrafia, ha permesso di migliorare la stratigrafia del

Calloviano superiore-Berriasiano inferiore alle basse latitudini. Le indagini biostratigrafiche sono state condotte su smear slides e su sezioni ultra-sottili: i nannofossili sono da rari a comuni e presentano conservazione da scarsa a moderata.

È stata eseguita un'esaustiva revisione tassonomica per separare inequivocabilmente alcune forme di transizione tra due specie diverse e per delineare la rapida evoluzione di alcuni taxa. Sono state descritte quattro nuove specie: *Zeugrhabdotus fluxus*, *Nannoconus puer*, *Nannoconus erbae*, *Hexalithus geometricus*. Particolare attenzione è stata rivolta agli aspetti tassonomici ed evolutivi dei nannoconidi primitivi, poi verificati su materiale proveniente dal Sito DSDP 534 A dell'Oceano Atlantico per gli intervalli Titoniano inferiore-superiore e limite Titoniano/Berriasiano.

I quarantotto eventi a nannofossili calcarei riconosciuti incrementano la risoluzione stratigrafica nell'intervallo di tempo studiato. Trentasette eventi appartenenti all'intervallo Kimmeridgiano superiore-Berriasiano inferiore sono stati direttamente correlati alla magnetostratigrafia (CM22-CM17) rivelando prime comparse sistematicamente precedenti a quanto riportato in letteratura.

È proposta una zonazione a nannofossili calcarei per l'intervallo Calloviano sommitale-Berriasiano inferiore valida per il dominio Tetideo: consiste in sette zone e otto sottozone basate su una sequenza di trentuno eventi, tredici dei quali basati su taxa resistenti alla dissoluzione e quindi riproducibili anche in sezioni diagenizzate. La zonazione proposta presenta una risoluzione stratigrafica maggiore alle precedenti riportate in letteratura, specialmente per l'intervallo Calloviano-Kimmeridgiano per il quale non esiste ancora uno schema valido per il dominio tetideo.

### Introduction

The Late Jurassic-earlier Cretaceous interval was a crucial time in calcareous nannoplankton evolution. The Jurassic/Cretaceous (J/K) boundary time interval in particular was characterized by a major calcareous nannofossil speciation episode: several genera and spe-

cies common in the Cretaceous appear and rapidly evolve (Perch-Nielsen 1985; Bralower et al. 1989; Roth 1989). The Jurassic nannofossils did not occur in massive forming proportion prior to the Tithonian, when nannoliths, and especially nannoconids, first appeared and showed a progressive increase in diversity, abundance and degree of calcification through time, as documented in both Atlantic and Tethys oceans (Roth 1989; Bornemann et al. 2003; Erba 2006; Casellato 2009). At low latitudes this event was associated with a major change in pelagic sedimentation from predominantly siliceous to mostly calcareous. Particularly in the Tethys Ocean it is represented by the transition from the Rosso ad Aptici/Rosso Ammonitico Superiore to the Maiolica/Biancone limestones. The begin of the Late Jurassic was a time of exceptionally low carbonate accumulation rates, while the latest Jurassic was characterized by high sedimentation rates and the widespread deposition of calcareous nannofossil oozes and carbonate platforms (Muttoni et al. 2005). Around the Middle-Late Jurassic transition, the Tethys Ocean was almost free of carbonate sediments (Dromart et al. 2003a, b): the pelagic sedimentation was dominated by radiolarian ooze and hardgrounds formed along shallow shelf environments and on submarine highs (Baumgartner 1987; Winterer 1998; Dromart et al. 2003a, b; Erba & Casellato 2010). A drastic change in sediment production occurred since the latest Jurassic with the explosion of calcareous nannofossil, reaching lithogenic abundances during the Tithonian (Roth 1983; Erba & Quadrio 1987; Bornemann et al. 2003; Erba 2006; Casellato 2009).

Two paleogeographic provinces were recognized in Late Jurassic time, namely the Boreal and the Tethyan realms, characterized by a different floral and faunal assemblages. This provincialism has been documented also for calcareous nannofossils, exhibiting distinctive latitudinal differences (Roth 1983, 1986; Cooper 1989; Mutterlose 1992; Mutterlose & Kessels 2000; Street & Bown 2000) and preventing a globally applicable calcareous nannofossil zonation. Therefore two different biostratigraphic schemes are available for the Boreal and Tethyan realms for the Middle-Late Jurassic interval. The Boreal biostratigraphic scheme is mainly based on Northern Europe sections (Bown 1987; Bown et al. 1988; Bown & Cooper 1998). The schemes valid for the Tethyan Realm, or low latitudes, are based on land sections from the Mediterranean province (Italy, France, Spain, Portugal and Morocco) and on DSDP sites from Central Atlantic Ocean (DSDP sites 105, 391 C, 534 A) (Thierstein 1976; Wise & Wind 1976; Roth 1978; Roth et al. 1983; Bralower et al. 1989; De Kaenel et al. 1996; Mattioli & Erba 1999). Most bioevents employed in the biostratigraphic schemes established for the Callovian-Kimmeridgian interval (Roth et al. 1983; De Kaenel et al. 1996) consist of last or first occurrences (LO, FO) of

delicate coccoliths (genera *Stephanolithion* and *Vagalapilla*) that are hardly preserved in condensed or diagenesis-affected limestones.

A Late Jurassic calcareous nannofossil biostratigraphic scheme was first proposed at the end of '70s based of land sections and few DSDP sites (Thierstein 1976; Wise & Wind 1976; Roth 1978). In recent years it has been applied, revised and improved by various authors (Roth et al. 1983; Bralower et al. 1989; Tavera et al. 1994; De Kaenel et al. 1996; Bown & Cooper 1998; Casellato 2009). However, no Tethyan zonation has been yet formalized for the late Bathonian-late Kimmeridgian time interval of the low latitudes since the extreme condensation and/or the siliceous content of pelagic sediments characterizing the pelagic successions hampered the developing of a standard biostratigraphic scheme.

Calcareous nannofossil biostratigraphy is an important stratigraphic tool to calibrate M-sequence magnetic chrons and to revise chronostratigraphy and time scales, and Late Jurassic chronostratigraphy still needs improvements.

The purpose of this study is to document the high-resolution nannofossil biostratigraphy of several sections spanning the Upper Jurassic to the lowermost Cretaceous of the Lombardian Basin (Torre de' Busi, Monte Pernice sections) and Trento Plateau (Colme di Vignola, Foza, Sciapala, Bombatierle, Frisoni sections) in order to achieve a revised Tethyan biostratigraphic framework for the Upper Jurassic-lowermost Cretaceous interval. Nannofossil events are directly calibrated with magnetostratigraphy to achieve an integrated stratigraphy.

A detailed taxonomic revision is needed to unambiguously characterize transitional forms of calcareous nannofossils. In particular a specific analyses of the genus *Nannoconus* is conducted to reconstruct its appearance and early evolution, with implications for biostratigraphy and lithogenesis. The nannoconid investigation is extended to the DSDP Site 534 A (Central Atlantic Ocean) to substantiate the revised taxonomy and biostratigraphy with well preserved material.

## Geological framework

The studied area is situated in the Southern Alps (Lombardian Basin and Trento Plateau), North-East Italy. In the Mesozoic, the Southern Alps were a part of the southern Tethyan passive margin and belonged to an Africa promontory, named Adria microplate, bordered to the North and West by the Liguria-Piemonte segment of the Tethys Ocean (Alpine Tethys), and to the East by the Tethys Ocean (Fig. 1A) (Bosellini et al. 1980; Winterer & Bosellini 1981). During the Late

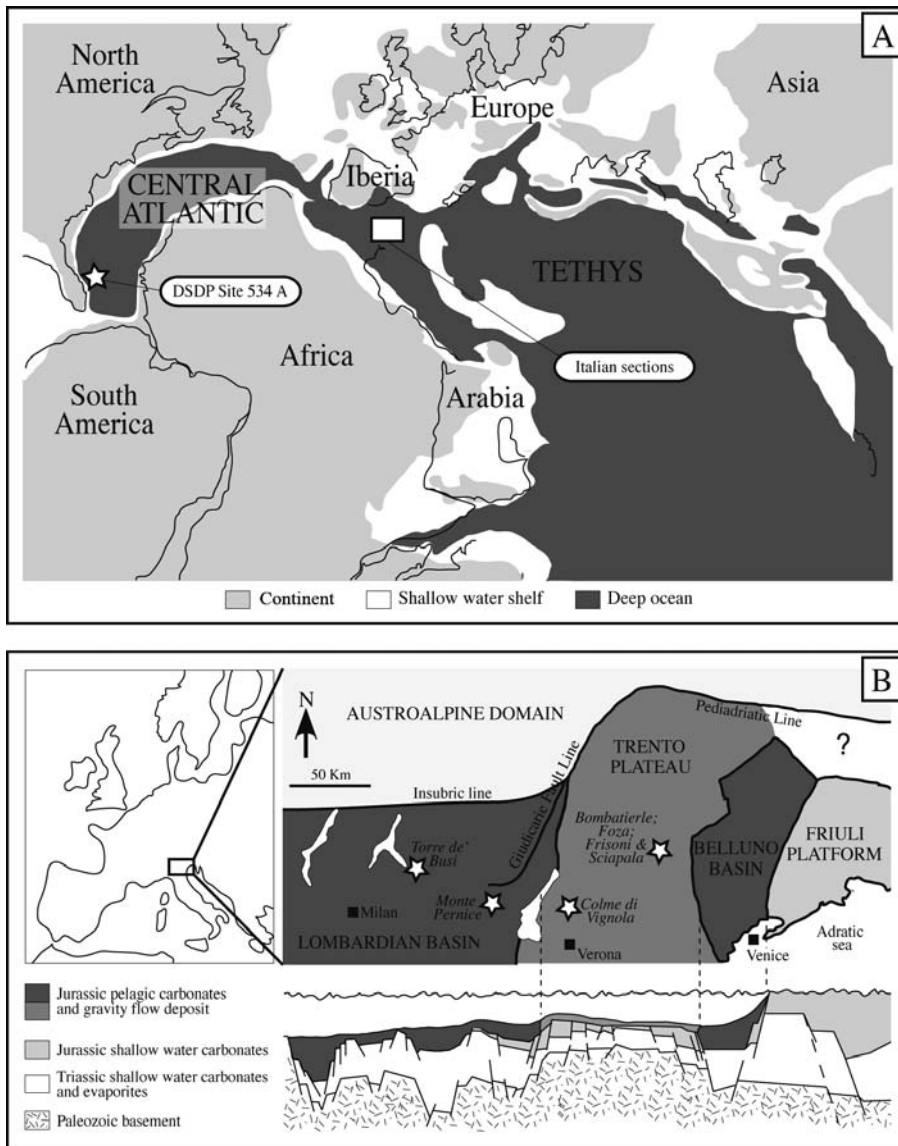


Fig. 1 - A: Paleogeographic reconstruction of Tethys Ocean during the Middle Jurassic, and position of studied sections on its southern margin (modified from Barrier & Vrielynck 2008). B: Paleogeographic units and schematic paleogeographic cross-section for latest Jurassic time (after Winterer & Bosellini 1981).

Triassic-Early Jurassic interval this continental margin experienced a incisive rifting phase that led to the progressive disintegration of the wide Norian carbonate platforms, fragmenting the margin in a horst and graben structure that lasted until the beginning of the Alpine Orogeny (Bernoulli & Jenkyns 1974; Winterer & Bosellini 1981; Baumgartner et al. 2001). This phase led to the formation of four different paleogeographic domains bounded by synsedimentary faults controlling sedimentation during the Jurassic: the deep pelagic Lombardian Basin; the pelagic submarine high of Trento Plateau; the relatively deep pelagic Belluno Basin; the shallow Friuli Platform (Fig. 1B). These domains are still arranged in their original pre-Alpine order, and allow a relatively clear paleogeographic reconstruction (Bernoulli et al. 1979; Winterer & Bosellini 1981; Baumgartner et al. 2001). The Upper Jurassic-Lower Cretaceous sedimentary sequences from Southern Alps are well known (Bernoulli 1964; Pasquarè 1965; Bernoulli

et al. 1979; Winterer & Bosellini 1981) and a number of studies have improved the stratigraphy of the Upper Jurassic sections (Channell & Grandesso 1987; Channell et al. 1987; Erba & Quadrio 1987; Channell et al. 1990; Baumgartner et al. 2001; Martire et al. 2006; Channell et al. 2010). The Middle Jurassic-lowermost Cretaceous sequence of the Trento Plateau comprises red condensed nodular pelagic limestones (Rosso Ammonitico and Calcare Selcifero di Fonzaso) overlain by white-grey micritic pseudo-nodular pelagic limestones with chert (Biancone) (Fig. 2). The coeval sequence deposited in the deeper Lombardian Basin consists of violet-red to greenish siliceous sediments (Radiolariti), transitionally followed by red siliceous to calcareous limestones with red chert lists and nodules (Rosso ad Aptici), transitionally changing into white limestones with grey chert nodules (Maiolica) (Fig. 2). The sedimentary sequence of the Southern Alps is everywhere characterized by a progressive upwards decrease of siliceous content, par-

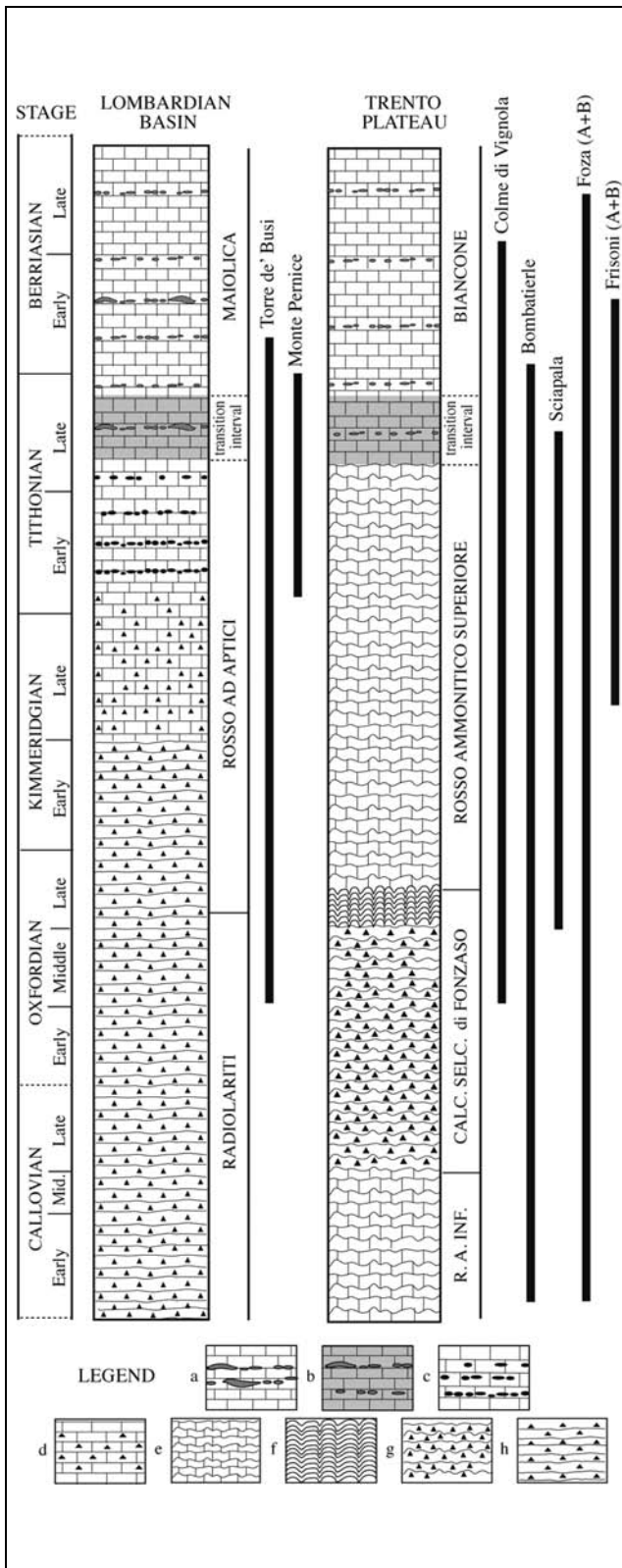


Fig. 2 - Schematic Jurassic lithostratigraphy of the studied sections, Southern Alps, Italy (after Baumgartner et al. 2001). a: Whitish limestone with grey chert nodules; b: Whitish-reddish limestone with grayish-reddish chert nodules; c: Red limestone with red-brown chert nodules; d: Reddish-brown siliceous limestone; e: Pale brown or reddish nodular cherty marlstone and limestone; f: red-brown cherty marls; g: reddish nodular chert; h: reddish-violet chert.

alleled by an increase of calcareous content (Roth 1986; Winterer 1998; Muttoni et al. 2005).

### Materials and Methods

New and/or historical sections from Lombardian Basin and Trento Plateau were studied in order to achieve an integrated bio-magnetostratigraphic framework for the Upper Jurassic-lowermost Cretaceous interval. Samples for biostratigraphic investigations were taken from un-heated magneto-core chips and, in some cases (Torre de' Busi section and Bombattierle quarry) supplemented with additional samples independently collected in the field. Samples for calcareous nannofossil investigations were chosen from different lithologies: marly claystones from the Radiolariti and from Calcare Selcifero di Fonzaso interbeds; marlstones and limestones from Rosso Ammonitico; limestones from Rosso ad Aptici and Maiolica/Biancone. Samples were taken at regular intervals, with sampling spacing varying from few decimetres to one meter (see appendix 3 for details regarding each studied section).

Calcareous nannofossil biostratigraphic investigations were performed on smear slides and ultra-thin sections. Smear slides were prepared powdering a small amount of rock material adding few drops of bi-distillate water. The obtained suspension was mounted onto a microscope slide, covered with a slide cover and fixed with Norland Optical Adhesive, without centrifuging, ultrasonic cleaning or settling the sediment in order to retain the original composition. Concentrated smear slide were also prepared to detect the rare taxa and particularly to study the appearance and evolution of nannoconids. Sections from Lombardian Basin were also analyzed using ultra-thin sections, in order to further investigate those specimens characterized by delicate ultrastructure and/or large dimensions (like nannoconids or large watznauerids) that can be easily destroyed by powdering hard rock material for smear slides. In order to make nannofossils visible ultra-thin sections were thinned to a 7  $\mu\text{m}$  thickness using an emery powder mixed with water. A total of 820 samples (630 smear slides and 190 ultra-thin sections) were inspected using a light polarizing microscope, at 1250X magnification.

The available biostratigraphic schemes of Bralower et al. (1989) and De Kaenel et al. (1996) were adopted for the biostratigraphic investigations (Fig. 3).

Preservation of calcareous nannofossils was characterized adopting the codes described by Roth (1983): E1 (slight etching); E2 (moderate etching); E3 (strong dissolution); O1 (slight overgrowth); O2 (moderate overgrowth); O3 (strong overgrowth).

Estimate of nannofossil total abundance was recorded as follows:

- A (abundant): > 11 specimens per field of view;
- C (common): 1-10 specimens per field of view;
- F (few): 1 specimens every 1-10 fields of view;
- R (rare): 1 specimens every 11-100 fields of view;
- B (barren): no specimen found.

### Biostratigraphy

Nannofossils are rare to few in the uppermost Callovian to uppermost Kimmeridgian, become common in the lower Tithonian and increase in abundance from the uppermost lower Tithonian upwards. The nannofossil assemblages recognized in the Rosso Ammonitico, Radiolariti-Rosso ad Aptici transition and the lower Rosso ad Aptici are dominated by the genera *Watznaueria* and *Cyclagelosphaera*, most resistant to diage-

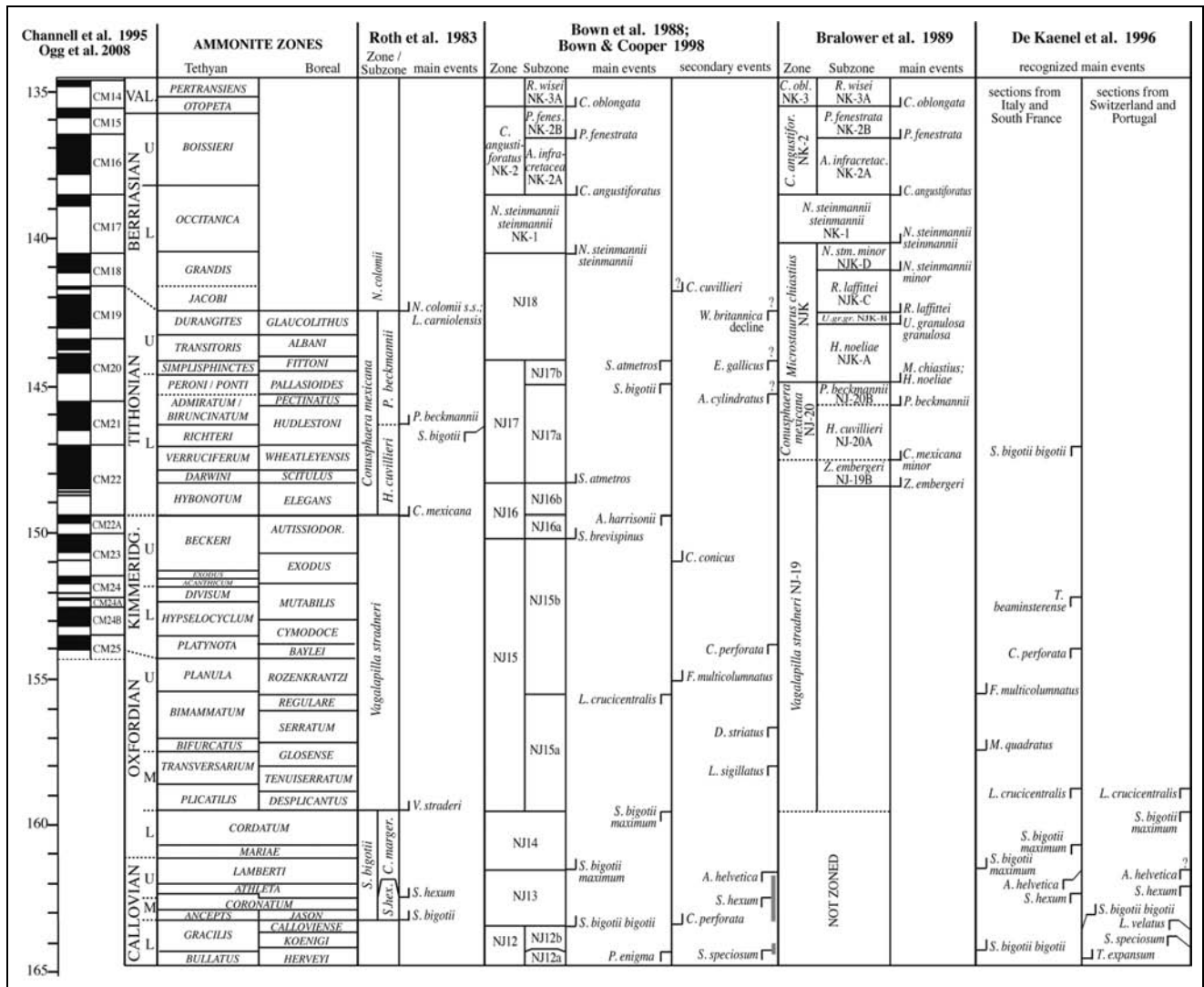


Fig. 3 - Comparative chart of calcareous nannofossil zonations available for the Tethyan Realm.

netic modifications (Roth 1986). The upper Rosso ad Aptici and upper Rosso Ammonitico are characterized by the appearance and sudden increase in abundance of highly-calcified nannoliths like *Conusphaera* and *Polycostella*, that dominate the nannofossil assemblages. From the Rosso ad Aptici-Maiolica and Rosso Ammonitico-Biancone transitions nannofossil abundance and diversification increase upwards with the appearance of genus *Nannoconus* that increases in abundance and size, reaching large dimensions and thus high calcification degree.

The investigated Callovian-Kimmeridgian interval has an extremely poor nannofossil preservation: only sparse and strongly etched specimens were observed. Nannofossil preservation in the Tithonian-lower Berriasian interval improves to poor till moderate, and most taxa described in literature were identified.

Calcareous nannofossil species recognized are listed in Appendix 1. The stratigraphic levels of marker events recognized are reported in Table 1. Range charts

of calcareous nannofossils in the studied sections are given in Appendix 2 along with a detailed lithostratigraphic description for each section, reported in Appendix 3.

*Torre de' Busi section, Lombardian Basin*

The Torre de' Busi section is the most expanded of the studied sections. In the upper Oxfordian-lowermost Berriasian thirty-two calcareous nannofossil bioevents are recognized (Fig. 4). The uppermost Radiolariti can be assigned to the latest Oxfordian based on the FO of *F. multicolumnatus* according to De Kaenel et al. (1996). At the same level the FO of *M. quadratus* is detected, however this taxon should appear before *F. multicolumnatus* according to De Kaenel et al. (1996) and Gardin (written communication, 2009), thus it might not represent here a real first occurrence. The middle Rosso ad Aptici is dated as earliest Tithonian, based on the FOs of *C. mexicana minor*, *C. mexicana mexicana* and *P. beckmannii*. Few meters above the FO

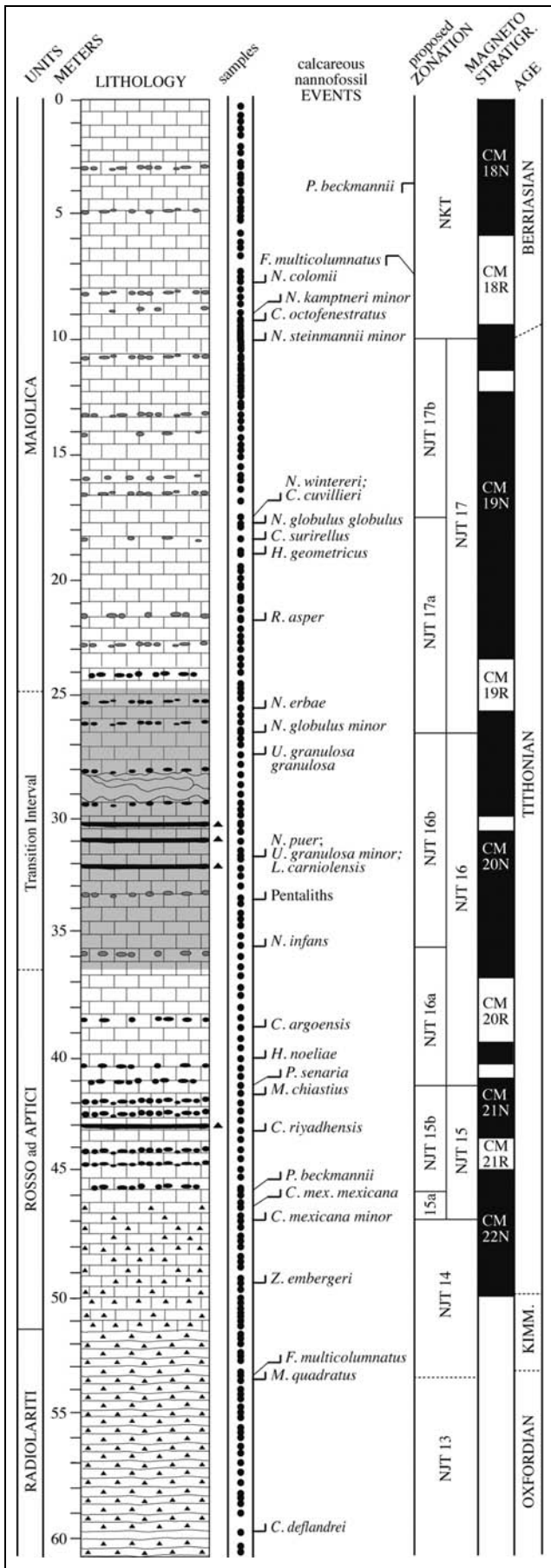


Fig. 4 - The lithostratigraphy, biostratigraphy and magnetostratigraphy of the Torre de' Busi section, Lombardian Basin.

of *C. riyadhensis* is recognized. The uppermost Rosso ad Aptici is dated as latest early Tithonian by the FO of *M. chiastius* shortly followed by the FOs of *P. senaria*, *H. noeliae* and *C. argoensis*. Few meters above the appearance of genus *Nannoconus* is recognized: primitive nannoconids (*N. infans*, *N. puer* and *N. erbae*) first occur close to the early/late Tithonian boundary, evolving upward across the Rosso ad Aptici-Maiolica transition. This interval is also characterized by the appearance of numerous new genera and species: the nannoliths genus *Lithraphidites*, the primitive penthalits (mainly genus *Micrantholithus*) and the murolith genus *Umbria*. The FO of *N. globulus minor* is recognized well before the appearance level reported in literature (Bralower et al. 1989). The lowermost Maiolica is assigned to the latest late Tithonian on the basis of the FO of *R. asper*, shortly followed by the FOs of *C. surirellus*, *N. globulus globulus*, *C. cuvillieri* and *N. wintereri*. In this study a new *Hexalithus* species (*H. geometricus*) is described, appearing after the FO of *R. asper* and slightly before the FO of *C. surirellus* (18.98 m, Tab. 1). The J/K boundary is approximated on the FO of *N. steinmannii minor*. In the Tithonian/Berriasian (J/K) boundary interval the FOs of *N. kamptneri minor*, *N. colomii* and *C. octofenestratus* are also reported.

*Monte Pernice section, Lombardian basin*

This section is short and condensed. Samples previously documented by Erba & Quadrio (1987) are re-analyzed (Fig. 5). Ultra-thin sections and newly prepared smear slides are investigated: a total of fifteen calcareous nannofossil events are identified from the early Tithonian to earliest Berriasian. In the Rosso ad Aptici-Maiolica transition the FOs of *M. chiastius* and *H. noeliae* are recognized, allowing the assignment of these strata to the early Tithonian; at the same level the FO of *N. infans* is reported shortly followed by the FO *N. globulus minor*. The FOs of *C. argoensis*, *U. granulosa granulosa*, *N. puer*, *N. erbae* and *H. geometricus* also occur during this interval. The lowermost Maiolica is late Tithonian in age on the basis of the FOs of *C. surirellus*, *N. wintereri* and *C. cuvillieri*. The J/K boundary is localized in the upper part of the section on the basis the FO of *N. steinmannii minor*.

*Colme di Vignola section, Trento Plateau*

The Colme di Vignola section (Fig. 6) covers the Calcare Selcifero di Fonzaso to Biancone interval. The succession shows an extreme nodularity that testify severe condensation. Twenty calcareous nannofossil bioevents allow dating the Rosso Ammonitico Superiore-Biancone interval to the Oxfordian-Berriasian. The lower Rosso Ammonitico Superiore could be Middle Oxfordian in age on the basis of the LO of *L. sigillatus* according to Bown et al. (1988) and Bown & Cooper

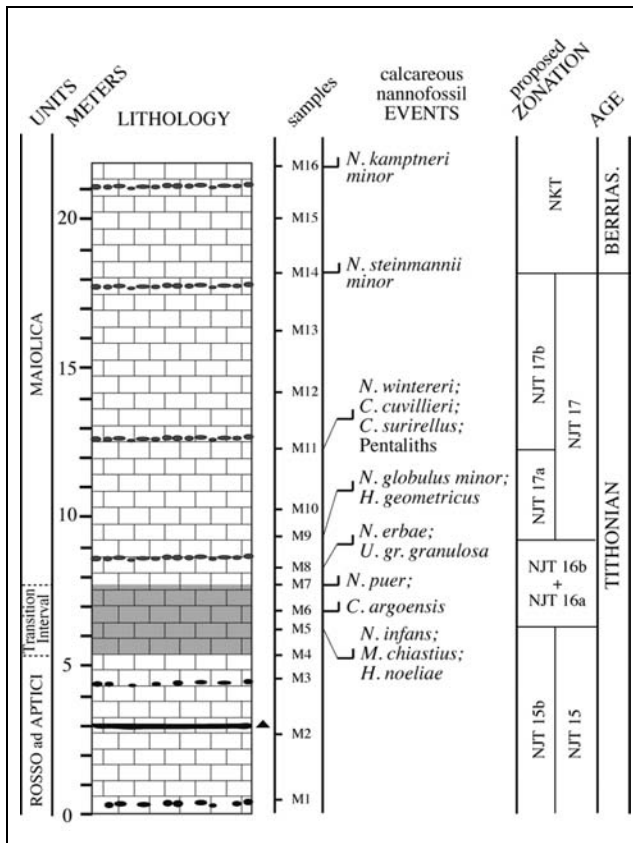


Fig. 5 - The lithostratigraphy, biostratigraphy and magnetostratigraphy of the Monte Pernice section, Lombardian Basin.

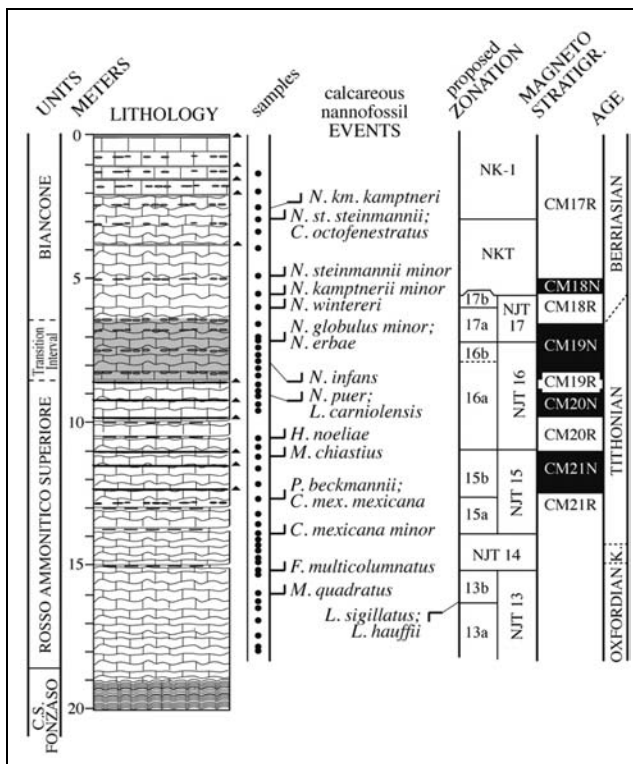


Fig. 6 - The lithostratigraphy, biostratigraphy and magnetostratigraphy of the Colme di Vignola section, Trento Plateau.

(1998). Few decimetres above the FO of *F. multicolumnatus* is identified deriving a latest Oxfordian age. In the middle Rosso Ammonitico Superiore the FOs of *C. mexicana minor*, *C. mexicana mexicana* and *P. beckmannii* are recognized and an earliest Tithonian age is given. The FOs of *M. chiastius* and *H. noeliae* fall in the upper Rosso Ammonitico Superiore. Across the Rosso Ammonitico-Biancone transition the FOs of *N. infans*, *N. puer* and *N. erbae* are observed along with the FOs of *L. carniolensis* and *N. globulus minor*. The lowermost Maiolica is dated as the latest Tithonian and the J/K boundary is recognized on the basis of the FOs of *N. wintereri*, *N. steinmannii minor* and *N. kamptneri minor*. In the upper part of the section the FOs of *N. steinmannii steinmannii*, *N. kamptneri kamptneri* and *C. octofenestratus* were detected and an early Berriasian age is derived.

*Foza composite section, Trento Plateau*

The Foza section (Figs 7, 8) represents the longest succession, covering the Rosso Ammonitico Inferiore to Biancone interval. Thirty-nine calcareous nannofossil bioevents characterizing the upper Callovian-Berriasian are recognized. Two intervals in the lowermost part of the section (35.4-36.0 m and 39.0-40.0 m, Fig. 7) are covered by vegetation and were not sampled. In the upper Calcare Selcifero di Fonzaso the LO of *C. wiedmannii* is recognized, assigning this level to the latest Callovian (Reale & Monechi 1994; Mattioli & Erba 1999). One meter above, the LO of *L. sigillatus* indicates a middle Oxfordian age. The uppermost strata of Calcare Selcifero di Fonzaso are here characterized by the FO of *C. deflandrei* followed by the FO of *M. quadratus*: according to De Kaenel et al. (1996) the latter event indicates a middle/late Oxfordian age (base of *Bifurcatus* Ammonite Zone), but other Authors suppose it indicates late early Oxfordian (upper part of *Cordatum* Ammonite Zone, Gardin, written communication, 2009). In the lowest part of Rosso Ammonitico Inferiore the FO of *F. multicolumnatus* is recognized, indicating a latest Oxfordian age. The FOs of *C. mexicana minor* and *C. mexicana mexicana* lie in the middle Rosso Ammonitico Superiore, consequently assigned to the earliest Tithonian. At the same level the FO of *C. riyadhensis* is recognized, occurring earlier than in the Lombardian Basin (Torre de' Busi section, Tab.1). The nannofossil events recognized indicate that the uppermost Callovian-Kimmeridgian interval is severely condensed and possibly partially discontinuous.

In the uppermost Rosso Ammonitico Superiore the FOs of *P. beckmannii*, along with the FOs of *C. argoensis* and *Z. embergeri* are identified, followed by the FO of *M. chiastius*. The Rosso Ammonitico Superiore-Biancone transition is characterized by the FOs of *N. infans*, *N. puer* and *U. granulosa granulosa*. In the



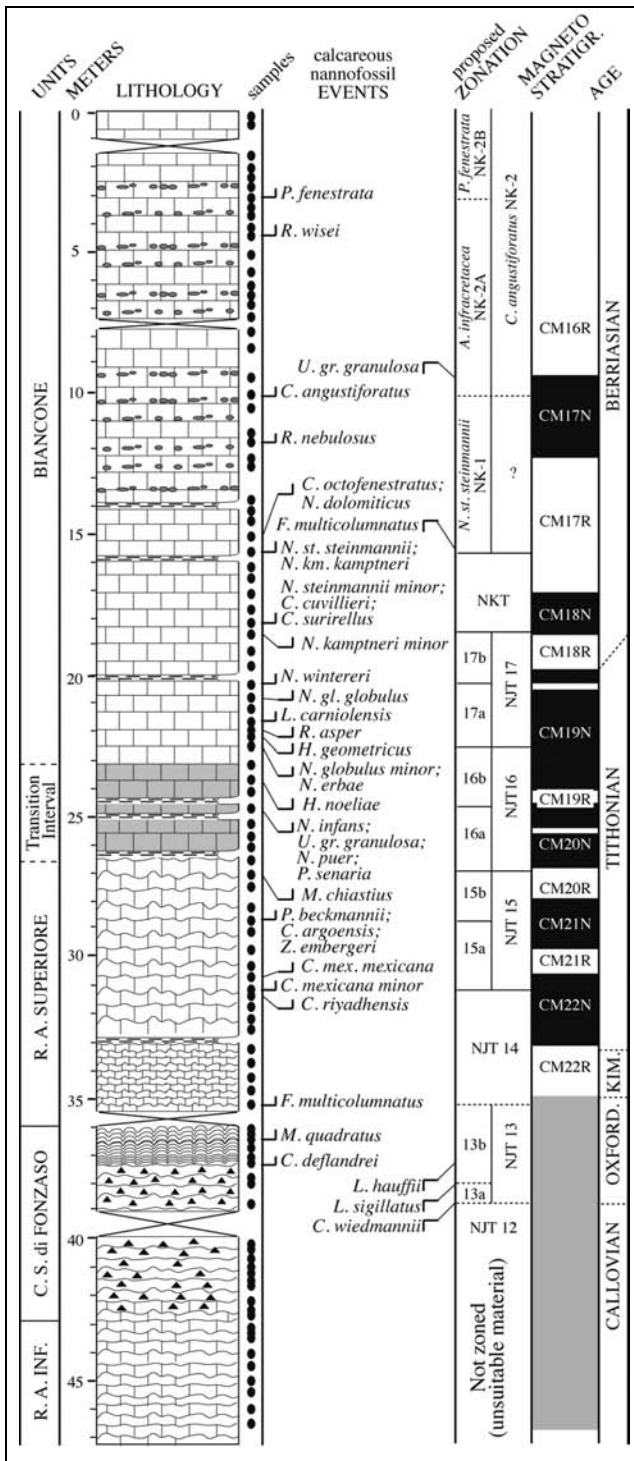


Fig. 7 - The lithostratigraphy, biostratigraphy and magnetostratigraphy of the Foza A section, Trento Plateau.

same interval the FO of *P. senaria* and, slightly after, the FO of *H. noeliae* were recognized, much later than in Torre de' Busi section. The lowermost Biancone is assigned to the latest Tithonian on the basis of the FOs of *N. globulus minor*, *H. geometricus*, *R. asper*, *L. carniolensis* and *N. globulus globulus* as well as the FO of *N. wintereri*. The J/K boundary interval is approximated on the basis of the FOs of *N. steinmannii minor* and *N.*

*kamptneri minor*. Several Berriasian bioevents (Brallower et al. 1989) are detected in the upper portion of the Foza section (data coming both from section A and B, Figs 7, 8): the FOs of *N. steinmannii steinmannii*, *N. kamptneri kamptneri*, *C. octofenestratus*, *C. angustiforatus*, *N. dolomiticus*, *R. nebulosus*, *R. wisei* and *P. fenestrata* as well as the LOs of *N. wintereri* and *U. granulosa granulosa* (see Tab. 1 for details).

*Bombatierle quarry, Trento Plateau*

The Bombatierle quarry (Fig. 9) represents an extremely well exposed section spanning the Rosso Ammonitico Inferiore to Rosso Ammonitico-Biancone transition. A bentonite layer (Bernoulli & Peters 1970; Martire et al. 2006) characterizes the lowermost part of Rosso Ammonitico Superiore and represents a marker level clearly distinctive in the quarry walls and useful for stratigraphic correlation on the Trento Plateau. On the basis of this datum is possible to correlate this section with the Kaberlaba one (Martire 1996), where calpionellid and ammonite biostratigraphies are available (Martire et al. 2006).

A total of nineteen calcareous nannofossil bioevents characterizing the Upper Callovian-Early Tithonian are recognized. The uppermost part of Rosso Ammonitico Inferiore is assigned to the latest Callovian on the basis of rare specimens of *A. helvetica* (Bown et al. 1988; De Kaenel et al. 1996; Bown & Cooper 1998). In the Rosso Ammonitico Medio (Calcare Selcifero di Fonzaso) the LOs of *C. wiedmannii* and *L. sigillatus* are recognized and a latest Callovian-middle Oxfordian age is inferred. In the lowermost part of the Rosso Ammonitico Superiore the FO of *F. multicolumnatus* is detected indicating a latest Oxfordian age. The FOs of *C. deflandrei* and *M. quadratus* are recognized in the lower Rosso Ammonitico Superiore above the FO of *F. multicolumnatus*. The FOs of *C. mexicana minor*, *C. mexicana mexicana* and *P. beckmannii* lie in the upper Rosso Ammonitico Superiore, consequently assigned to the earliest Tithonian. The Rosso Ammonitico-Biancone transition is thinner and stratigraphically older than in the other sections, based on the FOs of *M. chiastius* and *H. noeliae*. The lowermost Biancone covers the early-late Tithonian interval as testified by the appearance of primitive nannoconids (*N. infans*, *N. puer* and *N. erbae*) and by the FOs of *L. carniolensis*, *C. argoensis* and *U. granulosa granulosa*.

*Sciapala quarry, Trento Plateau*

The Sciapala quarry is characterized by an expanded section of Rosso Ammonitico Medio-Superiore and covers the older interval studied (Fig. 10). A total fifteen bioevents characterizing the upper Callovian-early Tithonian were detected. The Rosso Ammonitico Medio (Calcare Selcifero di Fonzaso) is characterized



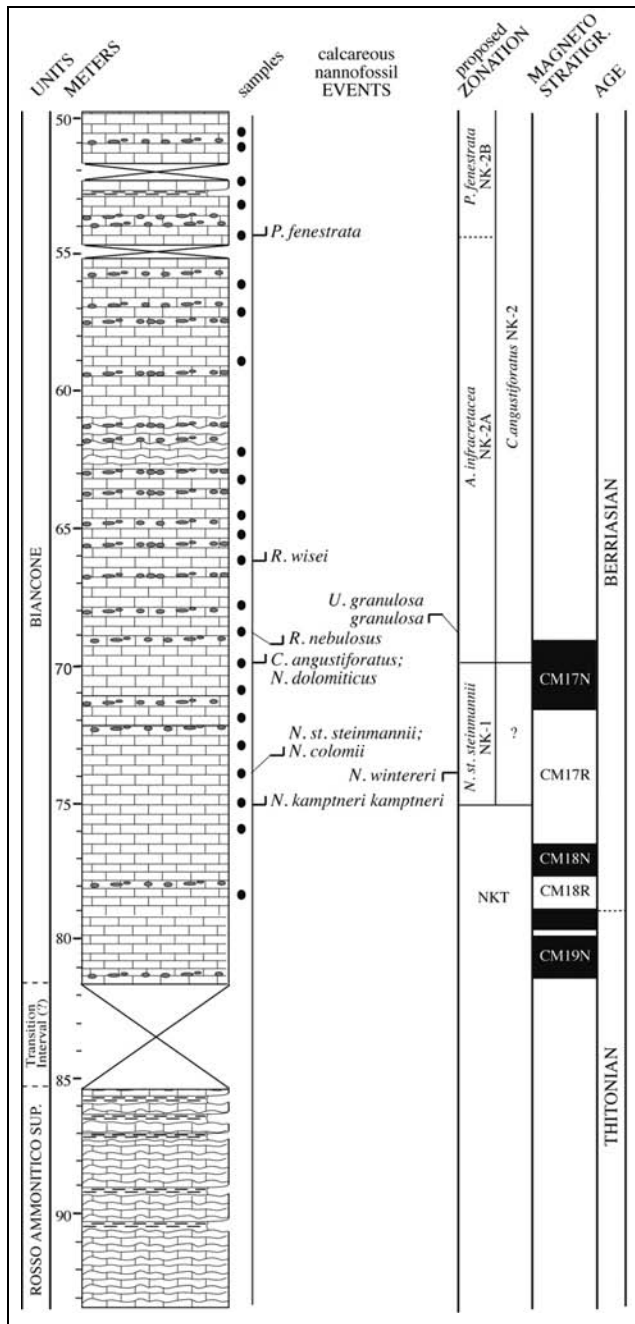


Fig. 8 - The lithostratigraphy, biostratigraphy and magnetostratigraphy of the Foza B section, Trento Plateau.

by the LOs of *C. wiedmannii* and *L. sigillatus*: these events suggest a latest Callovian-middle Oxfordian age. In the lowermost strata of Rosso Ammonitico Superiore the FO of *F. multicolumnatus* indicates a latest Oxfordian age. At the same level the FO of *C. deflandrei* is detected. Few meters above the FO of *M. quadratus* is identified. The middle Rosso Ammonitico Superiore is assigned to the earliest Tithonian on the basis of the FOs of *C. mexicana minor*, *C. mexicana mexicana* shortly followed by the FOs of *P. beckmannii* and *C. argoensis*. The uppermost Rosso Ammonitico Superiore spans the early-late Tithonian interval on the

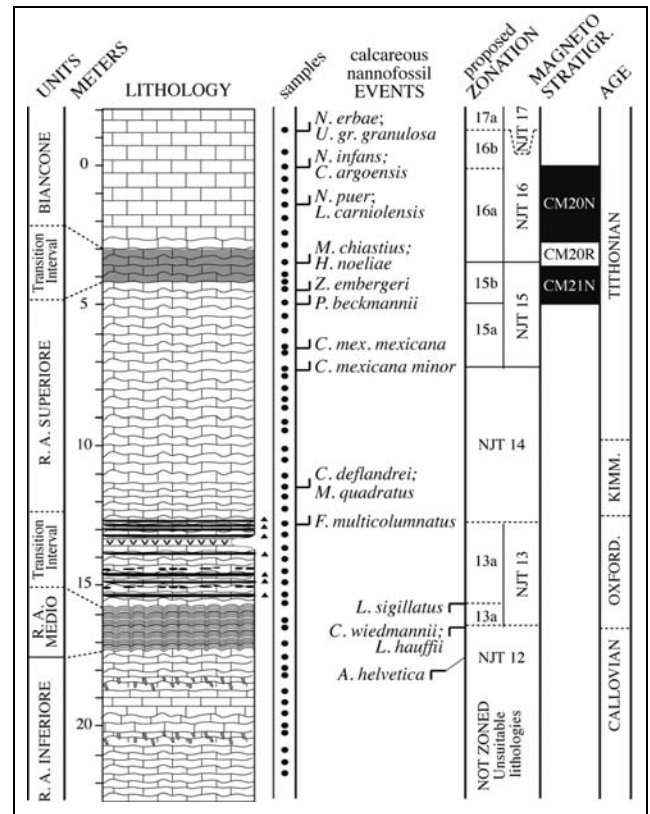


Fig. 9 - The lithostratigraphy, biostratigraphy and magnetostratigraphy of the Bombatierle quarry, Trento Plateau.

basis of the FO of *M. chiastius*, followed by the FOs of *P. senaria* and *U. granulosa minor*. The primitive nannofossils *N. infans* and *N. puer* appear in the uppermost strata of Rosso Ammonitico Superiore, before the Rosso Ammonitico-Biancone transition.

*Frisoni composite section, Trento Plateau*

The Frisoni composite section covers the Rosso Ammonitico Superiore (Fig. 11) to lower Biancone (Fig. 12) interval. The stratigraphic succession, and especially the Rosso Ammonitico Superiore, shows severe nodularity and condensation: in both Frisoni A and B sections calcareous nannofossils are rare to few and very poorly preserved. However, seventeen events and four events are recognized at Frisoni A and Frisoni B respectively. The FOs of *C. mexicana minor*, *C. mexicana mexicana* and *P. beckmannii* are identified in the upper Rosso Ammonitico Superiore in both sections. At Frisoni A the FOs of *M. chiastius* and *P. senaria* are recognized in the middle Rosso Ammonitico Superiore. In this section the FOs of *N. infans*, *N. puer* and *N. erbae* are identified below the Rosso Ammonitico-Biancone transition, as in the Sciapala quarry. The FO of *U. granulosa granulosa* is recognized in the middle part of Rosso Ammonitico-Biancone transition. In the lowermost part of Biancone is recognized the J/K boundary interval approximated on the FOs of *N. steinmannii minor*.

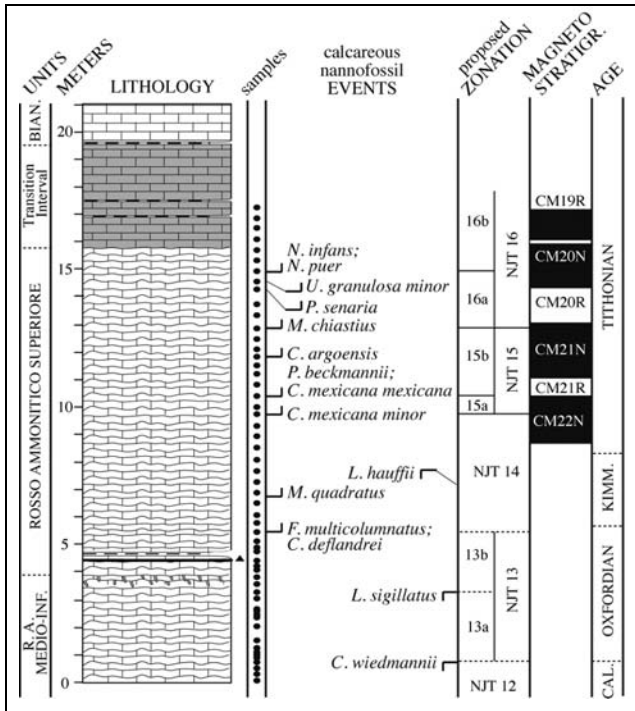


Fig. 10 - The lithostratigraphy, biostratigraphy and magnetostratigraphy of the Sciapala quarry, Trento Plateau.

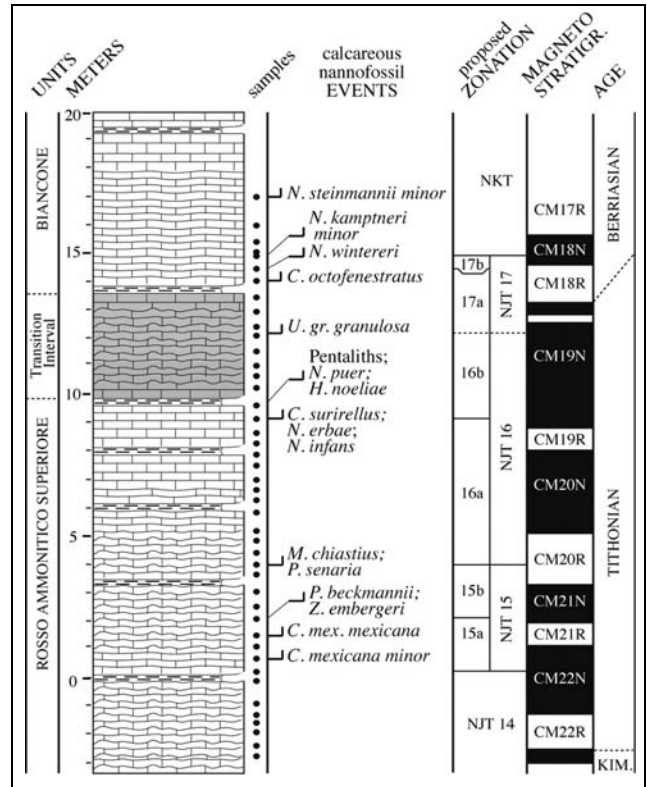


Fig. 12 - The lithostratigraphy, biostratigraphy and magnetostratigraphy of the Frisoni A section, Trento Plateau.

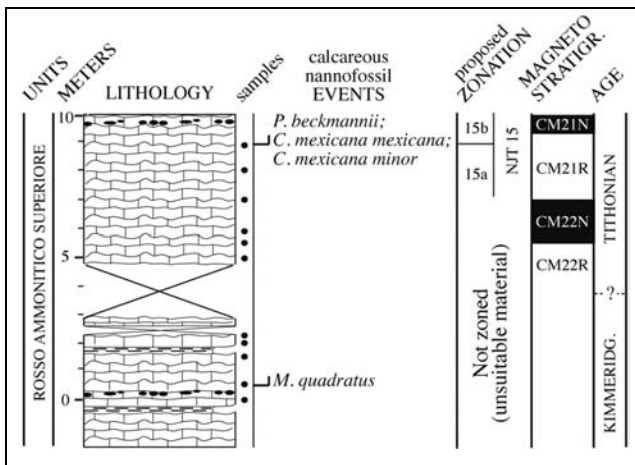


Fig. 11 - The lithostratigraphy, biostratigraphy and magnetostratigraphy of the Frisoni B section, Trento Plateau.

The FOs of *N. kamptneri minor*, *C. octofenestratus* and *N. wintereri* are also observed in the uppermost part of the section.

**Nannoconids**

During this study special attention was paid to the nannoconid group, first appearing and evolving during the Tithonian. The genus *Nannoconus* has received detailed investigations by several Authors in the past (Brönnimann 1955; Trejo 1960; Wind 1978; Deres & Achéritéguy 1980; Bralower et al. 1989), indicating that

several Lower Cretaceous nannoconid species have a precursor smaller in size in the Tithonian. Particularly, Bralower et al. (1989) investigated the evolution of Tithonian nannoconids and described several new species and subspecies. Here the Tithonian interval has been carefully studied on both smear slides and ultra-thin sections and two new primitive species, *N. puer* (Pl. 3, figs 4-9; Pl. 9, fig. 4) and *N. erbae* (Pl. 4, figs 7-12), were described (see Systematic Palaeontology). The nannoconid primitive forms appear and rapidly evolve through the early/late Tithonian time interval (Fig. 13).

The results obtained permit to interpret the evolutionary behaviour of Tithonian nannoconids. Two morphological groups are distinguished on the basis of the nannolith outlines: spherical or subspherical forms (*N. infans*, *N. puer* and *N. globulus*), subconical and conical forms (*N. erbae*, *N. wintereri*, *N. steinmannii*, *N. kamptneri*). Evolutionary links connecting the species belonging to the same group are inferred.

A first evolutionary lineage is hypothesized for the smaller forms *N. infans* and *N. puer*, which seems to evolve toward *N. globulus minor* (Pl. 4, figs 1-6), which, in turn, evolves upwards increasing in size and calcification degree generating *N. globulus globulus* (Pl. 5, figs 5-8; Pl. 9, figs 5-6) (Fig. 13). Another possible lineage is hypothesized for the conical morphotypes that characterized the latest Tithonian and the Tithonian/Berriasian boundary interval. A lineage involves

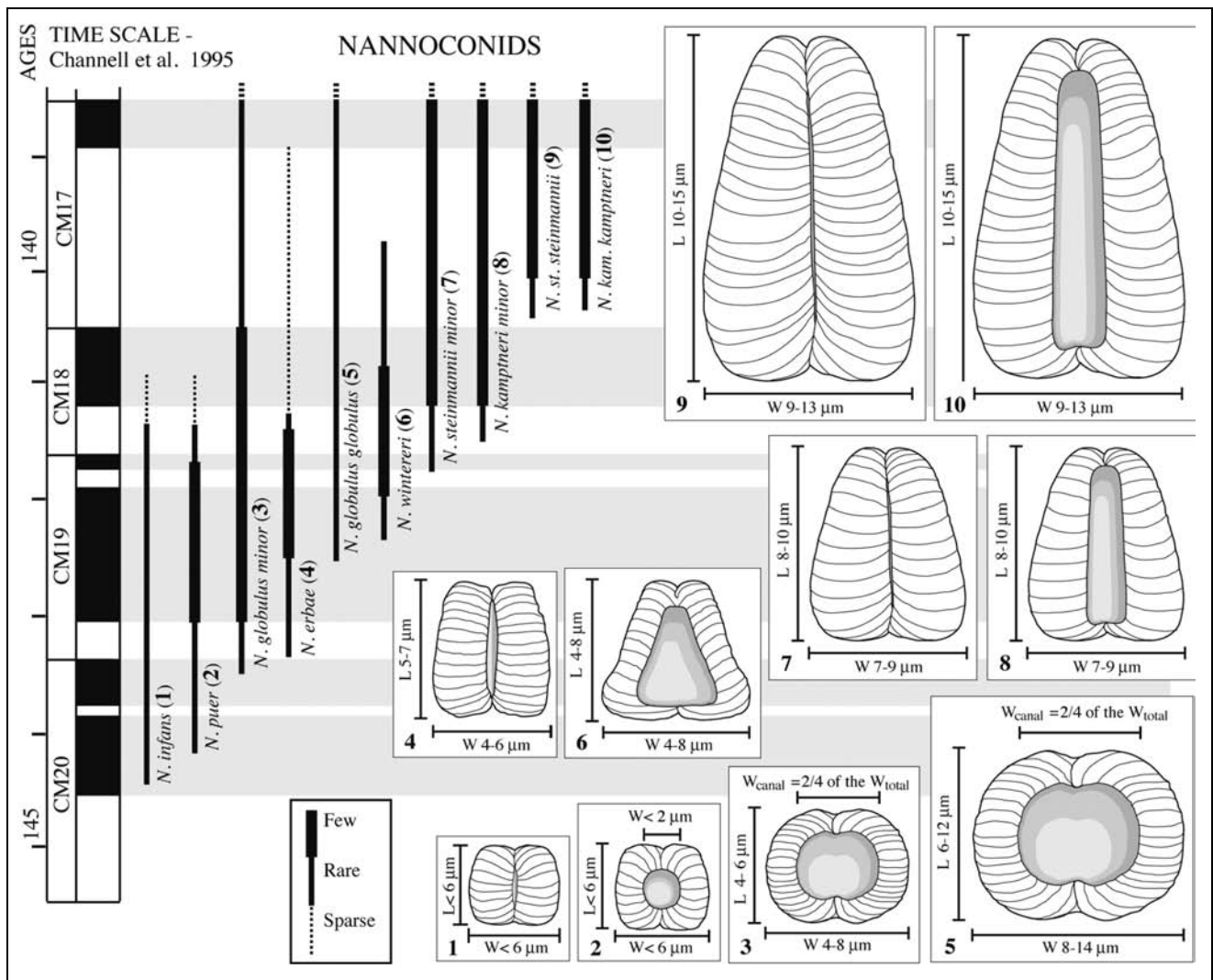


Fig. 13 - Distribution and abundance of Tithonian nannoconids and corresponding sketches correlated with indications of their dimensions. Sketches are plotted at the same scale.

*N. erbae*, which increases in size, and thus in calcification degree, evolving in *N. steinmannii minor* (Pl. 5, figs 10-11), which, in turn, grows culminating in *N. steinmannii steinmannii* (Pl. 6, figs 1-2) (Fig. 13). Another lineage possibly links *N. wintereri* (Pl. 5, figs 1-4; Pl. 9, fig. 7) and *N. kamptneri* (Pl. 5, figs 9, 12; Pl. 6, figs 3-4) (Fig. 13) but more accurate investigations are needed to check its validity.

The nannoconids diversification, dimensions, calcification degree and abundance (Fig. 13) increase upwards during the Tithonian: the primitive and spherical forms show an increase in abundance, becoming a common components of the nannofossil assemblages of late Tithonian; the conical morphotypes as well show a huge and sudden increase in abundance and dimensions across the J/K boundary interval becoming the dominant components of the nannofossil assemblages. These abundance increases induced changes in the pelagic micrite composition (Erba & Quadrio 1987; Weissert & Erba 2004; Erba 2006; Casellato 2009), best decipher-

able observing ultra-thin sections, and representing one of the most relevant events in the Tithonian. Particularly in most of the studied section the spherical nannoconid increase characterizes the transition intervals between Rosso ad Aptici-Maiolica (Lombardian Basin) and upper Rosso Ammonitico Superiore-Biancone (Trento Plateau). On the other hand, the dramatic increase in abundance of conical nannoconids across the Tithonian/Berriasian boundary interval controlled completely the composition of Maiolica/Biancone, therefore regarded as a “nannoconites” by previous authors (Erba 1990 and references therein).

The results achieved from the Southern Alps sections were tested on the DSDP Site 534 A (Fig. 14), in order to verify on well preserved material nannoconid taxonomical features and stratigraphic distribution, especially for the new species, and the potential evolutionary relationships. The species *N. puer* and *N. erbae* were recognized in the DSDP Site 534 A, as well as the other new species defined in this paper (*Z. fluxus* and *H.*

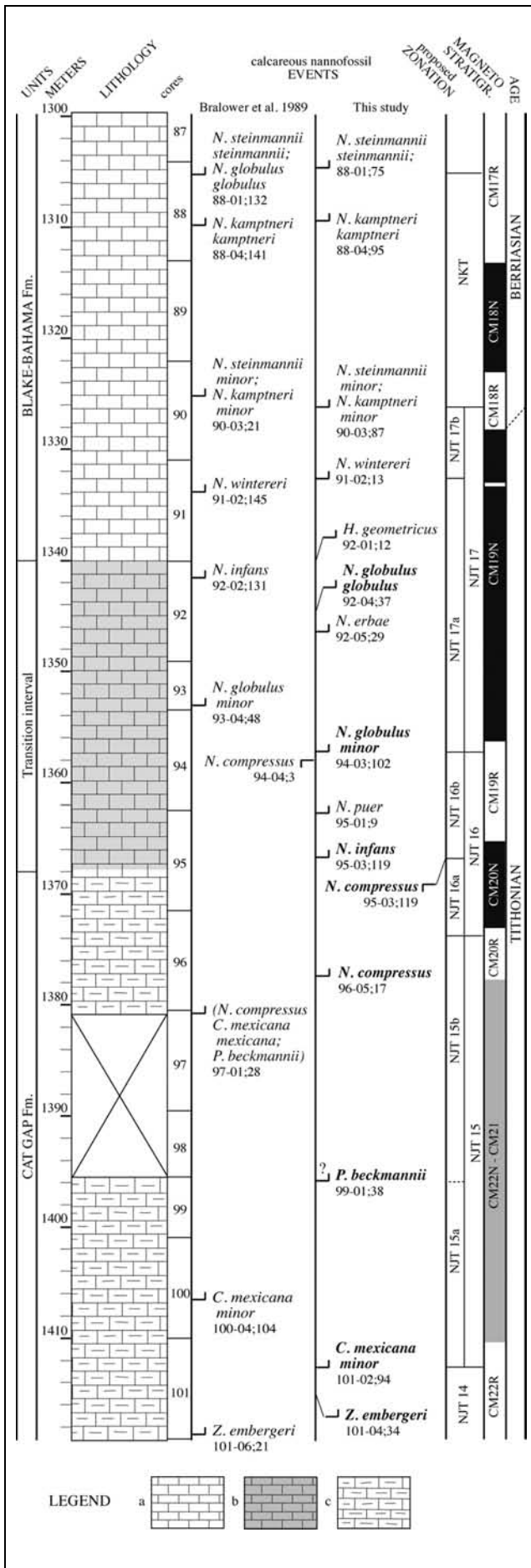


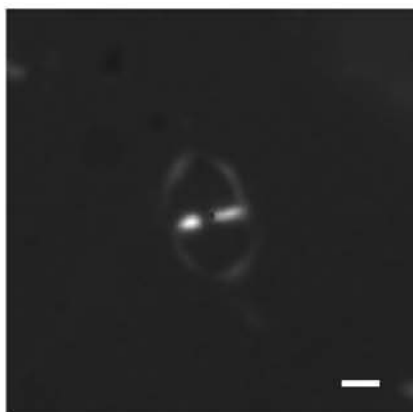
Fig. 14 - The lithostratigraphy, biostratigraphy and magnetostratigraphy of the DSDP Site 534 A, Central Atlantic Ocean. Calcareous nannofossil data regard mainly the nannocoid group. Each bioevent is plotted along with informations regarding the sample (xx-yy; z = core # - core section #; centimetre). Bioevents found at older stratigraphic levels than reported by previous Authors (Bralower et al. 1989) are in bold font. a: Gray to white nannofossil limestone and chalk; b: Grayish to reddish calcareous marly limestone; c: Reddish calcareous claystone and marly limestone.

geometricus): all of them display similar distribution than in the Tethyan sections. Similar variations in dimension, abundance increases and comparable evolutionary behaviours were also observed confirming their supra-regional validity. The investigation of DSDP Site 534 A has pointed out that the FOs of *N. infans*, *N. globulus minor* and *N. globulus globulus* occur at older stratigraphic levels than reported by previous Authors (Bralower et al. 1989), at analogous levels of Southern Alps sections. Nevertheless, the nannocoid population of Atlantic Ocean differs from the Tethyan one for the presence of *N. compressus* (Bralower et al. 1989, pl. VIII, figs 7-12, pp. 226). This species is abundant in the DSDP Site 534 A and dominates the nannofossil assemblage across the CM20, between the FO of *M. chiastius* and the FO of *N. infans* (Fig. 14). As a matter of fact, this species was defined at DSDP Site 105 and reported from the Atlantic Ocean (DSDP sites 534 A and 391 C). Only rare specimens were documented from land sections in Spain (Carcabuey) and France (Broyon) (Bralower et al. 1989), but no *N. compressus* specimens were observed in the studied sections. Therefore, this taxon is here considered an endemic nannoco-

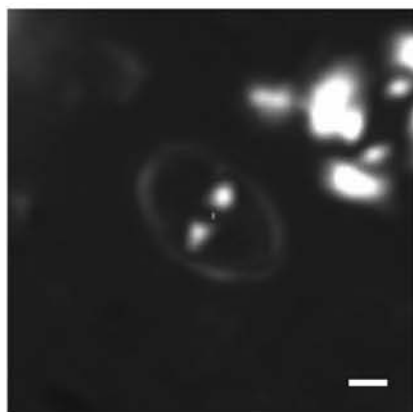
PLATE 1

Scale bar represents 1 µm.

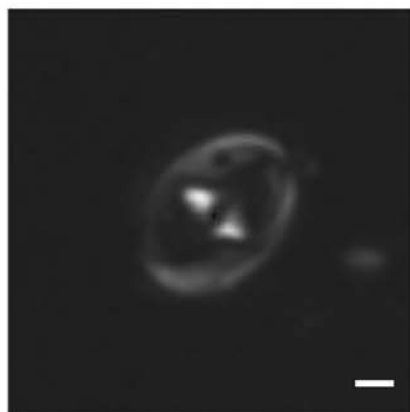
Fig. 1 - *Z. erectus*, cross-polarized light, DSDP Site 534 A 100-03;102-103, smear slide. Fig. 2 - *Z. erectus*, cross-polarized light, DSDP Site 534 A 101-05;104-105, smear slide. Fig. 3 - *Z. fluxus* n. sp., cross-polarized light, DSDP Site 534 A 101-02;92-93, smear slide. Fig. 4 - *Z. fluxus* n. sp., cross-polarized light, DSDP Site 534 A 101-04;98-99, smear slide. Fig. 5 - *Z. fluxus* n. sp., cross-polarized light, DSDP Site 534 A 100-03; 102-103, smear slide. Fig. 6 - *Z. fluxus* n. sp., cross-polarized light, DSDP Site 534 101-02; 92-93, smear slide, holotype MPUM 10473. Fig. 7 - *Z. fluxus*, n. sp. cross-polarized light, Torre de' Busi 17.54, smear slide. Fig. 8 - *Z. fluxus*, n. sp. cross-polarized light, DSDP Site 534 A 96-02;99-100, smear slide. Fig. 9 - *Z. fluxus*, n. sp. cross-polarized light, Torre de' Busi 2.95, smear slide. Fig. 10 - *Z. embergeri*, cross-polarized light, Foza A 6.55, smear slide. Fig. 11 - *Z. embergeri*, cross-polarized light, Monte Pernice MP13, smear slide. Fig. 12 - *Z. embergeri*, cross-polarized light, Torre de' Busi 0.28, smear slide.



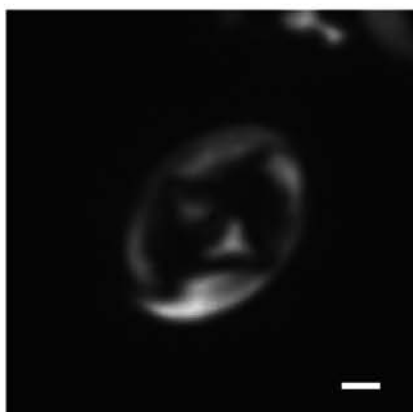
1. *Z. erectus*



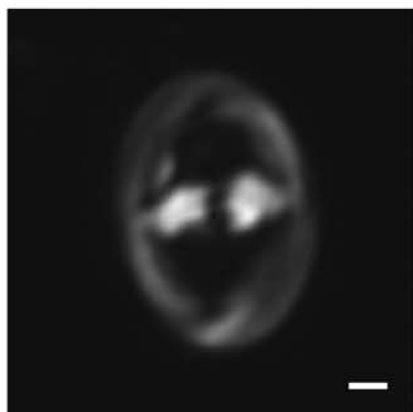
2. *Z. erectus*



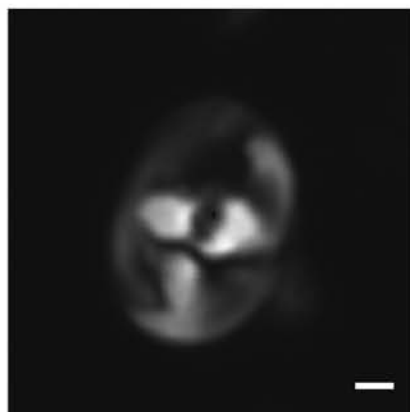
3. *Z. fluxus* n. sp.



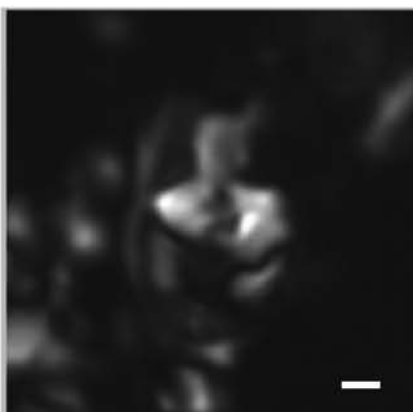
4. *Z. fluxus* n. sp.



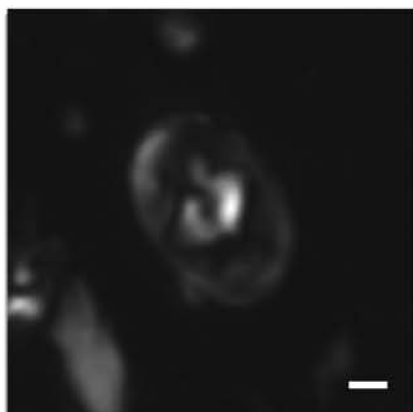
5. *Z. fluxus* n. sp.



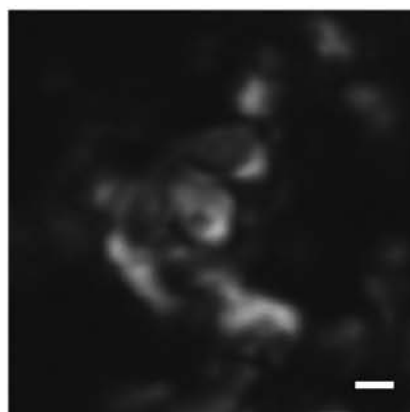
6. *Z. fluxus* n. sp.



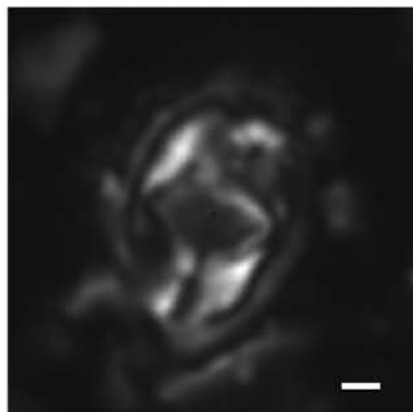
7. *Z. fluxus* n. sp.



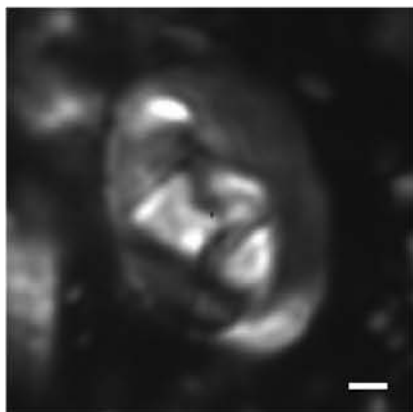
8. *Z. fluxus* n. sp.



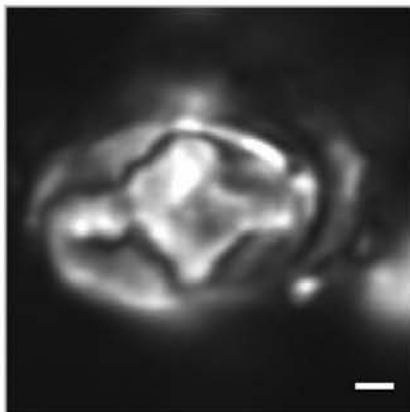
9. *Z. fluxus* n. sp.



10. *Z. embergeri*



11. *Z. embergeri*



12. *Z. embergeri*

mid species characterizing the nannofossil assemblages of Atlantic Ocean.

### Systematic Palaeontology

Calcareous nannofossil species quoted in this study are listed in Appendix 1. In this paragraph, alphabetically ordered per Order name, four new species (*Z. fluxus*, *N. puer*, *N. erbae*, *H. geometricus*) are described and remarks concerning mainly dimensional features of six species (*Z. erectus*, *Z. embergeri*, *W. britannica*, *W. communis*, *W. manivittiae*, *F. multicolumnatus*) are reported.

Kingdom **Chromista** Cavalier-Smith, 1981

Division (Phylum) **Haptophyta** Hibberd  
ex Cavalier-Smith, 1986

Class **Prymnesiophyceae** Hibberd, 1976

Subclass **Prymnesiophyceae** Cavalier-Smith, 1986

Order **Eiffellithales** Rood, Hay & Barnard, 1971

Family Chiastozygaceae (Rood, Hay & Barnard 1973)  
Varol & Giris, 1994

Genus *Zeugrhabdotus* Reinhardt, 1965

**Zeugrhabdotus erectus** (Deflandre in Deflandre & Fert,  
1954) Reinhardt, 1965

Pl. 1, figs 1, 2

**Remarks.** In this study this species is distinguished from *Z. embergeri* and *Z. fluxus* by the following features: it has lower interference colour (from grey to white); it shows smaller dimension (coccolith length < 5 µm); in the light microscope it displays two open areas; the bridge is lath-shaped; the bridge width is less than one quarter of the maximum coccolith axis (bridge width < 1/4 coccolith length).

**Zeugrhabdotus fluxus** n. sp.

Pl. 1, figs 3-9; Pl. 9, figs 1, 2

**Origin of the name:** Named for its morphology, displaying features transitional between *Z. erectus* and *Z. embergeri* (*fluxus* lat. = transitory).

**Holotype:** MPUM 10473; DSDP Site 534 A 101-02; 92-93, Pl.1, fig. 6

**Repository:** Museo di Paleontologia Università degli Studi di Milano (MPUM), Dipartimento di Scienze della Terra "A. Desio", Milano, Italy.

**Description.** Small, elliptic coccolith characterized by a smoothed rim and interference colour from grey to bright white. The central area can be narrow until completely close by a calcified membrane; the

central area contains a bridge, composed by two triangular elements that can be merged forming one thick rhomboidal bridge in more calcified specimens; the bridge is oriented parallel to the short axis of the ellipse; the bridge width is slightly smaller or approximates one third of the coccolith maximum axis (bridge width = 1/3 coccolith length). The coccolith maximum length is usually 5-8 µm (5 µm < coccolith length < 8 µm).

**Comparison with related species.** It is distinguished from *Z. erectus* by its larger coccolith size, brighter colours, wider central bridge and closer central area. It is distinguished from *Z. embergeri* by its smaller coccolith size, smaller central bridge and less calcified or narrower central openings.

**Discussion.** This species represent a transitional term between *Z. erectus* and *Z. embergeri*. The former increases through time in shield size and thickness; the outline of the central bridge changes from lath-shape to rhomboid increasing in size and thickness as well; the delicate and perforated membrane which fills the central openings of *Z. erectus* becomes more calcified and thick. A minimum diameter of 5 µm was used to separate *Z. fluxus* from *Z. erectus*; a maximum diameter less than 8 µm is adopted to discriminate this species from *Z. embergeri*. Further investigations are needed to best clarify the evolutionary relations between the three morphotypes and to better constrain the stratigraphic utility of *Z. fluxus*.

**Range.** Late Kimmeridgian - Tithonian

**Zeugrhabdotus embergeri** (Noël, 1958)

Perch-Nielsen, 1984

Pl. 1, figs 10-12

**Remarks.** In this study *Z. embergeri* includes specimens with a maximum diameter greater than 8 µm, as well as very highly calcified specimens of *Z. cooperi* (Bown 1992).

Order **Watznaueriales** Bown, 1987

Family Watznaueriaceae Rood, Hay & Barnard, 1971

Genus *Watznaueria* Reinhardt, 1964

**Watznaueria britannica** (Stradner, 1963) Reinhardt, 1964

Pl. 2, figs 1, 2

**Remarks.** In the studied sections, along with normal size *W. britannica* (Cobianchi et al. 1992), several large specimens were observed: they have an identical ultrastructure to *W. britannica* holotype, but their coccolith maximum diameter is always greater than 9 µm. Those specimens were systematically separated and are

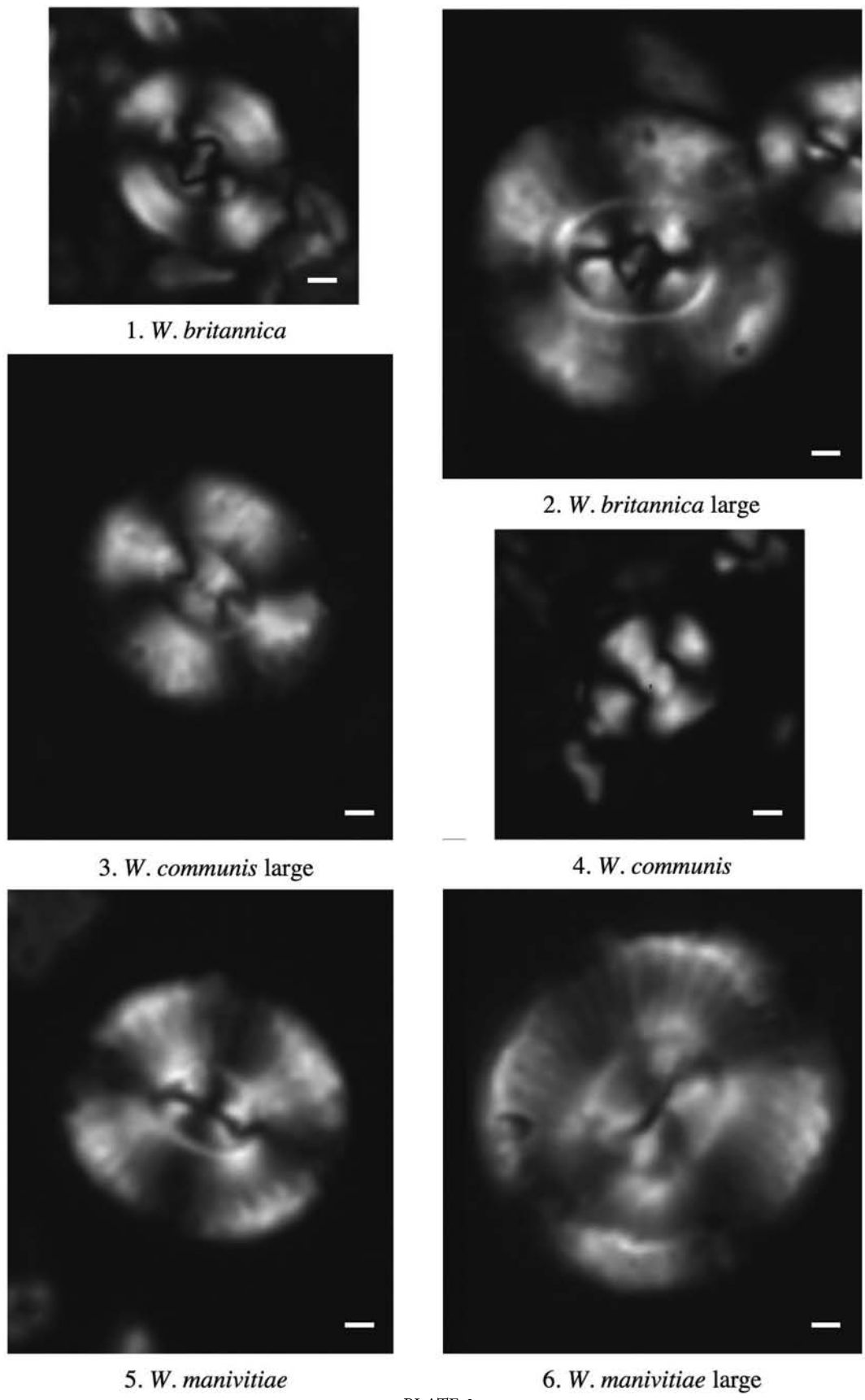
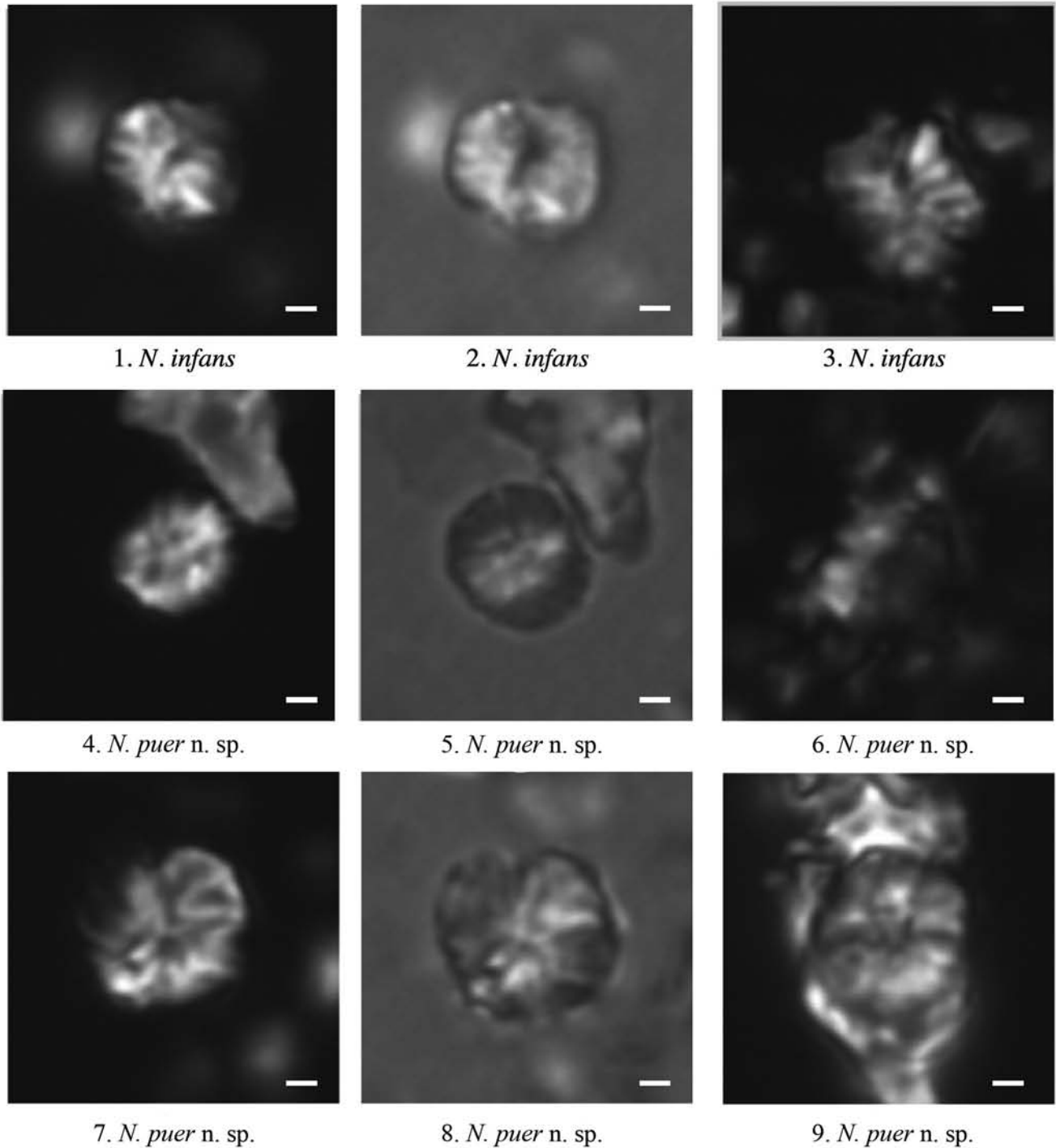


PLATE 2

Scale bar represents 1 µm.

Fig. 1 - *W. britannica*, cross-polarized light, Foza A 9.60, smear slide. Fig. 2 - *W. britannica* large, cross-polarized light, DSDP Site 534 A 99-04;14-15, smear slide. Fig. 3 - *W. communis* large, cross-polarized light, DSDP Site 534 A 101-06;32-33, smear slide. Fig. 4 - *W. communis*, cross-polarized light, Foza A 14.15, smear slide. Fig. 5 - *W. manivitiae*, cross-polarized light, DSDP Site 534 A 99-01;93-94, smear slide. Fig. 6 - *W. manivitiae* large, cross-polarized light, DSDP Site 534 A 102-05;24-25, smear slide.





## PLATE 3

Scale bar represents 1  $\mu\text{m}$ .

Fig. 1 - *N. infans*, cross-polarized light, DSDP Site 534 A 93-04; 31-32, smear slide. Fig. 2 - *N. infans*, cross-polarized light, quartz lamina, DSDP Site 534 A 93-04; 31-32, smear slide. Fig. 3 - *N. infans*, cross-polarized light, Foza A 12.38, smear slide. Fig. 4 - *N. puer n. sp.*, cross-polarized light, DSDP Site 534 A 95-01; 9-10, smear slide. Fig. 5 - *N. puer n. sp.*, cross-polarized light, quartz lamina, DSDP Site 534 A 95-01; 9-10, smear slide. Fig. 6 - *N. puer n. sp.*, cross-polarized light, Torre de' Busi 21.25, smear slide. Fig. 7 - *N. puer n. sp.*, cross-polarized light, DSDP Site 534 A 93-01; 133-134, smear slide, holotype MPUM 10474. Fig. 8 - *N. puer n. sp.*, cross-polarized light, quartz lamina, DSDP Site 534 A 93-01; 133-134, smear slide, holotype MPUM 10474. Fig. 9 - *N. puer n. sp.*, cross-polarized light, Torre de' Busi 10.60 (J), smear slide.

reported as *W. britannica* large in the range charts (Appendix 2).

**Watznaueria communis** Reinhardt, 1964

Pl. 2, figs 3, 4

**Remarks.** In the studied sections along with normal size *W. communis* (Cobianchi et al. 1992), several large specimens displaying an identical ultrastructure to *W. communis* holotype, but greater size were observed. Those specimens are reported in the range charts as *W. communis* large.

**Watznaueria manivittiae** (Bukry, 1973) Moshkovitz & Ehrlich, 1987

Pl. 2, figs 5, 6; Pl. 9, fig. 8

**Remarks.** In the studied sections several large specimens of *W. manivittiae* were observed and the ones with a size greater than 12 µm in length were systematically separated and reported as *W. manivittiae* large in the range charts (Appendix 2).

*Incertae sedis*

Family Nannoconacea Deflandre, 1959

Genus *Nannoconus* Kamptner, 1931

**Nannoconus puer** n. sp.

Pl. 3, figs 4-9; Pl. 9, fig. 4

**Origin of the name:** Named for its small size and primitive morphology.

**Holotype:** MPUM 10474; DSDP 534 A 93-01; 133-134, axial view, Pl. 3, fig. 7, 8.

**Repository:** Museo di Paleontologia Università degli Studi di Milano (MPUM), Dipartimento di Scienze della Terra "A. Desio", Milano, Italy.

**Description.** Very small and primitive nannocoid with a subcircular to slightly squared shape. This form has a large canal and narrow apical and basal apertures. The test thickness is usually comparable to the canal width; individual wedges outline are very difficult to be seen in the light microscope. Dimensions are less than 6 µm both in length and width, typically 4 µm on average.

**Comparison with related species.** It is distinguished from *N. infans* by its larger axial canal, and from *N. globulus minor* by its more symmetric nannolith morphology and its narrower canal. This species could be rare in smear slides since it is very small and delicate. It is one of the first (primitive) nannoconids to appear.

**Discussion.** This species is inferred being a precursor of *N. globulus minor*.

**Known range.** Late Tithonian (Tethyan Nannofossil Zone NJT 16; CM20N) - early Berriasian (Tethyan Nannofossil Zone NKT; CM18N).

**Nannoconus erbae** n. sp.

Pl. 4, figs 7-12

**Origin of the name:** Named after Prof. E. Erba for her major contribution to the Jurassic and Cretaceous paleoceanography.

**Holotype:** MPUM 10475; Torre de' Busi 12.80 (A), axial view, Pl. 4, fig. 12

**Repository:** Museo di Paleontologia Università degli Studi di Milano (MPUM), Dipartimento di Scienze della Terra "A. Desio", Milano, Italy.

**Description.** Small nannoconid with rectangular to elongate oval toward slightly conical outline. Adjacent walls are well defined and closely juxtaposed, individual wall wedges are not visible in the light microscope. The walls are thicker than other primitive forms (*N. infans*, *N. puer* and *N. globulus minor*), giving the nannolith a very distinctive soft aspect. This form has a slightly narrow canal and narrow apical and basal apertures.

**Comparison with related species.** It is distinguished from *N. infans* by its more elongated outline and larger nannolith size; from *N. wintereri* by its outline and narrow axial canal; from *N. steinmannii minor* by its less conical outline and smaller dimensions.

**Discussion.** This species is inferred being a precursor of *N. steinmannii minor*.

**Range.** Late Tithonian (Tethyan Nannofossil Zone NJT 16b-17a; CM19) - earliest Berriasian (Tethyan Nannofossil Zone NKT; CM18N).

Genus *Faviconus* Bralower in Bralower et al., 1989

**Faviconus multicolumnatus** Bralower

in Bralower et al., 1989

Pl. 6, figs 5-7; Pl. 7, figs 1, 2

**Remarks.** This species is originally described as an elongated nannolith characterized by numerous stacked wedges separated by thin axial canals. The columns may have very disorganized arrangements. Bralower et al. (1989) reported for every single element (one canal, two wedges stack) a dimension range of 6-12 µm in length and 4-6 µm in width. The authors also pointed out that earliest species are characterized by one canal and two wedge stacks, while later forms could have more, up to five wedge stacks. During this study several specimens were observed both in thin sections and simple smear slides: this species could reach greater

dimension than previously reported (Pl. 6, figs 5-7) and no systematic changing in the number of elements through time has been noticed. Since its appearance this species is characterized by numerous elements, sometimes randomly organized and rarely structured as semi-sphere (Pl. 7, figs 1-2). Each single element can reach dimension up to 15-18  $\mu\text{m}$  in length and 5  $\mu\text{m}$  in width (Pl. 6, fig. 7). Moreover, the aggregate (or spheres) can reach dimensions of 27-30  $\mu\text{m}$  (diameter). Such a huge dimensions and the nannolith ultrastructure arrangement in itself are believed to reduce the probability of finding entire and preserved specimens in smear slides, where this species has been always observed as broken pieces.

Family Polycyclolithaceae (Forchheimer, 1972)

Varol, 1992

Genus *Hexalithus* Gardet, 1955

***Hexalithus geometricus* n. sp.**

Pl. 8, figs 4-9

**Origin of the name:** Named after its linear, geometric margin.

**Holotype:** MPUM 10476; Torre de' Busi 3.25, Pl. 8, fig. 6

**Repository:** Museo di Paleontologia Università degli Studi di Milano (MPUM), Dipartimento di Scienze della Terra "A. Desio", Milano, Italy.

**Description.** Mono-lamellar, hexagonal nannolith composed of six distinct triangular elements juxtaposed one each other. The inter-element sutures of diametrically opposed elements are aligned. The external border of each element has no flare. At the optical microscope, using crossed nicols, each element has its own optical orientation, thus get extinct in different moment turning the microscope table. Diameter (measured as double apothem) is comprised between 4-8  $\mu\text{m}$ .

**Comparison with related species.** This form is distinguished from *H. noeliae* by the lack of flares at the end of each element; from *H. hexalithus* for its greater dimensions; from *H. magharensis* for its smaller dimensions. It is distinguished from *P. senaria* as the latter presents embriated elements, a concave outer margin and has a greater relief.

**Range.** Late Tithonian (Tethyan Nannofossil Zone NJT 17a; lower CM19N) - Berriasian.

#### Upper Jurassic Tethyan Nannofossil Zones

The calcareous nannofossil events detected in this study were calibrated with magnetostratigraphy, available for the studied sections (except for Monte Pernice) and spanning the CM22 to the lower part of CM17 (Channell et al. 2010). The correlations of some nanno-

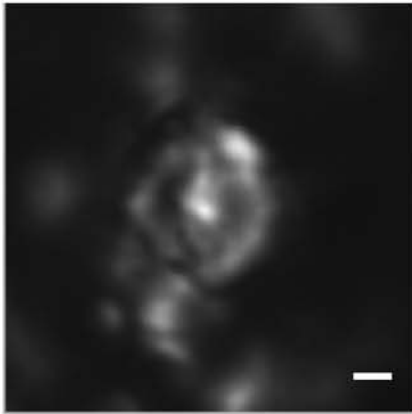
fossil events to polarity chrons are consistent among the studied sections (the FOs of *C. mexicana minor*, *N. steinmannii minor*, *N. kamptneri minor*), but the calibrations of several events indicate discrepancies among the different studied localities (Tab.1). The results of this study were also compared to the data collected by other Authors on land sections (Bralower et al. 1989; Michalík et al. 2009) and on the DSDP Site 534 A from Central Atlantic Ocean (Bralower et al. 1989). The data comparison (Fig. 15) point out additional discrepancies in the calibration of bioevents (FOs) with the Tithonian polarity chron sequence. The majority of the calcareous nannofossil FOs recognized in this study occurs systematically at older stratigraphic levels than reported by previous Authors, even when the same stratigraphic section was analyzed, as for Foza section and DSDP Site 534 A (Bralower et al. 1989 and this study, Fig. 14 and 15). In particular, data from Torre de' Busi display the older occurrences of most events. The discrepancies between Torre de' Busi and the Trento Plateau sections are possibly related to higher abundances and better preservation, along with a faster sedimentation rate with no gap allowing a better resolution in the Lombardian Basin. Calcareous nannofossil results from Torre de' Busi show much more similarities with the ones from DSDP Site 534 A, nevertheless some bioevents still display diachronism when compared (Fig. 15), possibly a consequence of the different resolution of biostratigraphic investigations (one sample every 10-20 cm *circa* at Torre de' Busi; one sample every 1-1.5 m *circa* at DSDP Site 534 A, both Bralower et al. 1989 and this study) as well as differences in the paleoceanographic settings.

The aim of this study is to select a succession of calcareous nannofossil bioevents useful for poorly pre-

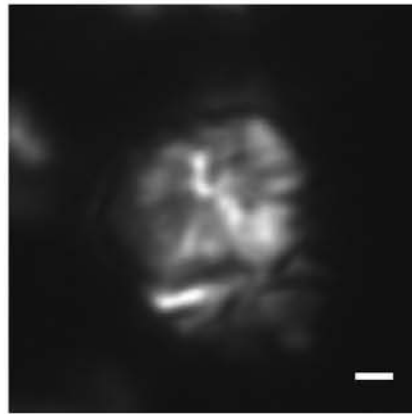
#### PLATE 4

Scale bar represents 1  $\mu\text{m}$ .

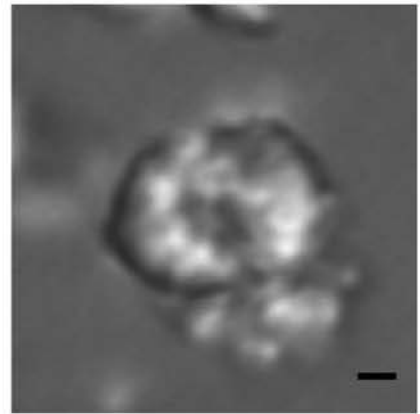
Fig. 1 - *N. globulus minor*, cross-polarized light, Torre de Busi 10.40 (K), smear slide. Fig. 2 - *N. globulus minor*, cross-polarized light, DSDP Site 534 A 91-06; 17-18, smear slide. Fig. 3 - *N. globulus minor*, cross-polarized light, quartz lamina, DSDP Site 534 A 91-06; 17-18, smear slide. Fig. 4 - *N. globulus minor*, cross-polarized light, Torre de' Busi 9.35 (Q), smear slide. Fig. 5 - *N. globulus minor*, cross-polarized light, Torre de' Busi 11.25 (G), smear slide. Fig. 6 - *N. globulus minor*, cross-polarized light, Torre de' Busi 4.46, smear slide. Fig. 7 - *N. erbae* n. sp., cross-polarized light, Torre de' Busi 12.80 (A), smear slide. Fig. 8 - *N. erbae* n. sp., cross-polarized light, quartz lamina, DSDP Site 534 A 91-06; 17-18, smear slide. Fig. 9 - *N. erbae* n. sp., cross-polarized light, quartz lamina, DSDP Site 534 A 91-06; 17-18, smear slide. Fig. 10 - *N. erbae* n. sp., cross-polarized light, DSDP Site 534 A 92-01;12-13, smear slide. Fig. 11 - *N. erbae* n. sp., cross-polarized light, quartz lamina, DSDP Site 534 A 92-01;12-13, smear slide. Fig. 12 - *N. erbae* n. sp., cross-polarized light, Torre de' Busi 12.80 (A), smear slide, holotype MPUM 10475.



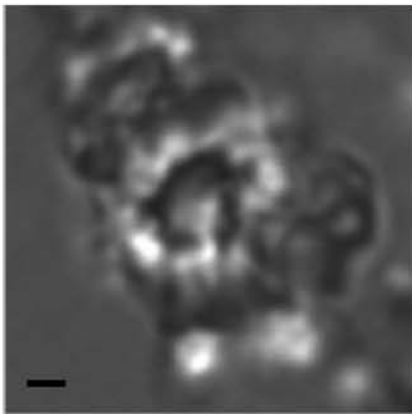
1. *N. globulus minor*



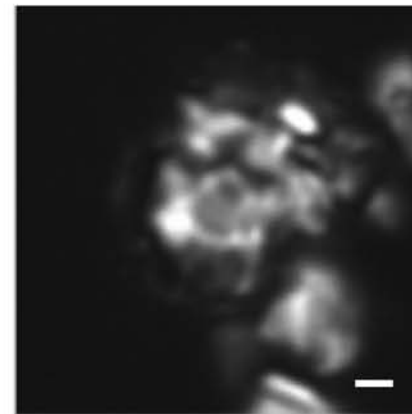
2. *N. globulus minor*



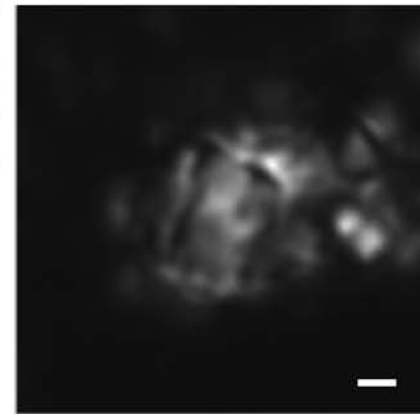
3. *N. globulus minor*



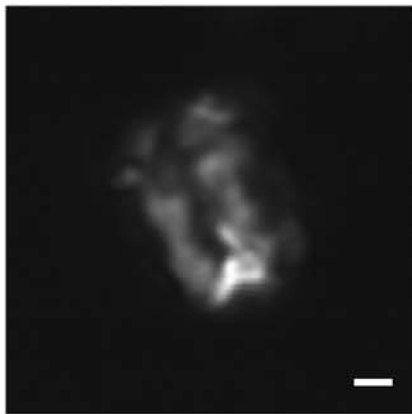
4. *N. globulus minor*



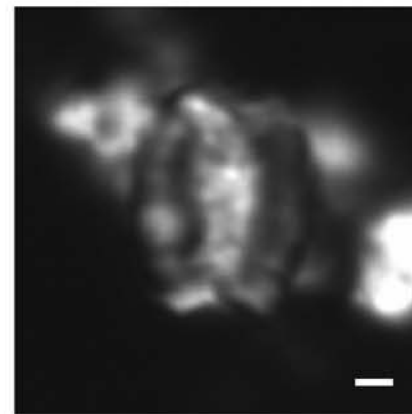
5. *N. globulus minor*



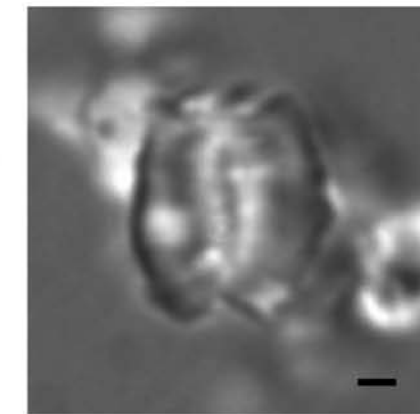
6. *N. globulus minor*



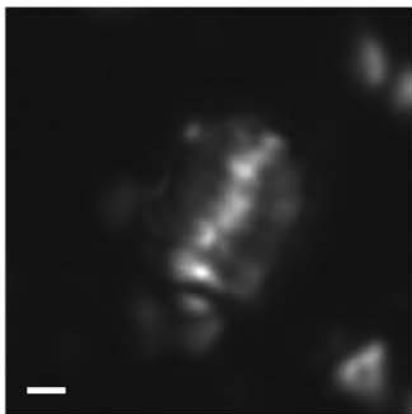
7. *N. erbae* n. sp.



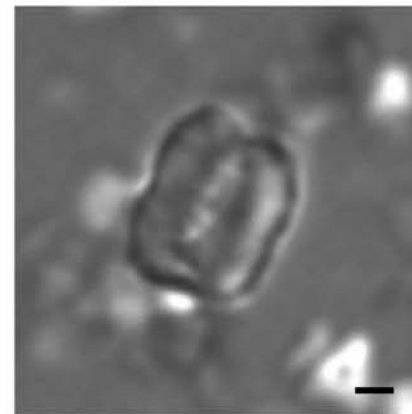
8. *N. erbae* n. sp.



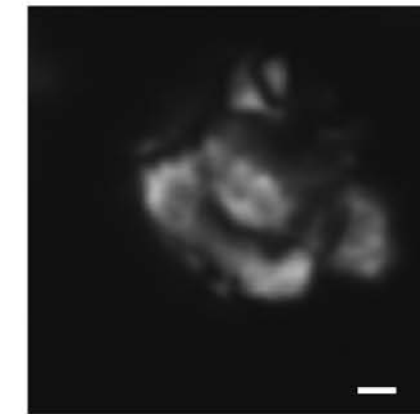
9. *N. erbae* n. sp.



10. *N. erbae* n. sp.



11. *N. erbae* n. sp.



12. *N. erbae* n. sp.

served land sections: for the reason exposed above the results from Torre de' Busi have been eventually considered referential for the uppermost Kimmeridgian-lowermost Berriasian time interval.

A synthesis of nannofossil events recognized in this work is presented in Table 1, where FOs and LOs are calibrated with magnetostratigraphy. These results were used to revise previous biostratigraphic schemes (Bralower et al. 1989; De Kaenel et al. 1996) and propose a Tethyan calcareous nannofossil zonation for the uppermost Callovian-lower Berriasian interval (Fig. 16). The proposed scheme consists of a succession of zones and subzones, whose boundaries are defined on individual biostratigraphic events, often FO of taxonomically distinctive and dissolution-resistant forms that should be broadly recognizable and replicable in the majority of the sections. Zones and subzones are characterized by secondary biostratigraphic events as well, considered less important, less accurately determinable or not recognizable in every section. A sequence of thirteen main events (eleven FOs and two LOs) is proposed for the uppermost Callovian-lowermost Berriasian interval. These events are mainly based on diagenesis-resistant taxa that were recognized in all the studied sections and thus are virtually easy to be recognized even in diagenetically altered material. A further sequence of eighteen secondary events (seventeen FOs and one LOs) is proposed, based on taxa displaying delicate and/or few peculiar features and/or lower abundance. Thirteen additional events (seven FOs and six LOs) require further investigations to be stratigraphically better constrained as they are rare or occur only sporadically in the studied sections. To be consistent with previous Lower-Middle Jurassic biostratigraphic scheme after Mattioli & Erba (1999) the same code of Tethyan Jurassic biozonation is adopted, therefore the lower zone in this study is NJT 12, subsequent to the *W. barnesiae* NJT 11 Zone of Bathonian age.

#### Description of Upper Jurassic Tethyan Nannofossil Zones

##### NJT 12 Zone

**Author:** Defined here.

**Definition:** Total range of *Cyclagelosphaera wiedmannii*.

**Range:** uppermost Bathonian-Callovian/Oxfordian boundary.

**Reference Section:** This interval has been observed at Bombatierle and Sciapala quarries and Foza section (Trento Plateau). Only the upper part of NJT 12 Zone was detected since the FO of *C. wiedmannii* was not observed.

**Remarks:** The uppermost part of this zone in the studied sections is also characterized by the LO of *A. helvetica*.

This zone is correlatable to the uppermost part of Boreal nannofossil zone NJ11, zones NJ12 and NJ13 to the lowermost part of NJ14 (Bown et al. 1988; Bown & Cooper 1998). Further studies are needed to better constrain the entire zone, which might register further bioevents as reported by other authors (Bown et al. 1988; De Kaenel et al. 1996; Bown & Cooper 1998; Cobianchi 2002).

**Associated species:** *W. barnesiae*, *W. britannica*, *W. britannica* large, *W. communis*, *W. fossacincta*, *W. manivittiae*, *W. manivittiae* large, *C. margerelii*, *D. lehmannii*, *L. hauffii*, *L. sigillatus*, *L. crucicentralis*, *C. perforata*, *Z. erectus*.

##### NJT 13 Zone

**Author:** Defined here.

**Definition:** From the last occurrence of *Cyclagelosphaera wiedmannii* to the first occurrence of *Favicolinus multicolumnatus*.

**Range:** Callovian/Oxfordian boundary-uppermost Oxfordian.

**Reference Sections:** This interval has been observed at Bombatierle and Sciapala quarries, and Foza section (Trento Plateau).

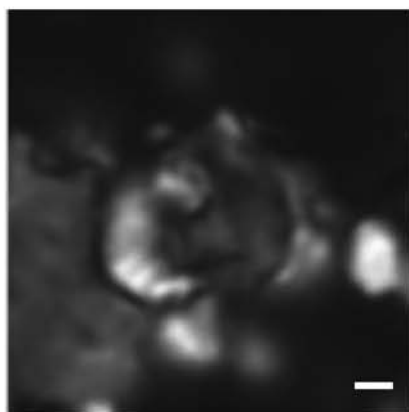
**Remarks:** This interval is also characterized by the LO *L. sigillatus* and the FO of *M. quadratus*.

This zone should correlate the lower part of *V. stradneri* Zone NJ-19 (Bralower et al. 1989). The *V. stradneri* Zone is only applicable to Northern Europe and the Western North Atlantic, whereas it is not identified in the Tethyan sections because *V. stradneri* does not appear until the Berriasian (Thierstein 1973; Bralower et al. 1989). This zone also corresponds to the

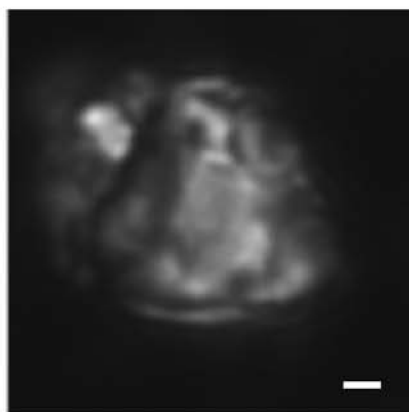
#### PLATE 5

Scale bar represents 1  $\mu$ m.

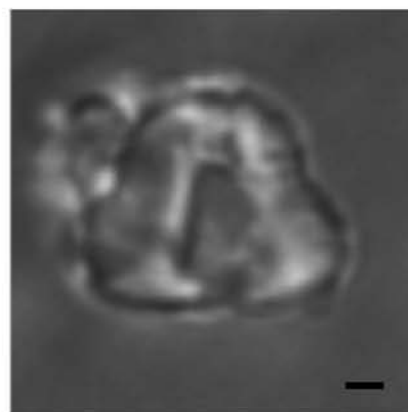
Fig. 1 - *N. wintereri*, cross-polarized light, Torre de' Busi 4.46, smear slide. Fig. 2 - *N. wintereri*, cross-polarized light, DSDP Site 534 A 88-06; 35-36, smear slide. Fig. 3 - *N. wintereri*, cross-polarized light, quartz lamina, DSDP Site 534 A 88-06; 35-36, smear slide. Fig. 4 - *N. wintereri*, cross-polarized light, Torre de' Busi 4.90, smear slide. Fig. 5 - *N. globulus globulus*, cross-polarized light, Foza A 10.52, smear slide. Fig. 6 - *N. globulus globulus*, cross-polarized light, Foza B 63.20, smear slide. Fig. 7 - *N. globulus globulus*, cross-polarized light, DSDP Site 534 A 92-04; 37-38, smear slide. Fig. 8 - *N. globulus globulus*, cross-polarized light, quartz lamina, DSDP Site 534 A 92-04; 37-38, smear slide. Fig. 9 - *N. kamptneri minor*, cross-polarized light, Foza B 50.50, smear slide. Fig. 10 - *N. steinmannii minor*, cross-polarized light, Foza B 50.50, smear slide. Fig. 11 - *N. steinmannii minor*, cross-polarized light, Foza A 3.40, smear slide. Fig. 12 - *N. kamptneri minor*, cross-polarized light, Foza B 73.85, smear slide.



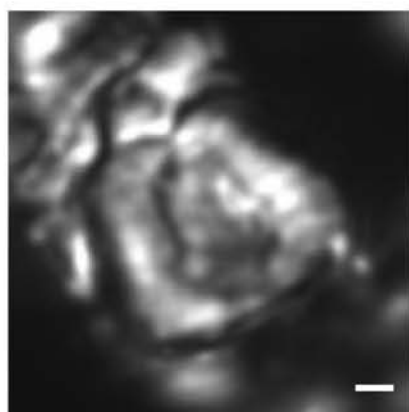
1. *N. wintereri*



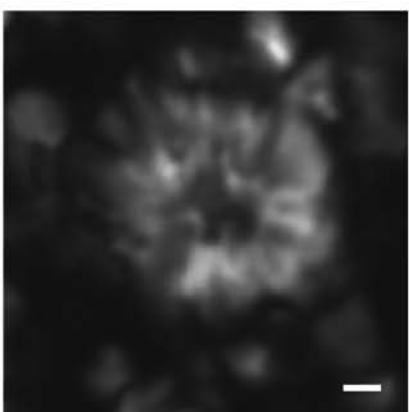
2. *N. wintereri*



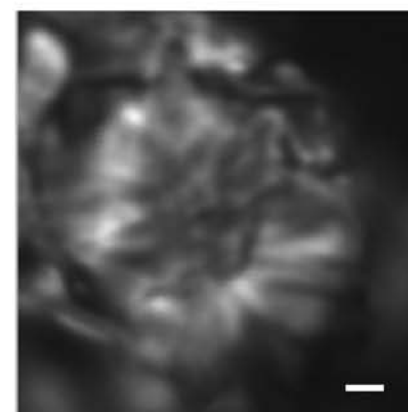
3. *N. wintereri*



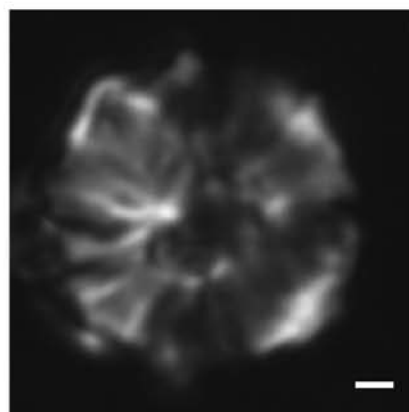
4. *N. wintereri*



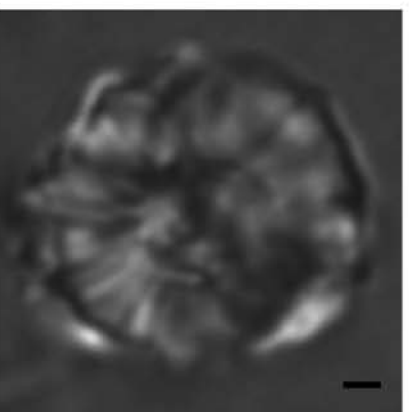
5. *N. globulus globulus*



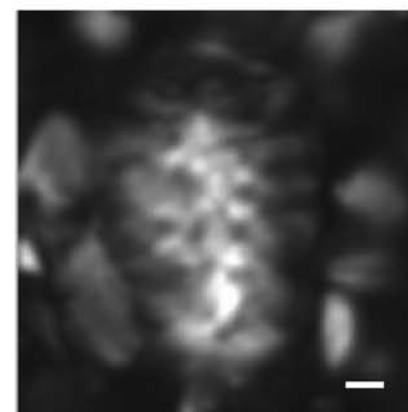
6. *N. globulus globulus*



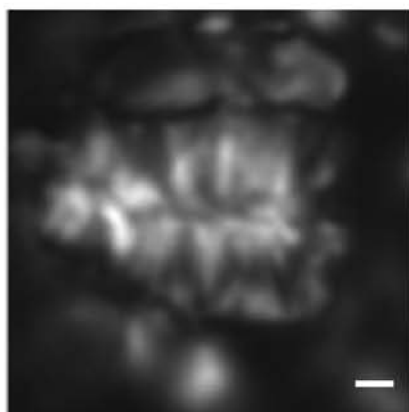
7. *N. globulus globulus*



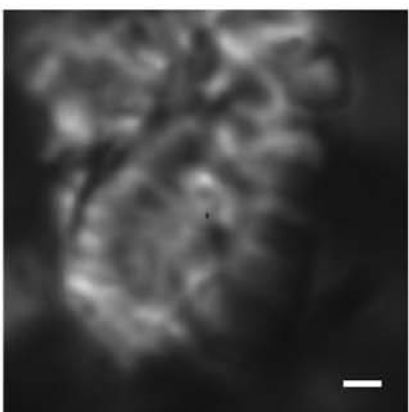
8. *N. globulus globulus*



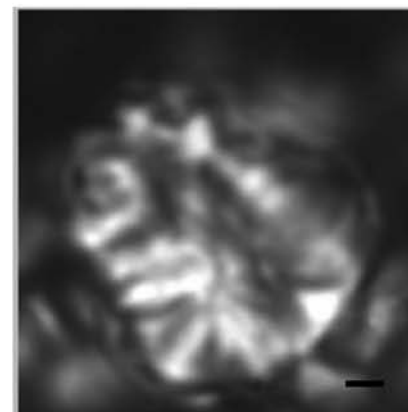
9. *N. kamptneri minor*



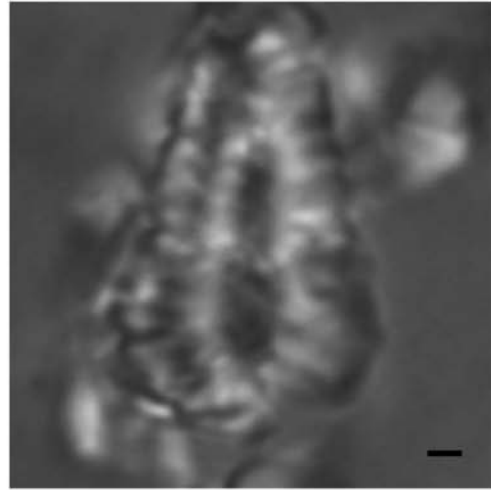
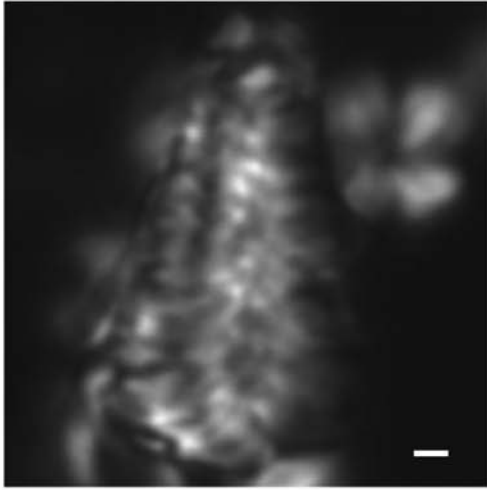
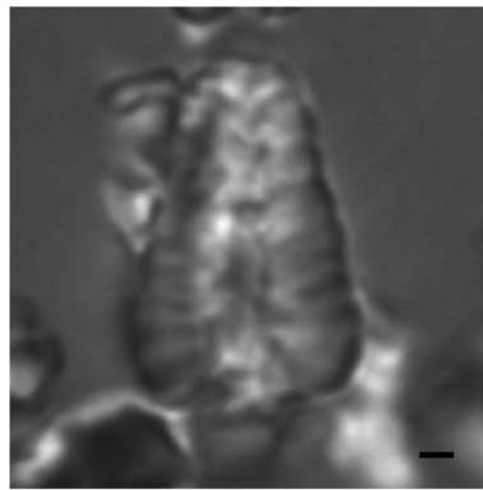
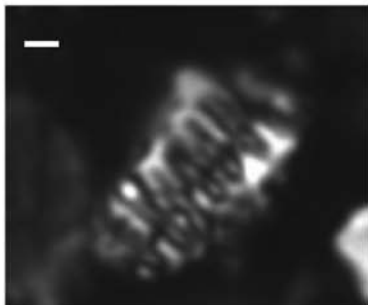
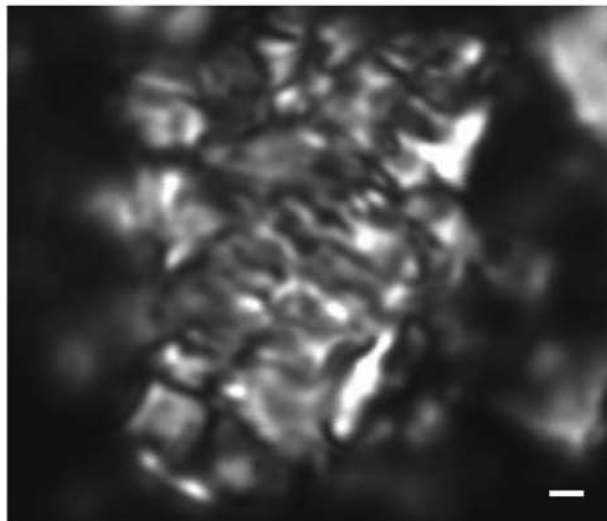
10. *N. steinmannii minor*



11. *N. steinmannii minor*



12. *N. kamptneri minor*

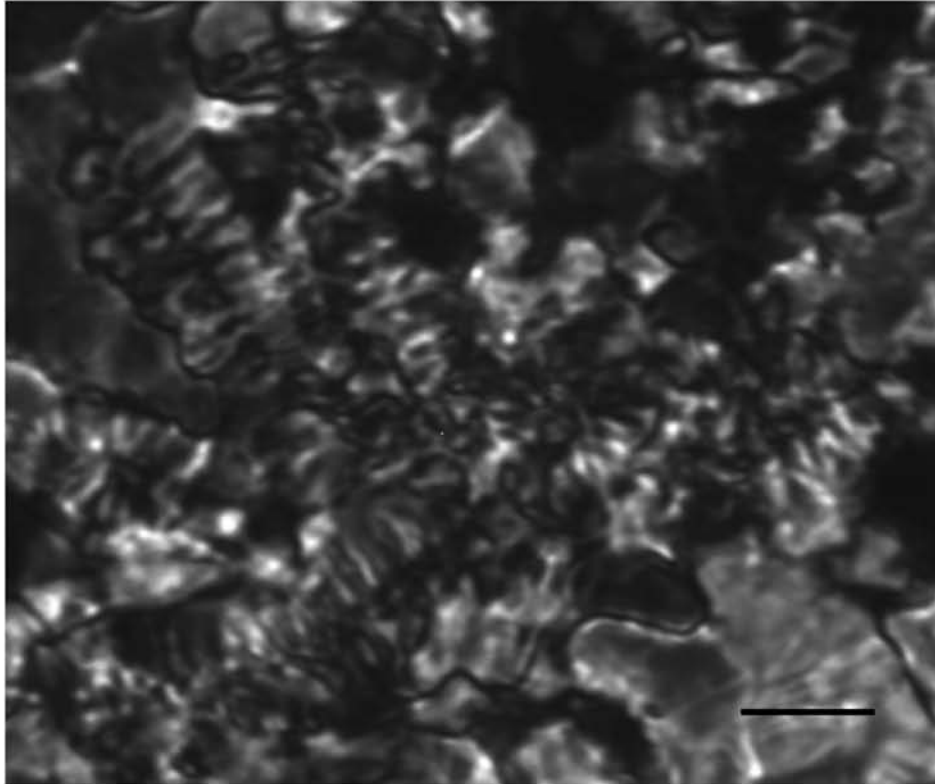
1-2. *N. steinmannii steinmannii*3-4. *N. kamptneri kamptneri*5. *F. multicolumnatus*6. *F. multicolumnatus*7. *F. multicolumnatus*

## PLATE 6

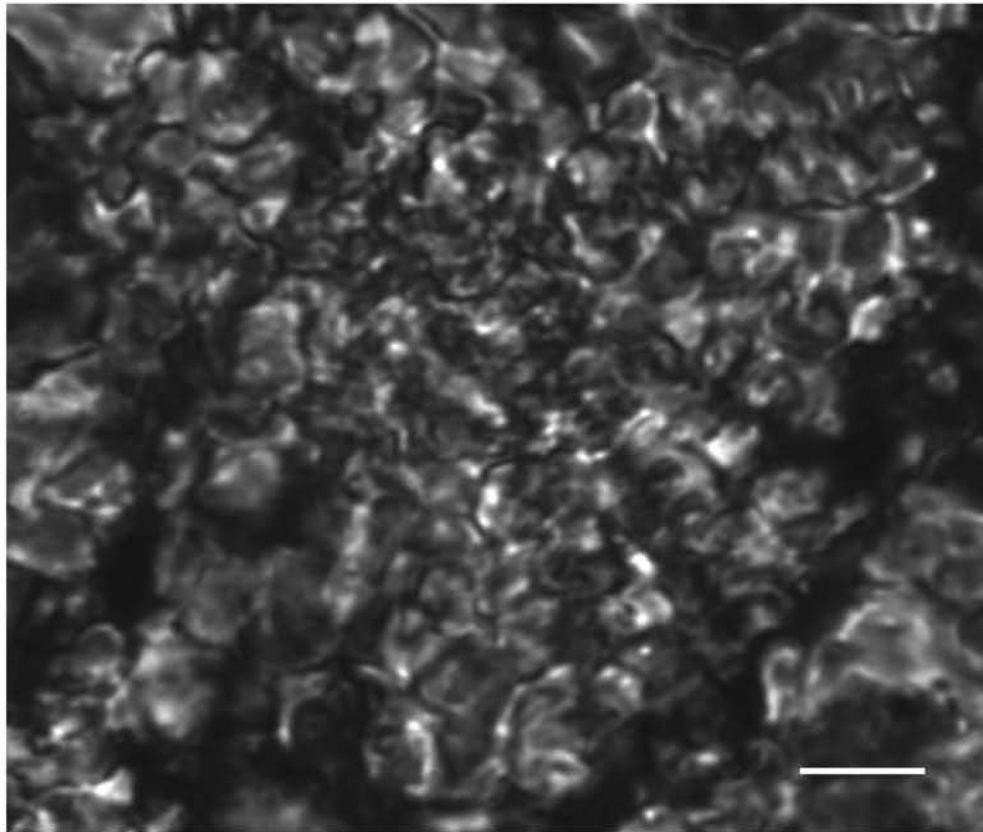
Scale bar represents 1  $\mu\text{m}$ .

Fig. 1 - *N. steinmannii steinmannii*, cross-polarized light, DSDP Site 534 A 87-03; 100-101, smear slide. Fig. 2 - *N. steinmannii steinmannii*, cross-polarized light, quartz lamina, DSDP Site 534 A 87-03; 100-101, smear slide. Fig. 3 - *N. kamptneri kamptneri*, cross-polarized light, DSDP Site 534 A 88-02;94-95, smear slide. Fig. 4 - *N. kamptneri kamptneri*, cross-polarized light, quartz lamina, DSDP Site 534 A 88-02;94-95, smear slide. Fig. 5 - *F. multicolumnatus*, cross-polarized light, DSDP Site 534 A 94-03;102-103, smear slide. Fig. 6 - *F. multicolumnatus*, cross-polarized light, Torre de' Busi 30.15, smear slide. Fig. 7 - *F. multicolumnatus*, cross-polarized light, Torre de' Busi 7.50, smear slide.





1. *F. multicolumnatus* aggregate



2. *F. multicolumnatus* aggregate

PLATE 7

Scale bar represents 5  $\mu\text{m}$ .

Fig. 1 - *F. multicolumnatus* aggregate, cross-polarized light, Torre de' Busi 45.35, ultra-thin section. Fig. 2 - *F. multicolumnatus* aggregate, cross-polarized light, Torre de' Busi 47.00, ultra-thin section.

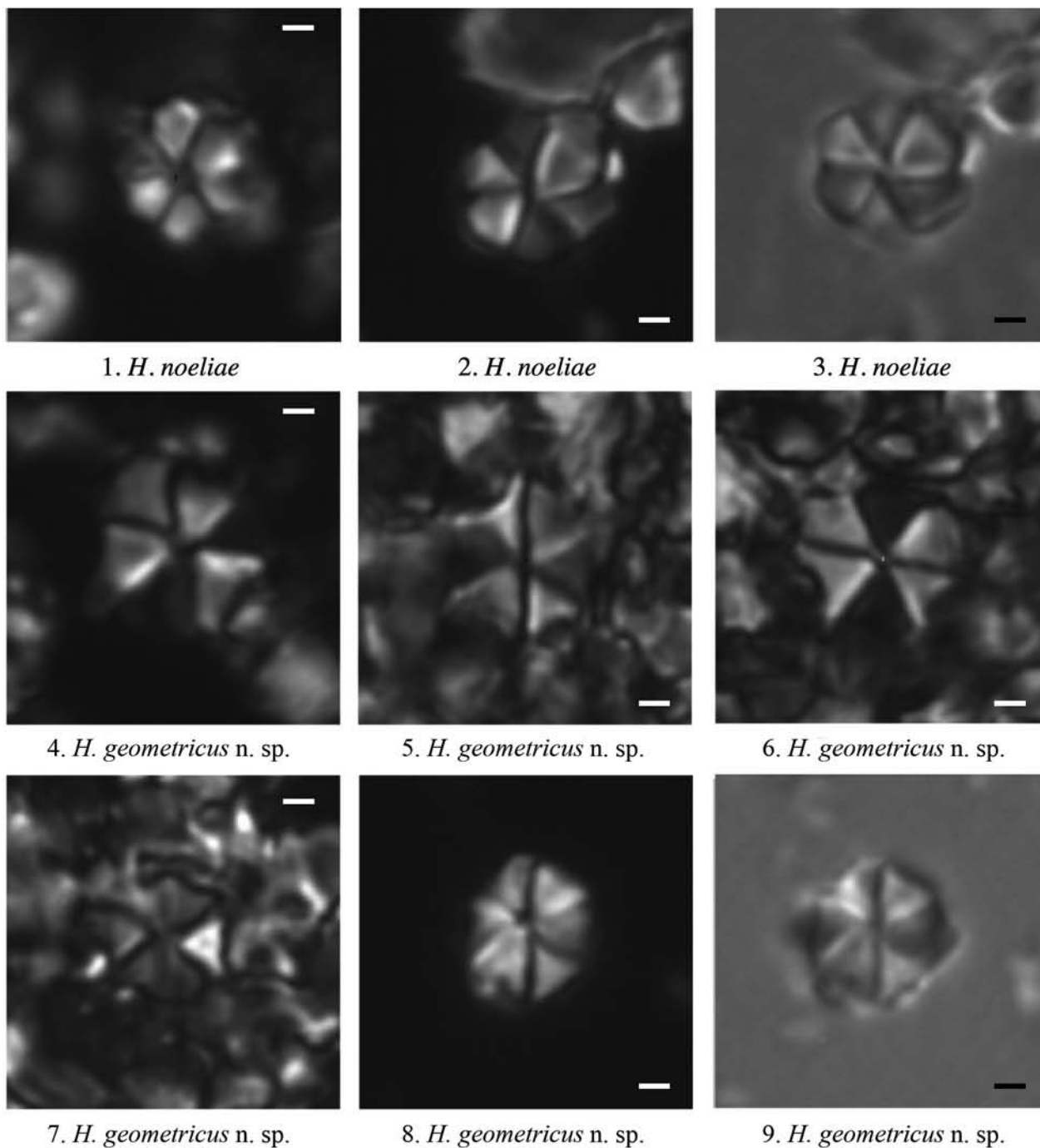


## PLATE 8

Scale bar represents 1  $\mu$ m.

Fig. 1 - *H. noeliae*, cross-polarized light, Torre de Busi 15.50, smear slide. Fig. 2 - *H. noeliae*, cross-polarized light, DSDP Site 534 A 91-06; 17-18, smear slide. Fig. 3 - *H. noeliae*, cross-polarized light, quartz lamina, DSDP Site 534 A 91-06; 17-18, smear slide. Fig. 4 - *H. geometricus* n. sp., cross-polarized light, Foza B 74.95, smear slide. Fig. 5, 6 - *H. geometricus* n. sp., cross-polarized light, Torre de' Busi 3.25, ultra-thin section, holotype MPUM 10476. Fig. 7 - *H. geometricus* n. sp., cross-polarized light, Torre de' Busi 11.17, smear slide. Fig. 8 - *H. geometricus* n. sp., cross-polarized light, DSDP Site 534 A 92-01; 12-13, smear slide. Fig. 9 - *H. geometricus* n. sp., cross-polarized light, quartz lamina, DSDP Site 534 A 92-01; 12-13, smear slide.

middle NJ14 and the lowermost part of NJ15b Boreal nannofossil Zone (Bown et al. 1988; Bown & Cooper 1998). De Kaenel et al. (1996) report the LO of *L. crucicentralis* before the LO of *L. sigillatus*, while *L. crucicentralis* disappears later in the Boreal Realm (Bown et al. 1988; Bown & Cooper 1998). Rare specimens of this species were observed in this study (Foza, Sciapala and Bombatierle), but further investigations are needed on additional sections to place unequivocally its LO. Cobianchi (2002) report in this interval the LO of *W. contracta* and suggests this bioevent may approximate the Oxfordian/Kimmeridgian boundary. No specimens of this species were observed in this study.

The FO of *F. multicolumnatus* could be used to approximate the Oxfordian/Kimmeridgian boundary, but further studies are needed to better calibrate this event with other stratigraphic tools.

**Associated species:** *W. barnesiae*, *W. britannica*, *W. britannica* large, *W. communis*, *W. fossacincta*, *W. manivittiae*, *W. manivittiae* large, *C. margerelii*, *D. lehmanii*, *L. hauffii*, *L. sigillatus*, *L. crucicentralis*, *C. perforata*, *Z. erectus*, *M. quadratus*.

#### NJT 13a Subzone

**Author:** Defined here.

**Definition:** From the last occurrence of *Cyclagelosphaera wiedmannii* to the last occurrence of *Lotharingius sigillatus*.

**Range:** Callovian/Oxfordian boundary-middle Oxfordian.

**Reference section:** This interval has been observed at Bombatierle and Sciapala quarries, and Foza section (Trento Plateau).

**Remarks:** Rare specimens of *L. crucicentralis* were recognized in one sample from Sciapala quarry.

This subzone correlates the NJ14 and the lower part of NJ15a Boreal nannofossil Zone (Bown et al. 1988; Bown & Cooper 1998).

#### NJT 13b Subzone

**Author:** Defined here.

**Definition:** From the last occurrence of *Lotharingius sigillatus* to the first occurrence of *Faviconus multicolumnatus*.

**Range:** middle Oxfordian-uppermost Oxfordian.

**Reference section:** This interval has been observed at Colme di Vignola and Foza sections and at Bombatierle and Sciapala quarries (Trento Plateau).

**Remarks:** This interval is characterized by the appearance of *M. quadratus* (Torre de' Busi, Colme di Vignola, Foza), which occurs before the appearance of *F. multicolumnatus*, as reported by De Kaenel et al. (1996) from Italy and South-East France. Nevertheless, *M. quadratus* was also observed slightly above the NJT 13b Subzone (Sciapala, Bombatierle, Frisoni). Specimens of *C. deflandrei* were observed in this Zone (Sciapala), before the appearance of *M. quadratus* (Torre de' Busi, Foza, Colme di Vignola), along with the appearance of *F. multicolumnatus* (Sciapala) or slightly after the FO of *F. multicolumnatus* (Bombatierle): for these reasons the event is not considered a marker in the zonation and further investigation are planned to better constrain it.

This subzone correlates with the lower part of the *V. stradneri* Zone (Bralower et al. 1989) and with the middle NJ15a to lowermost NJ15b Boreal nannofossil Zone (Bown et al. 1988; Bown & Cooper 1998).

#### NJT 14 Zone

**Author:** Defined here.

**Definition:** From the first occurrence of *Faviconus multicolumnatus* to the first occurrence of *Conusphaera mexicana minor*.

**Range:** uppermost Oxfordian-lower Tithonian.

**Reference sections:** This interval has been observed at Torre de' Busi (Lombardian Basin), Colme di Vignola and Foza sections, Bombatierle and Sciapala quarries (Trento Plateau).

**Remarks:** The lower Kimmeridgian is characterized by the LOs of *C. perforata* and *T. beaminsterense* according to De Kaenel et al. (1996). Rare specimens of these taxa were observed only in one sample from Bombatierle. Their distribution is strongly controlled by dissolution and investigation on more suitable material is needed to better constrain their occurrence: for this reason the events are not considered a marker in the zonation.

As reported by previous Authors (Thierstein 1976; Wind 1978; Roth 1983) *Z. erectus* clearly evolves into *Z. embergeri* increasing in shield size and thickness and changing the outline of the central bridge from lath-shaped to rhomboid. Bralower et al. (1989) discriminated the two species by the dimensions and the coccolith outlines, trying to minimize the number of transitional species belonging neither to *Z. erectus* nor to *Z. embergeri*. Nevertheless several morphotypes displaying intermediate features were recognized in this study. It is believed that these specimens might have a stratigraphic importance. For these two reasons a new species, *Z. fluxus*, grouping the morphotypes displaying transitional features, is described (see Systematic paleontology). The FO of this species is reported in this zone, but further analysis on more suitable material are needed to better constrain its stratigraphic significance: for this reason the event is not considered a marker in the zonation. The upper part of this zone is characterized by the appearance of *Z. embergeri* at Torre de' Busi section.

This interval correlates with the middle and upper part of the *V. stradneri* NJ-19 Zone (Bralower et al. 1989) and with the NJ15b to the lower part of NJ17a

Boreal nannofossil zones (Bown et al. 1988; Bown & Cooper 1998). The top of this interval correlates the upper part of CM22 (Channell et al. 2010).

**Associated species:** *W. barnesiae*, *W. britannica*, *W. britannica* large, *W. communis*, *W. communis* large, *W. fossacincta*, *W. manivittiae*, *W. manivittiae* large, *C. margerelii*, *C. tubulata*, *D. lehmanii*, *C. perforata*, *Z. erectus*, *Z. fluxus*, *M. quadratus*, *F. multicolumnatus*.

#### NJT 15 Zone

**Authors:** Thierstein (1975); revised by Bralower et al. (1989); revised in this paper on the basis of an older first occurrence of *M. chiastius*.

**Definition:** From the first occurrence of *Conusphaera mexicana minor* to the first occurrence of *Microstaurus chiastius*.

**Range:** lower Tithonian (upper CM22N-upper CM21N).

**Reference sections:** This interval has been observed at Torre de' Busi (Lombardian Basin) and Colma di Vignole, Foza, and Frisoni sections, Sciapala and Bombatierle quarries (Trento Plateau).

**Remarks:** The definition of this zone is slightly altered from the *C. mexicana* Zone NJ-19 of Bralower et al. (1989) on the base of an older FO of *M. chiastius* recognized in this study (Fig. 15). This interval is also characterized by the first occurrence of *C. mexicana mexicana* and *P. beckmannii*, both increasing in abundance and becoming the dominant taxa through this zone. At Torre de' Busi and Foza sections the FO of *C. riyadhensis* lies in this zone. At Sciapala and Foza the FO of *C. argoensis* was detected in the upper part of this zone. This interval is also characterized by the appearance of *Z. embergeri* at Foza, Bombatierle and Frisoni sections.

This interval correlates with the NJ17a Boreal nannofossil zones (Bown et al. 1988; Bown & Cooper 1998).

**Associated species:** The nannofossil assemblages is dominated by large morphotypes of ellipsoglobo-sphaerids and by the nannoliths *C. mexicana minor*, *C. mexicana mexicana* and *P. beckmannii*. Quantitative studies performed on ultra-thin sections at Torre de' Busi and Monte Pernice, as well as on DSDP Site 534 A (Casellato 2009) indicate that these nannolith taxa increase significantly in abundance, size and calcification degree gaining lithogenetic proportion (Nannofossil Calcification Event - NCE, Bornemann et al. 2003; NCE-1, Casellato 2009): the abundance acmes are reached in discrete steps in this zone and in the following one (NJT 16).

#### NJT 15a Subzone

**Author:** Roth et al. (1983); emended by Bralower et al. (1989); the upper boundary of this subzone is

revised in this study on the basis of older first occurrences of the marker bioevents.

**Definition:** From the first occurrence of *Conusphaera mexicana minor* to the first occurrence of *Polycostella beckmannii*.

**Range:** lower Tithonian (upper CM22N-base of CM21R).

**Remarks:** This interval is also characterized by the FO of *C. mexicana mexicana*. This subzone, originally defined by Roth et al. (1983), was emended by Bralower et al. (1989) who preferred to use the first occurrence of *P. beckmannii* instead of the last occurrence of *S. bigotii* to define the top, as the former taxa is more dissolution resistant and thus more reliable in land sections. In this study this zone has the same definition of the *H. cuvillieri* Subzone NJ-20a of Bralower et al. (1989), however the top is older as *P. beckmannii* appears earlier than reported by the latter authors.

This interval correlates with the NJ17a Boreal nannofossil zones (Bown et al. 1988; Bown & Cooper 1998).

#### NJT 15b Subzone

**Author:** Roth et al. (1983); emended by Bralower et al. (1989). The boundaries of this subzone are revised in this study on the basis of older first occurrences of the marker bioevents.

**Definition:** From the first occurrence of *Polycostella beckmannii* to the first occurrence of *Microstaurus chiastius*.

**Range:** lower Tithonian (base of CM21R-base of CM20).

**Remarks:** This subzone has the same definition of the *P. beckmannii* Subzone NJ-20b of Bralower et al. (1989), however its boundaries are older, as the FOs of *P. beckmannii* and *M. chiastius* where found significantly before that previously reported.

This interval correlates with the NJ17a Boreal nannofossil zones (Bown et al. 1988; Bown & Cooper 1998).

#### NJT 16 Zone

**Author:** Defined here

---

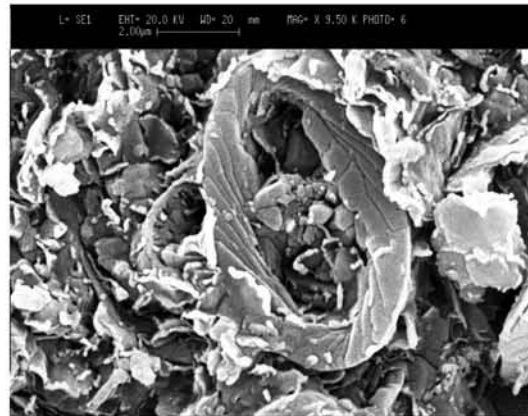
#### PLATE 9

Each picture has been taken using a Stereoscan Cambridge 360 scanning electron microscope. Scale bars are quoted on each picture.

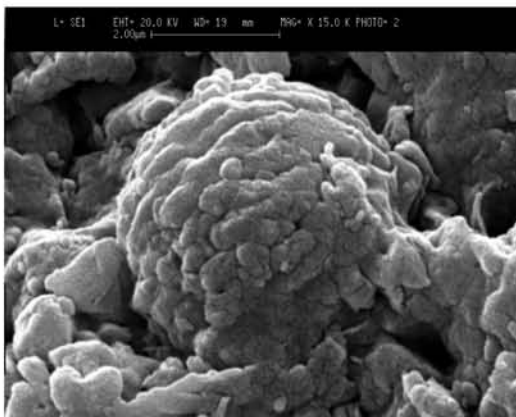
Fig. 1 - *Z. fluxus* n. sp., DSDP Site 534 A 102-05; 24-25. Fig. 2 - *Z. fluxus* n. sp., DSDP Site 534 A 101-02; 92-93. Fig. 3 - *N. infans* (?), DSDP Site 534 A 95-01; 9-10. Fig. 4 - *N. puer* n. sp., DSDP Site 534 A 95-01; 9-10. Fig. 5 - *N. globulus globulus*, DSDP Site 534 A 92-01; 12-13. Fig. 6 - *N. globulus globulus*, DSDP Site 534 A 92-03; 49-50. Fig. 7 - *N. wintereri*, DSDP Site 534 A 90-02; 22-23. Fig. 8 - *W. manivittiae* large, DSDP Site 534 A 97-01; 43-44.



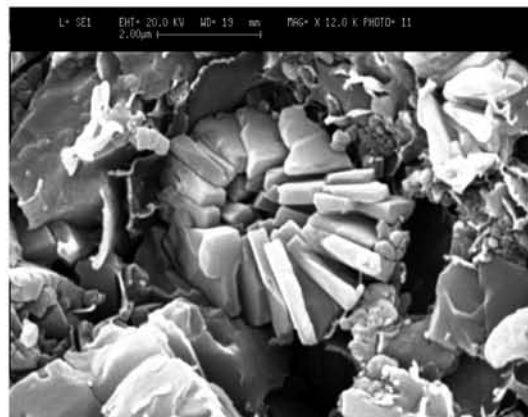
1. *Z. fluxus* n. sp.



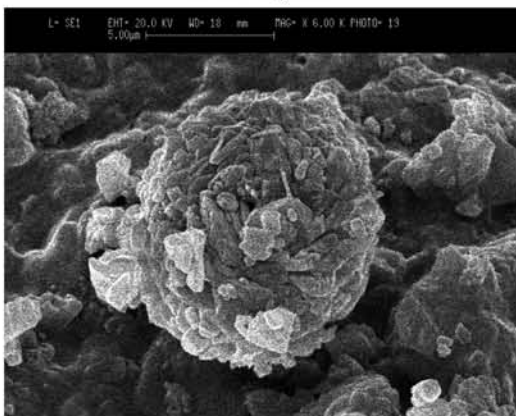
2. *Z. fluxus* n. sp.



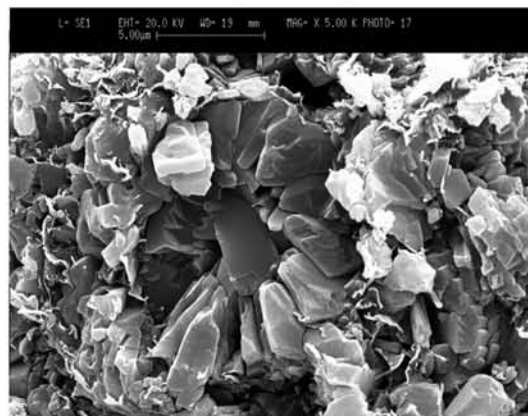
3. *N. infans*



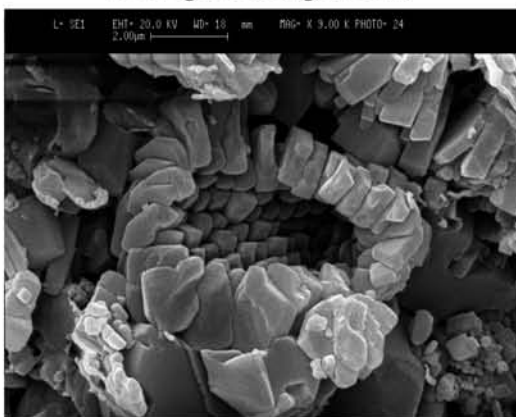
4. *N. puer* n. sp.



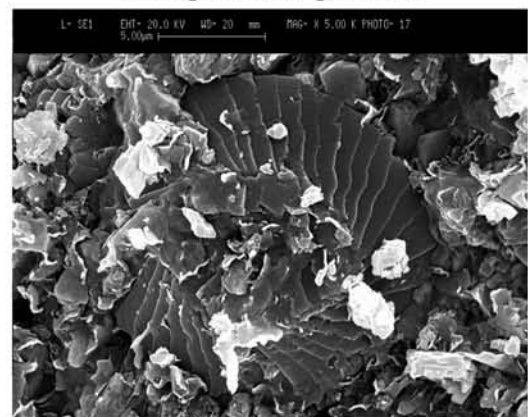
5. *N. globulus globulus*



6. *N. globulus globulus*



7. *N. wintereri*



8. *W. manivittiae* large

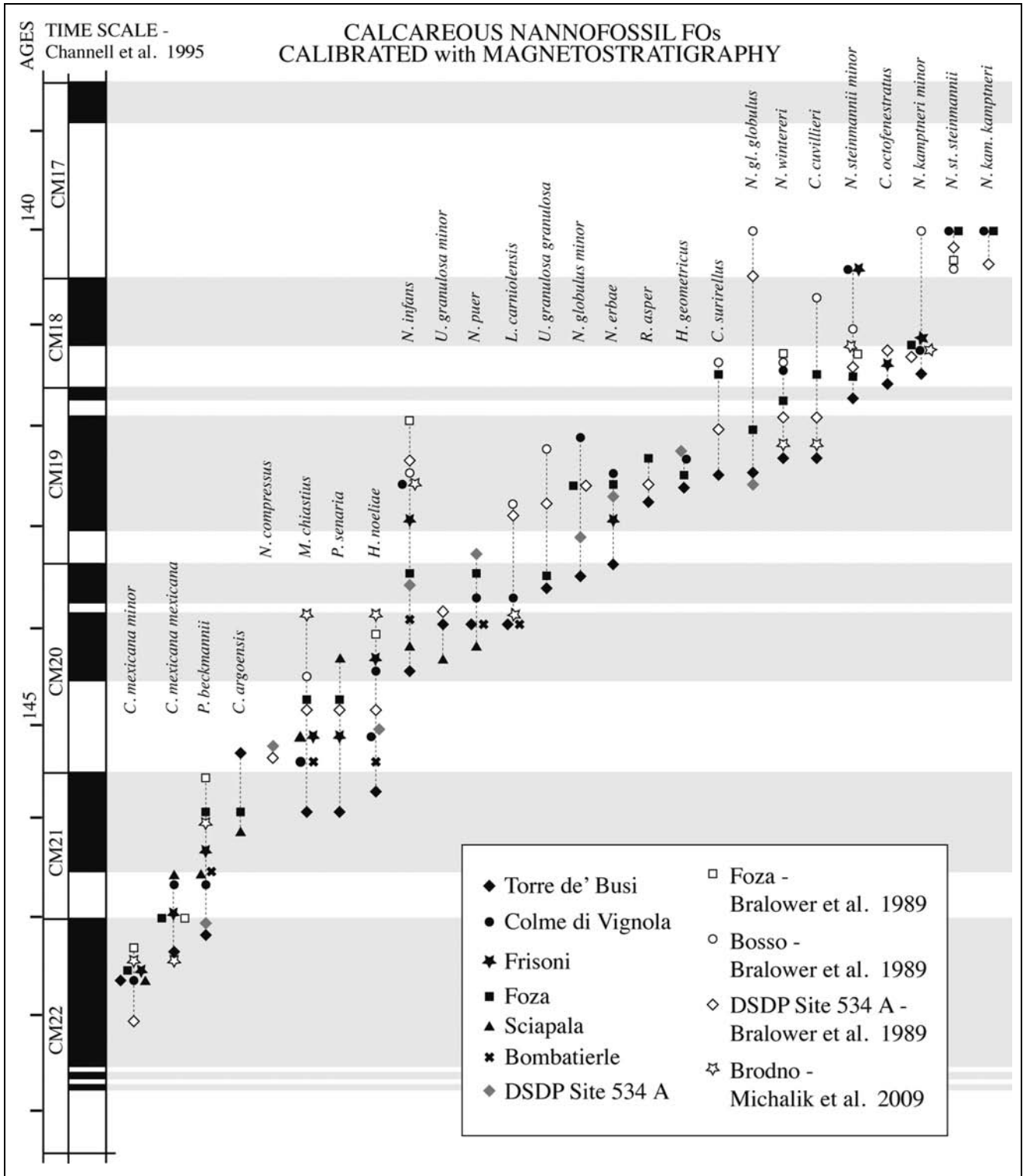


Fig. 15 - Calibration against time scale (Channell et al. 1995) of twenty-six bioevents (FOs only) recognized in each studied sections (full symbols). Some bioevents, previously detected and calibrated against magnetostratigraphy by previous Authors (Bralower et al. 1989 and Michalik et al. 2009) in other land sections and DSDP sites (empty symbols) are also plotted for comparison.

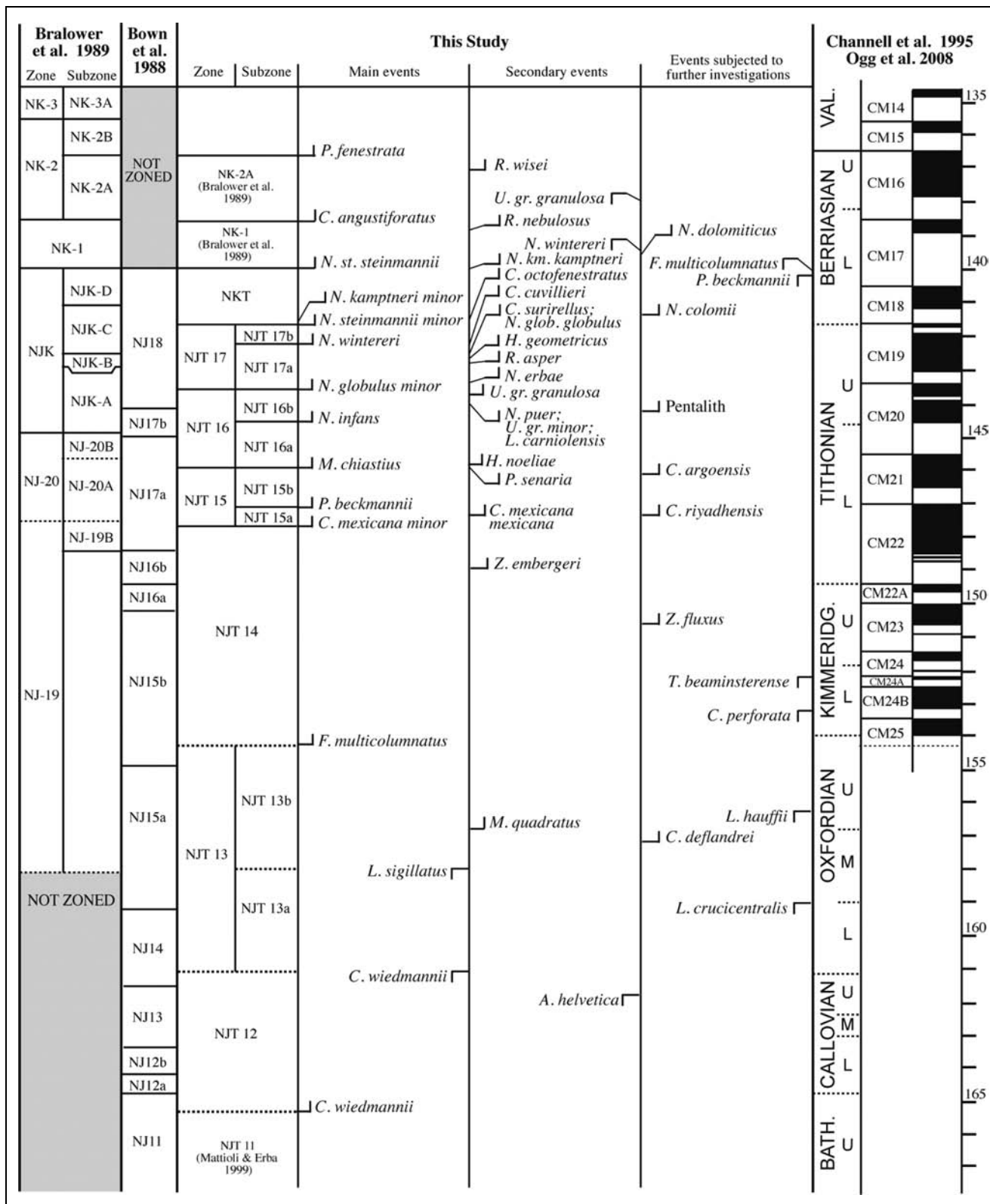


Fig. 16 - Upper Jurassic Tethyan Nannofossil Zonation proposed in this study. Note that only the species newly described or discussed in the paragraph on Systematic Palaeontology are reported in the plates. Other index taxa reported in the proposed zonation are exhaustively described and figured out by previous authors (Thierstein 1971; Thierstein 1976; Roth 1983; Bralower et al. 1989; Cobianchi et al. 1992; Reale & Monechi 1994; Mattioli & Erba 1999; Casellato 2009).



**Definition:** From the first occurrence of *Microstaurus chiastius* to the first occurrence of *Nannoconus globulus minor*.

**Range:** upper lower Tithonian-upper Tithonian (base of CM20-uppermost CM20N).

**Reference sections:** This interval has been observed at Torre de' Busi and Monte Pernice (Lombardian Basin), Colme di Vignola and Foza (Trento Plateau).

**Remarks:** This zone is essentially the same of the *H. noeliae* Subzone NJK-A of Bralower et al. (1989). However, its lower boundary is older, as the FOs of *M. chiastius* was found significantly before than what has been reported by Bralower et al. (1989). Originally the top of *H. noeliae* Subzone NJK-A was defined based on the FO of *U. granulosa granulosa*. Bralower et al. (1989) defined two subspecies of *U. granulosa*: a small one (*U. granulosa minor*) and a later, larger and dominant one (*U. granulosa granulosa*). The smaller subspecies was not distinguished in land material, and Bralower et al. (1989) paid attention to the fact that, if *U. granulosa* is unseparated, its range will result substantially different. Developing a high-resolution biostratigraphy on the studied sections, it was possible to distinguish the two subspecies, but a clear distinction was often hampered by poor preservation and overgrowth, that could bias the recognition of the real first occurrence of *U. granulosa granulosa*. Nevertheless, when undoubtedly detected, this event lies near the first occurrence on *N. globulus minor*. As the proposed zonation aims to be useful in poorly preserved land material, the latter event is preferred as it is easily identifiable and detectable even in poorly preserved material. Therefore, the NJK-A Subzone definition is here emended and elevated to a zone level, and the first occurrence of *U. granulosa granulosa* is considered an additional event useful in approximating this zone top.

The lowermost part of this interval is characterized by FOs of *P. senaria* and *H. noeliae*: these events lie very close to the first occurrence of *M. chiastius* and could be used as additional markers to approximate the base of this zone, as previously pointed out by Bralower et al. (1989).

This interval correlates the upper part of NJ17 and the base of NJ18 Boreal nannofossil zones (Bown et al. 1988; Bown & Cooper 1998).

**Associated species:** Ellipsagelosphaerids, *Z. erectus*, *Z. embergeri*, *Z. fluxus*, *C. mexicana mexicana*, *P. beckmannii*, *M. chiastius*, *H. noeliae*, *P. senaria*, *U. granulosa minor*, *C. argoensis*, *L. carniolensis*, primitive nannoconids.

#### NJT 16a Subzone

**Author:** Defined here

**Definition:** From the first occurrence of *Microstaurus chiastius* to the first occurrence of *Nannoconus infans*.

**Range:** upper lower Tithonian (upper CM21N-base of CM20N).

**Remarks:** This zone correlates with the *H. noeliae* Subzone NJK-A of Bralower et al. (1989), but has a shorter duration and older base boundary on the base of older FOs of *M. chiastius* and *N. infans* recognized in this study (Fig. 15).

No other events are reported within this subzone. The nannofossil assemblage is dominated by the nannolith genera *Polycostella* and *Conusphaera*, the latter showing pronounced abundance fluctuation during this interval upwards.

This interval correlates with the upper part of NJ17a and the lower part of NJ17b Boreal nannofossil zones (Bown et al. 1988; Bown & Cooper 1998).

#### NJT 16b Subzone

**Author:** Defined here

**Definition:** From the first occurrence of *Nannoconus infans* to the first occurrence of *Nannoconus globulus minor*.

**Range:** lower upper Tithonian (CM20N)

**Remarks:** This interval is characterized by the appearance of the primitive nannoconids *N. infans* and *N. puer*: these small species first occur close to the early/late Tithonian boundary evolving upwards and culminating in the appearance of *N. globulus minor*.

This interval is also characterized by the appearance of the murolith genus *Umbria*, the nannoliths genus *Lithraphidites* and of the primitive penthalits (mainly genus *Micrantholithus*).

This interval correlates with the upper part of NJ17b and the lowermost part of NJ18 Boreal nannofossil zones (Bown et al. 1988; Bown & Cooper 1998).

#### NJT 17 Zone

**Author:** Defined here.

**Definition:** From the first occurrence of *Nannoconus globulus minor* to the first occurrence of *Nannoconus steinmannii minor* and/or *Nannoconus kamptneri minor*.

**Range:** upper Tithonian to lowermost Berriasian (uppermost CM20N-lower CM18R).

**Reference section:** This interval has been observed at Torre de' Busi and Monte Pernice (Lombardian Basin), Colme di Vignola and Foza (Trento Plateau).

**Remarks:** This zone is correlatable with the uppermost part of *H. noeliae* Subzone NJK-A, the *U. granulosa granulosa* Subzone NJK-B and *R. laffittei* Subzone NJK-C of Bralower et al. (1989). *R. laffittei* is virtually absent in the investigated sections, while *U.*

*granulosa granulosa* is considered as a secondary event due to poor preservation and to a very gradual change from *U. granulosa minor* to *U. granulosa granulosa*. For these reasons the NJK-B and NJK-C subzones have been merged.

Several genera and species characterizing the Lower Cretaceous nannofloral associations appear in this interval: the FOs of *R. asper*, *C. surirellus* and *C. cuvillieri*, as well as the appearance of conical nannoconids, namely the FOs of *N. erbae*, *N. wintereri* and the FOs of *N. steinmannii minor* and *N. kamptneri minor* at the top of this zone. The FO of *H. geometricus*, is also reported from the middle part of this zone.

This zone correlates with the *U. granulosa granulosa* NJK-B and *R. laffitei* NJK-C subzones of Bralower et al. (1989) and with the NJ18 Boreal nannofossil zones of Bown et al. (1988) and Bown & Cooper (1998).

**Associated species:** The nannofossil assemblages of this zone are dominated by nannoconids that increase in abundance and dimensions upwards. Other components are the Ellipsagelosphaerids and *C. mexicana mexicana*. *Z. erectus*, *Z. embergeri*, *Z. fluxus*, *P. beckmannii*, *M. chiastius*, *H. noeliae*, *P. senaria*, *U. granulosa minor*, *C. argoensis*, *L. carniolensis*, *U. granulosa granulosa*, *R. asper*, *C. surirellus* and *C. cuvillieri* constitute just the smaller amount of the assemblages.

#### NJT 17a Subzone

**Author:** Defined here.

**Definition:** From the first occurrence of *Nannoconus globulus minor* to the first occurrence of *Nannoconus wintereri*.

**Range:** upper Tithonian (CM19R-upper CM19N).

**Remarks:** This subzone is correlatable with the uppermost part of *H. noeliae* Subzone NJK-A, the *U. granulosa granulosa* Subzone NJK-B and the lowermost part of *R. laffitei* Subzone NJK-C of Bralower et al. (1989).

This interval is characterized by the appearance of *N. erbae* and of *N. globulus globulus*, the latter occurring at a much older level compared to Brönnimann (1955), Deres & Achéritéguy (1980) and Bralower et al. (1989). The appearance of the genera *Cretarhabdus* and *Rhabdogiscus* is also observed within this subzone.

This zone correlates with the lower part of NJ18 Boreal nannofossil zones of Bown et al. (1988) and Bown & Cooper (1998).

#### NJT 17b Subzone

**Author:** Defined here.

**Definition:** From the first occurrence of *Nannoconus wintereri* to the first occurrence of *Nannoconus steinmannii minor* and/or *Nannoconus kamptneri minor*.

**Range:** Tithonian/Berriasian boundary interval (upper CM19N-lower CM18R).

**Remarks:** This subzone is characterized by a dramatic increase in abundance of nannoconids becoming the dominant component of the nannofossil association.

This zone correlates with the *R. laffitei* NJK-C Subzone of Bralower et al. (1989) and with the lower part of NJ18 Boreal nannofossil zones of Bown et al. (1988) and Bown & Cooper (1998).

#### NKT Zone

**Author:** Bralower et al. (1989). Re-named in this paper to be consistent with the proposed Zonation.

**Definition:** From the first occurrences of *Nannoconus steinmannii minor* and/or *Nannoconus kamptneri minor* to the first occurrence of *Nannoconus steinmannii steinmannii*.

**Range:** lowermost Berriasian (lower CM18R-lower CM17R).

**Reference section:** This interval has been observed at Colme di Vignola and Foza (Trento Plateau).

**Remarks:** The FOs of *N. steinmannii minor* and/or *N. kamptneri minor*, along with the base of CM18, were adopted in this study as markers in approximating the J/K boundary.

In few of the studied sections, the LOs of *P. beckmannii* and *F. multicolumnatus* and the FO of *N. colomii* were observed in this interval: the precise levels of these events are still to be identified and further investigations are needed.

This zone is also characterized by the FO of *C. octofenestratus*.

This zone corresponds to the upper part of NJ18 Boreal nannofossil zones of Bown et al. (1988) and Bown & Cooper (1998).

**Associated species:** The nannofossil assemblages of this zone are dominated by large nannoconids. Additional species are the Ellipsagelosphaerids, *C. mexicana mexicana*, *M. chiastius*, *H. noeliae*, *H. geometricus*, *P. senaria*, *L. carniolensis*, *U. granulosa granulosa*, *R. asper*, *C. surirellus*, *C. cuvillieri* and *C. octofenestratus*.

### Nannofossil bioevents and chronostratigraphy of the Callovian-Berriasian interval

Calcareous nannofossil bioevents maybe used to approximate stage boundaries, especially when detailed ammonite investigations are not available or are insufficient as in the studied sections. The Callovian/Oxfordian stage boundary can be approximated by the LO of *Cyclagelosphaera wiedmannii*, at least in the Tethyan Realm (Reale & Monechi 1994; Cobianchi 2002), whereas this bioevent is not used in the Boreal Realm (De Kaenel et al. 1996; Bown & Cooper 1998).

According to previous Authors (De Kaenel et al. 1996; Bown & Cooper 1998) the FO of *Faviconus multicolumnatus* is latest Oxfordian in age (uppermost part of *Bimammatum* Ammonite Zone after De Kaenel et al. 1996; *Rosenkrantzi* Ammonite Zone after Bown & Cooper 1998), while the LO of *C. perforata* is dated as earliest Kimmeridgian (De Kaenel et al. 1996). Consequently the Oxfordian/Kimmeridgian boundary can be placed between these two nannofossil bioevents.

The Kimmeridgian/Tithonian boundary is defined as the base of the *Hybonotum* Ammonite Zone and calibrated to the base of CM22AN (Ogg et al. 1984; Channell et al. 1995; Gradstein et al. 2004). The FO of *Conusphaera mexicana minor* is the calcareous nannofossil event falling within the upper part of *Hybonotum* Ammonite Zone (Carcabuey section, Spain, Bralower et al. 1989) and correlating the upper part of CM22N (DSDP Site 534 A, Bralower et al. 1989; Xausa section, Channell et al. 1987). To date, no nannofossil events approximate the Kimmeridgian/Tithonian boundary and the FO of *C. mexicana minor* can be used to identify an early Tithonian age. The definition of the Jurassic/Cretaceous boundary (Tithonian/Berriasian boundary) is subject to debate since 40 years. Faunal and floral endemism and paleoprovincialism (Tethyan, Boreal

realms) characterized the end of the Jurassic and the beginning of the Cretaceous, hampering an agreement on a practical, widely applicable marker that could act as a base for the Cretaceous (Remane et al. 1986; Remane 1991; Zakharov et al. 1996). The Jurassic/Cretaceous Working Group constituted by the International Subcommission on Cretaceous Stratigraphy (ISCS), has recently compiled a list of primary and secondary markers characterizing the J/K boundary interval (Wimbledon 2007; Wimbledon 2009; Wimbledon et al. submitted); among the others, the FOs of *N. steinmannii minor* and *N. kamptneri minor* and the base of Magnetic Chron 18R were indicated as primary workable markers useful to approximate the boundary.

## Conclusion

– The nannofossil assemblages from Tethyan land sections are dominated by dissolution resistant genera while fragile forms occur occasionally: for this reason the available biostratigraphic schemes were severely revised and alternative bioevents useful for poorly preserved land sections were pointed out.

– All nannofossil events were calibrated with magnetostratigraphy. A Tethyan calcareous nannofossil

EVENTS	Torre de' Busi		M. Pernice	Colme di Vignola		Foza A		Foza B		Sciapala		Bombatierle		Frisoni 1		Frisoni 2	
	meter	CM	meter	meter	CM	meter	CM	meter	CM	meter	CM	meter	CM	meter	CM	meter	CM
FO <i>P. fenestrata</i>						FO 3.05	...	FO 54.20	...								
FO <i>R. wisei</i>						FO 4.56	...	FO 66.10	16R(?)								
LO <i>U. gr. granulosa</i>						LO 9.60	17.9N	LO 68.95	16R								
FO <i>C. angustifloratus</i>						FO 10.05	17.7N	FO 69.90	17N								
FO <i>R. nebulosus</i>						FO 11.80	17.2N										
LO <i>N. wintereri</i>								LO 73.85	17.3R								
FO <i>N. dolomiticus</i>								FO 69.90	17N								
FO <i>N. km. kamptneri</i>						FO 15.20	17.4R	FO 74.95	17.3R								
FO <i>N. st. steinmannii</i>						FO 15.65	17.3R	FO 73.85	17.3R								
FO <i>N. colomii</i>						FO 15.65	17.3R	FO 73.85	17.3R								
LO <i>F. multicolumnatus</i>						FO 2.47	17R										
LO <i>P. beckmannii</i>						FO 2.99	17R										
FO <i>N. kamptneri minor</i>						FO 5.57	18.9R	FO 18.57	18.0N								
FO <i>N. octofenestratus</i>						(2.99)	(17R)	(15.20)	(17.4R)								
FO <i>N. steinmannii minor</i>						FO 4.94	17.1R	FO 18.16	18.2R								
FO <i>C. cuvillieri</i>						?	?	FO 18.16	18.3N								
FO <i>N. wintereri</i>						FO 5.97	18.5R	FO 20.27	19.9N								
FO <i>N. globulus globulus</i>								(LO 73.85)	(17.3R)								
FO <i>C. surirellus</i>						?	?	FO 20.87	19.7N								
FO <i>H. geometricus</i>						FO 7.04	19.5N	FO 18.16	18.3N								
FO <i>R. asper</i>						?	?	FO 22.00	19.5N								
FO <i>N. erbae</i>						FO 7.30	19.5N	FO 22.62	19.4N								
FO <i>N. globulus minor</i>						FO 7.04	19.8N	FO 22.62	19.4N								
FO <i>U. gr. granulosa</i>								FO 24.70	20.9N								
FO <i>L. carnioleensis</i>						FO 9.12	20.7N	(21.75)	(19.6N)								
FO <i>N. puer</i>						FO 9.12	20.7N	FO 24.70	20.9N								
FO <i>U. granulosa minor</i>						(8.30)		(23.17)	(19.3N)								
FO Pentoliths								(1.65)	...								
FO <i>N. infans</i>						FO 7.87	19.4N	FO 24.70	20.9N								
FO <i>M. favula</i>						?	?	(12.65)	(17.9R)								
FO <i>H. noelliae</i>						FO 10.52	20.4R	FO 23.66	19.1N								
FO <i>P. senaria</i>						(8.30)	(7.04)	(19.7N)									
FO <i>M. chiastius</i>						FO 10.87	20.1R	FO 27.05	20.8R								
FO <i>C. riyadhensis</i>								FO 32.22	22.8N								
FO <i>C. argoensis</i>						(7.52)	(19.5N)	FO 28.72	21.6N								
FO <i>P. beckmannii</i>						FO 12.76	21.7R	FO 28.72	21.6N								
FO <i>C. mex. mexicana</i>						FO 12.76	21.7R	FO 30.60	21.0R								
FO <i>C. mexicana minor</i>						FO 13.90	22N	FO 31.15	22.7N								
FO <i>Z. emberegeri</i>						(9.28)	(20.5N)	FO 28.72	21.6N								
FO <i>C. deflandrei</i>						from the base	...	FO 37.25	...								
LO <i>T. beaminsterense</i>																	
LO <i>C. perforata</i>																	
FO <i>F. multicolumnatus</i>						FO 15.14	...	FO 35.15	...								
FO <i>M. quadratus</i>						FO 15.93	...	FO 36.33	...								
LO <i>L. hauffii</i>						LO 16.18	...	LO 37.25	...								
LO <i>L. sigillatus</i>						LO 16.18	...	LO 38.00	...								
LO <i>L. crucicentralis</i>								?	?								
LO <i>C. wiedmannii</i>								LO 38.75	...								
LO <i>A. helvetica</i>								?	?								

Tab. 1 - Position of nannofossil events by meter level and within polarity zone, where polarity zone position is denoted by decimal from the base of each zone. The events in brackets are not true FOs or LOs, thus are not plotted on the corresponding figure.

zonation scheme is proposed for the uppermost Callovian-lower Berriasian interval. It consists of seven zones and eight subzones based on a total of thirty-five bioevents. The zones and subzones were defined on dissolution resistant taxa assuring highest reproducibility even in heavily diagenized sections. The proposed biostratigraphic scheme gives higher resolution than previous zonations, especially for the latest Callovian-Kimmeridgian interval, where no biozonation was available for the Tethyan Realm. The integration with the magnetostratigraphy points out that the majority of calcareous nannofossil events detected from the latest Kimmeridgian to earliest Berriasian occurs systematically at older stratigraphic levels than previously reported.

– A taxonomic revision was performed to unambiguously separate transitional forms and better delineate rapidly evolving groups. As a result the new species *Hexalithus geometricus* is defined in the upper Tithonian; also the evolution of *Zeugrhabdotus erectus* toward *Zeugrhabdotus embergeri* was quantitatively char-

acterized based on morphometric analyses and a new transitional species, *Zeugrhabdotus fluxus* is described. The early evolution of the genus *Nannoconus* was investigated in the Tethyan land sections and verified at DSDP Site 534 A from Central Atlantic Ocean: two new species of primitive nannoconids, *Nannoconus puer* and *Nannoconus erbae*, were described. The species *Nannoconus compressus* results to be endemic, occurring only in the Atlantic Ocean.

*Acknowledgments.* I am so much grateful to Elisabetta Erba for her teachings and stimulating discussions, for having introduced me to the intriguing world of micropaleontology.

Jörg Mutterlose and Jens Herrle provided valuable reviews of the manuscript and improved both the text and the English language. The thoughtful comments of Elisabetta Erba led to improvements in the whole manuscript.

This paper is one of the results of the author's PhD research, funded by "Progetto Giovani Promettenti", Università degli Studi di Milano, and by MIUR-COFIN 2005044839\_001 to I. Premoli Silva.

This research project used samples and data provided by the Ocean Drilling Program (ODP).

## REFERENCES

- Barrier E. & Vrielynck B. (2008) - Palaeotectonic maps of the Middle East. Tectono-Sedimentary-Palinspastic maps from Late Norian to Pliocene. *CCGM/CGMW*: 14 maps, Paris.
- Baumgartner P.O. (1987) - Age and genesis of the Tethyan Jurassic Radiolarite. *Ecl. Geol. Helv.*, 80(3): 831-879.
- Baumgartner P.O., Bernoulli D. & Martire L. (2001) - Mesozoic pelagic facies of the Southern Alps: Paleotectonics and paleoceanography. *IAS 2001 Davos, Field-trip Guide*, Excursion A1, Davos.
- Bernoulli D. (1964) - Zur Geologie des Monte Generoso (Lombardische Alpen). Ein Beitrag zur Kenntnis der sudalpinen Sedimente. *Beitr. Geol. Karte Schweiz*, 118: 134 pp.
- Bernoulli D. & Peters T. (1970) - Traces of rhyolitic-trachytic volcanism in the Upper Jurassic of Southern Alps. *Ecl. Geol. Helv.*, 67: 209-213.
- Bernoulli D. & Jenkyns H.C. (1974) - Alpine, Mediterranean and central Atlantic Mesozoic facies in relation to the early evolution of the Tethys. *SEPM special publication*, 19: 129-160.
- Bernoulli D., Caron C., Homewood P., Kälin O. & Stuijvenberg J.V. (1979) - Evolution of continental margin in the Alps. *Schweiz. Mineral. Petrogr. Mitt.*, 59: 165-170.
- Bornemann A., Aschwer U. & Mutterlose J. (2003) - The impact of calcareous nannofossils on the pelagic carbonate accumulation across the Jurassic-Cretaceous boundary. *Palaeogeogr., Palaeoclimatol., Palaeoecol.*, 199: 187-228.
- Bosellini A., Lobitzer H., Brandner R., Resch W. & Castellarin A. (1980) - The complex basin of the Calcareous Alps and Paleomargins. *Abh. Geol. B-A.*, 34: 287-325.
- Bown P.R. (1987) - Taxonomy, evolution and biostratigraphy of Late Triassic-Early Jurassic calcareous nannofossil. *Palaeont. Ass., Special pap. Paleont.*, 32: 118 pp.
- Bown P.R. (1992) - New calcareous nannofossil taxa from the Jurassic/Cretaceous boundary interval of sites 765 and 261, Argo Abyssal Plain. *Initial Reports of the Ocean Drilling Program, Scientific Results*, 123: 369-379.
- Bown P.R. & Cooper M.K.E. (1998) - Jurassic. In: Bown P.R. (Ed.) - *Calcareous nannofossil biostratigraphy*. Kluwer Academic Publishers: 34-85, Cambridge.
- Bown P.R., Cooper M.K.E. & Lord A.R. (1988) - A calcareous nannofossil biozonation scheme for the early to mid Mesozoic. *Newsl. Stratigr.*, 20: 91-114.
- Bralower T.J., Monechi S. & Thierstein H.R. (1989) - Calcareous nannofossils Zonation of the Jurassic-Cretaceous Boundary interval and correlations with the Geomagnetic Polarity Timescale. *Mar. Micropal.*, 14: 153-235.
- Brönnimann P. (1955) - Microfossil *incertae sedis* from the Upper Jurassic and Lower Cretaceous of Cuba. *Micropaleont.*, 1: 28-51.

- Casellato C.E. (2009) - Causes and consequences of calcareous nannoplankton evolution in the Late Jurassic: implications for biogeochronology, biocalcification and ocean chemistry. PhD thesis, Università degli Studi di Milano, 122 pp., Milano.
- Channell J.E.T. & Grandesso P. (1987) - A revised correlation of Mesozoic polarity chrons and calpionellid zones. *Earth Planet. Sci. Lett.*, 85: 222-240.
- Channell J.E.T., Bralower T.J. & Grandesso P. (1987) - Biostratigraphic correlation of Mesozoic polarity chrons CM1 to CM23 at Capriolo and Xausa (Southern Alps, Italy). *Earth Planet. Sci. Lett.*, 85: 203-221.
- Channell J.E.T., Massari F. & Benedetti A. (1990) - Magnetostratigraphy and biostratigraphy of Callovian-Oxfordian limestones from Trento plateau (Monte Lessini, Northern Italy). *Palaeogeogr., Palaeoclimatol., Palaeoecol.*, 79(3-4): 289-303.
- Channell J.E.T., Erba E., Nakanishi I. & Tamaki K. (1995) - Late Jurassic - Early Cretaceous time scales and oceanic magnetic anomaly block models. In: Berggren W.A., Kent D.V., Aubry M. & Hardenbol J. (Eds) - Geochronology, Time Scales and Global Stratigraphic Correlation, SEPM special publication, 54: 51-64, Tulsa.
- Channell J.E.T., Casellato C.E., Muttoni G. & Erba E. (2010) - Polarity and polar wander at the Jurassic/Cretaceous boundary in the Southern Alps, Italy. *Palaeogeogr., Palaeoclimatol., Palaeoecol.*, 293: 51-75.
- Cobianchi M. (2002) - I nannofossili calcarei del Giurassico Medio e Superiore del Bacino di Belluno (Alpi Calcareae Meridionali). *Atti Tic. Sci. Terra*, 43: 3-24.
- Cobianchi M., Erba E. & Pirini Radrizzani C. (1992) - Evolutionary trends of calcareous nannofossil genera *Lotharingius* and *Watznaueria* during the Early and Middle Jurassic. *Mem. Sc. Geol. Padova*, 43: 19-25.
- Cooper M.K.E. (1989) - Nannofossil provincialism in the Late Jurassic-Early Cretaceous (Kimmeridgian to Valanginian) period. In: Crux J.A. & van Heck S.E. (Eds) - Nannofossils and their Applications, Ellis Horwood: 223-246, Chichester.
- De Kaenel E., Bergen J.A. & Perch-Nielsen K. (1996) - Jurassic calcareous nannofossil biostratigraphy of Western Europe. Compilation of recent studies and calibration of bioevents. *Bull. Soc. géol. Fr.*, 167(1): 15-28.
- Deres F. & Achéritéguy J. (1980) - Biostratigraphie des Nannoconidés. *Bull. Cent. Rech. Explor.*, 4(1): 1-53.
- Dromart G., Garcia J.P., Gaumet F., Picard S., Rousseau M., Atrops F., Lecuyer C. & Sheppard S.M.F. (2003a) - Perturbation of the carbon cycle at the Middle/Late Jurassic transition: geological and geochemical evidences. *Am. J. Sci.*, 303: 667-707.
- Dromart G., Garcia J.P., Picard S., Atrops F., Lecuyer C. & Sheppard S.M.F. (2003b) - Ice age at the Middle-Late Jurassic transition? *Earth Planet. Sci. Lett.*, 213: 205-220.
- Erba E. (1990) - Upper Jurassic to Lower Cretaceous *Nannoconus* distribution in some sections from Northern and Central Italy. *Mem. Sci. Geol.*, 41: 255-261.
- Erba E. (2006) - The first 150 million years history of calcareous nannoplankton: Biosphere - Geosphere interaction. *Palaeogeogr., Palaeoclimatol., Palaeoecol.*, 232: 237-250.
- Erba E. & Quadrio B. (1987) - Biostratigrafia a Nannofossili calcarei, Calpionellidi e Foraminiferi planctonici della Maiolica (Titoniano superiore-Aptiano) nelle Prealpi Bergamasche (Italia settentrionale). *Riv. It. Paleont. Strat.*, 93(1): 3-108.
- Erba E. & Casellato C.E. (2010) - Paleocceanografia del Giurassico nella Tetide occidentale: l'archivio geologico del Bacino Lombardo. *Rendiconti dell'Istituto Lombardo, Accademia di Scienze e Lettere. Special Publication on "Una nuova Geologia per la Lombardia"*, 447: 115-140, Milano.
- Gradstein F.M., Ogg J.G. & Smith A.G. (2004) - A geologic time scale. V. of 589 pp. Cambridge University Press, Cambridge.
- Martire L. (1996) - Stratigraphy, facies and synsedimentary tectonics in the Jurassic Rosso Ammonitico Veronese (Altopiano di Asiago, NE Italy). *Facies*, 35: 209-236.
- Martire L., Clari P., Lozar F. & Pavia G. (2006) - The Rosso Ammonitico Veronese (Middle-Upper Jurassic of the Trento Plateau): a proposal of lithostratigraphic ordering and formalization. *Riv. It. Paleont. Strat.*, 112(2): 227-250.
- Mattioli E. & Erba E. (1999) - Synthesis of calcareous nannofossil events in tethyan Lower and Middle Jurassic successions. *Riv. It. Paleont. Strat.*, 105(3): 343-376.
- Michalík J., Reháková D., Halásová E. & Linterová O. (2009) - The Brodno section - a potential regional stratotype of the Jurassic/Cretaceous boundary (Western Carpathians). *Geologica Carpathica*, 60(3): 213-232.
- Mutterlose J. (1992) - Biostratigraphy and palaeobiogeography of Early Cretaceous calcareous nannofossils. *Cretaceous Res.*, 13, 167-189.
- Mutterlose J. & Kessels K. (2000) - Early Cretaceous calcareous nannofossils from High latitudes: implications for paleobiogeography and paleoclimate. *Palaeogeogr. Palaeoclimatol. Palaeoecol.*, 160(2): 347-372.
- Muttoni G., Erba E., Kent D., Bachtadse V. (2005) - Mesozoic Alpine facies deposition as a result of past latitudinal plate motion. *Nature*, 434: 59-63.
- Ogg J.G. (1981) - Sedimentology and paleomagnetism of Jurassic pelagic limestones: "Ammonitico Rosso" facies. Unpublished PhD thesis, Scripps Institution of Oceanography, University of California, 212 pp., San Diego.
- Ogg J.G., Steiner M.B., Oloriz F. & Tavera J.M. (1984) - Jurassic magnetostratigraphy, 1. Kimmeridgian-Tithonian of Sierra Gorda and Carcabuey, southern Spain. *Earth Planet. Sci. Lett.*, 71: 147-162.
- Ogg J.G., Ogg G. & Gradstein F. (2008) - The Concise Geologic Time Scale. V. of 177 pp. Cambridge University Press, Cambridge.
- Pasquarè G. (1965) - Il Giurassico Superiore nelle Prealpi Lombarde. *Mem. Riv. It. Paleont. Strat.*, XI: 237 pp.
- Perch-Nielsen K. (1985) - Mesozoic calcareous nannofossil. In: Bolli H.M., Saunders J.B., Perch-Nielsen K. (Eds)

- Plankton Stratigraphy. Cambridge University Press: 329-426, Cambridge.
- Reale V. & Monechi S. (1994) - *Cyclagelosphaera wiedmannii* new species, a marker for the Callovian. *J. Nanopl. Res.*, 16(3): 117-119.
- Remane J. (1991) - The Jurassic-Cretaceous boundary: problems of definition and procedure. *Cretaceous Res.*, 12: 447-453.
- Remane J., Borza K., Nagy I., Bakalova-Ivanova D., Knauer J., Pop G. & Tardi-Filácz E. (1986) - Agreement on the subdivision of the standard calpionellid zones defined at the 2nd Planktonic Conference, Roma 1970. *Acta Geol. Hung.*, 29: 4-14.
- Roth P.H. (1978) - Cretaceous nannoplankton biostratigraphy and oceanography of the northwestern Atlantic Ocean. *Initial Reports of the Deep Sea Drilling Project*, 44: 731-759.
- Roth P.H. (1983) - Jurassic and Lower Cretaceous calcareous nannofossil in the Western North Atlantic (Site 534): biostratigraphy, preservation and some observation on biogeography and paleoceanography. *Initial Reports of the Deep Sea Drilling Project*, 76: 587-621.
- Roth P.H. (1986) - Mesozoic paleoceanography of the North Atlantic and Tethys Oceans. In: Summerhays C.P. & Shackleton N.J. (Eds) - North Atlantic Paleogeography. *Geol. Soc., Spec. Pub.*, 26: 299-320, London.
- Roth P.H. (1989) - Ocean circulation and calcareous nannoplankton evolution during the Jurassic and Cretaceous. *Palaeogeogr., Palaeoclimatol., Palaeoecol.*, 74: 111-126.
- Roth P.H., Medd A.W. & Watkins D.H. (1983) - Jurassic calcareous nannofossils zonation, an overview with evidence from Deep Sea Drilling Project Site 534. *Initial Reports of the Deep Sea Drilling Project*, 76: 573-580.
- Street C. & Bown P.R. (2000) - Paleobiogeography of Early Cretaceous (Berriasian-Barremian) calcareous nannoplankton. *Mar. Micropal.*, 39: 265-291.
- Tavera J.M., Aguado R., Company M. & Oloriz F. (1994) - Integrated biostratigraphy of the Durangites and Jacobi zones (J/B boundary) at the Puerto Escaño section in Southern Spain (Province of Cordoba). *Geobios*, 17: 469-476.
- Thierstein H.R. (1971) - Tentative Lower Cretaceous calcareous nannoplankton biostratigraphy. *Ecl. Geol. Helv.*, 29: 1-52.
- Thierstein H.R. (1973) - Lower Cretaceous calcareous nannoplankton biostratigraphy. *Abb. Geol. Bundesanst.*, 29: 1-52.
- Thierstein H.R. (1975) - Calcareous nannoplankton biostratigraphy at the Jurassic-Cretaceous boundary. In: Colloqui sur la limite Jurassique-Crétacé, Lyon, Neuchâtel, Sept. 1973. *Mém. B.R.G.M.*, 86: 84-94.
- Thierstein H.R. (1976) - Mesozoic calcareous nannoplankton biostratigraphy of marine sediments. *Mar. Micropal.*, 1: 325-362.
- Trejo M. (1960) - La familia Nannoconidae y su alcance stratigrafico en America (Protozoa Inc. saed.). *Boll. Ass. Mex. Geol. Petrol.* 12: 259-314.
- Weissert H. & Erba E. (2004) - Volcanism, CO<sub>2</sub> and palaeoclimate: a Late Jurassic - Early Cretaceous carbon and oxygen isotope record. *Jour. Geol. Soc.*, 161: 1-8.
- Wimbledon W.A.P. (2007) - The Jurassic-Cretaceous boundary: an age-old correlative enigma. *Episodes*, 31: 423-428.
- Wimbledon W.A.P. (2009) - Fixing a basal Berriasian and J/K boundary. In: Hart M.B. (Ed.) - 8<sup>th</sup> International Symposium on the Cretaceous System, 6<sup>th</sup>-12<sup>th</sup> September, 2009, Abstract Volume: 196-198, Plymouth.
- Wimbledon W.A.P., Casellato C.E., Reháková D., Bulot L.G., Erba E., Gardin S., Verreussel R.M.C.H., Munsterman D.K. & Hunt C.O. (*submitted*) - Fixing a basal Berriasian and Jurassic/Cretaceous (J-K) boundary - perhaps there is some light at the end of the tunnel? *Riv. It. Paleont. Strat.*
- Wind F.H. (1978) - Western North Atlantic Upper Jurassic-Cretaceous calcareous nannofossil biostratigraphy. *Initial Reports of the Deep Sea Drilling Project*, 44: 761-773.
- Winterer E.L. (1998) - Paleobathymetry of Mediterranean Tethyan Jurassic pelagic sediments. *Mem. Soc. Geol. It.*, 53: 97-131.
- Winterer E.L. & Bosellini A. (1981) - Subsidence and sedimentation on Jurassic Passive Continental Margin, Southern Alps, Italy. *AAPG Bulletin*, 65: 394-421.
- Wise S.W. & Wind F.H. (1976) - Mesozoic and Cenozoic calcareous nannofossil recovered by Deep Sea Drilling Project Leg 36 drilling on the Falkland Plateau, Southwest Atlantic sector of the Southern Ocean. *Initial Reports of the Deep Sea Drilling Project*, 36: 269-492.
- Zakharov V., Bown P. & Rawson P.F. (1996) - The Berriasian Stage and the Jurassic-Cretaceous boundary. *Bull. Inst. Roy. Sciences Natur. Belgique - Proceedings of the "Second International Symposium on Cretaceous Stage Boundaries", Brussel 8-16 September 1995*, Vol. 66-Supplement: 7-10.

## Appendix 1

Taxonomic index of calcareous nannofossil taxa reported in this study. Genera, species and subspecies are listed in alphabetic order. Authors and date of the original description and, when necessary, emendations are provided. See Perch-Nielsen (1985), Bralower et al. (1989), Bown & Cooper (1998), Mattioli & Erba (1999) and references therein for full information regarding taxonomy and authorships.

*Anfractus harrisonii* Medd, 1979  
*Ansulaspheera helvetica* Grün & Zweili, 1980  
*Assipetra infracretacea* (Thierstein, 1973) Roth, 1973  
*Axopodorhabdus cylindricus* (Noël, 1965) Wind & Wise in Wise & Wind 1976  
*Biscutum constans* (Górka, 1957) Black, 1967  
*Calcicalathina oblongata* (Worsley, 1971) Thierstein, 1971  
*Conusphaera mexicana* (Trejo, 1969) subsp. *mexicana* Bralower in Bralower et al. 1989  
*Conusphaera mexicana* (Trejo, 1969) subsp. *minor* (Bown & Cooper, 1989) Bralower in Bralower et al. 1989  
*Crepidolithus crassus* (Deflandre in Deflandre & Fert, 1954) Noël, 1965  
*Crepidolithus perforata* (Medd, 1979) Grün & Zweili, 1980  
*Cretarhabdus angustiforatus* (Black, 1971) Bukry, 1973  
*Cretarhabdus conicus* Bramlette & Martini, 1964  
*Cretarhabdus octofenestratus* Bralower in Bralower et al. 1989  
*Cretarhabdus surirellus* (Deflandre in Deflandre & Fert, 1954) Reinhardt, 1970  
*Crucibiscutum salebrosum* (Black, 1971) Jakubowski, 1986  
*Cruciellipsis cuvillieri* (Manivit, 1956) Thierstein, 1971  
*Cyclagelosphaera argoensis* Bown, 1992  
*Cyclagelosphaera deflandrei* (Manivit, 1966) Roth, 1973  
*Cyclagelosphaera margerelii* Noël, 1965  
*Cyclagelosphaera riyadhensis* Varol, 2006  
*Cyclagelosphaera tubulata* (Grün & Zweili, 1980) Cooper, 1987  
*Cyclagelosphaera wiedmannii* Reale & Monechi, 1994  
*Diazomatolithus lehmanii* Noël, 1965  
*Discorhabdus striatus* Moshkovitz & Ehrlich, 1976  
*Ethmorhabdus gallicus* Noël, 1965  
*Faviconus multicolumnatus* Bralower in Bralower et al. 1989  
*Hexalithus noeliae* (Noël, 1956) Loeblich & Tappan, 1966  
*Hexalithus geometricus*, this study  
*Hexapodorhabdus cuvillieri* Noël, 1965  
*Lithraphidites carniolensis* Deflandre, 1963  
*Lotharingius crucicentralis* (Medd, 1971) Grün & Zweili, 1980  
*Lotharingius hauffii* Grün & Zweili in Grün et al. 1974  
*Lotharingius sigillatus* (Stradner, 1971) Prins in Grün et al. 1974  
*Lotharingius velatus* Bown & Cooper, 1989  
*Manivittella pemmatoidea* (Deflandre ex Manivit, 1965) Thierstein, 1971  
*Markalius circumradiatus* (Stover, 1966) Perch-Nielsen, 1968  
*Markalius ellipticus* Grün in Grün & Alleman, 1975  
*Microstaurus chistiensis* (Worsley, 1971) Bralower et al., 1989  
*Microstaurus quadratus* Black, 1971  
*Miravetesina favula* Grün in Grün & Alleman, 1975  
*Nannoconus boneti* Trejo, 1959  
*Nannoconus brönnimannii* Trejo, 1959  
*Nannoconus colomii* (de Lapparent, 1931) Kamptner, 1938  
*Nannoconus compressus* Bralower & Thierstein in Bralower et al. 1989  
*Nannoconus dolomiticus* Cita and Pasquarè, 1959  
*Nannoconus erbae*, this study  
*Nannoconus globulus* (Brönnimann, 1955) subsp. *globulus* Bralower in Bralower et al. 1989  
*Nannoconus globulus* (Brönnimann, 1955) subsp. *minor* Bralower in Bralower et al. 1989  
*Nannoconus infans* Bralower in Bralower et al. 1989  
*Nannoconus kamptneri* (Brönnimann, 1955) subsp. *kamptneri* Bralower in Bralower et al. 1989

*Nannoconus kamptneri* (Brönnimann, 1955) subsp. *minor* Bralower in Bralower et al. 1989  
*Nannoconus puer*, this study  
*Nannoconus steinmannii* (Kamptner, 1931) subsp. *minor* Deres & Achéritéguy, 1980  
*Nannoconus steinmannii* (Kamptner, 1931) subsp. *steinmannii* Deres & Achéritéguy, 1980  
*Nannoconus wintereri* Bralower & Thierstein in Bralower et al. 1989  
*Percivalia fenestrata* (Worsley, 1971) Wise, 1983  
*Pikelhaube furtiva* (Roth, 1983) Applegate et al., 1987  
*Polycostella beckmannii* Thierstein, 1971  
*Polycostella senaria* Thierstein, 1971  
*Pseudoconus enigma* Bown & Cooper, 1989  
*Pseudolithraphidites* Keupp, 1976  
*Rhagodiscus asper* (Stradner, 1963) Reinhardt, 1967  
*Rhagodiscus nebulosus* Bralower in Bralower et al. 1989  
*Rotellapillus laffittei* (Noël, 1956) Noël, 1973  
*Rucinolithus wisei* Thierstein, 1971  
*Schizosphaerella punctulata* Deflandre & Dangeard, 1938  
*Stephanolithion atmetros* Cooper, 1987  
*Stephanolithion bigotii* (Deflandre, 1939) subsp. *bigotii* Medd, 1979  
*Stephanolithion bigotii* (Deflandre, 1939) subsp. *maximum* Medd, 1979  
*Stephanolithion brevispinus* (Wind & Wise in Wind 1988) Bown, 1998  
*Stephanolithion hexum* Rood & Barnard, 1972  
*Stephanolithion speciosum* Deflandre in Deflandre & Fert, 1954  
*Triscutum beaminsterense* Dockerill, 1987  
*Triscutum expansum* (Medd, 1979) Dockerill, 1987  
*Umbria granulosa* subsp. *granulosa* Bralower & Thierstein in Bralower et al. 1989  
*Umbria granulosa* subsp. *minor* Bralower & Thierstein in Bralower et al. 1989  
*Vagalapilla stradneri* (Rood et al., 1971) Thierstein, 1973  
*Watznaueria barnesiae* (Black in Black & Barnes, 1959) Perch-Nielsen, 1968  
*Watznaueria biporta* Bukry, 1969  
*Watznaueria britannica* (Stradner, 1963) Reinhardt, 1964  
*Watznaueria contracta* (Bown & Cooper, 1989) Cobianchi et al., 1992  
*Watznaueria communis* Reinhardt, 1964  
*Watznaueria fossacincta* (Black, 1971a) Bown in Bown & Cooper 1989  
*Watznaueria manivittiae* (Bukry, 1973) Moshkovitz & Ehrlich, 1987  
*Watznaueria rawsonii* Crux, 1987  
*Zeugrhabdotus cooperi* Bown, 1992b  
*Zeugrhabdotus embergeri* (Noël, 1958) Perch-Nielsen 1984  
*Zeugrhabdotus erectus* (Deflandre in Deflandre & Fert, 1954) Reinhardt, 1965  
*Zeugrhabdotus fluxus*, this study

## Appendix 2

In this appendix calcareous nannofossil range charts of the studied sections are given. Every chart reports the distribution, relative and total abundance estimations as well as preservation evaluation of each taxon observed. Question marks quoted in each chart correspond to elements that cannot be unequivocally classified but just tentatively assigned to a taxa. Those elements are represented by fragments or by heavily dissolved specimens, thus the classification is unsure. As show in the charts, question marks are often associated with uncertain zone boundaries testifying diagenetic effects on the nannofossil assemblages.























FRISONI B - meters	PRESERVATION	TOTAL ABUNDANCE											This study	Bralower et al. 1989 SUBZONES										
		<i>W. barnesiae</i>	<i>W. manivittae</i>	<i>W. manivittae</i> large	<i>W. britannica</i>	<i>W. fossacincta</i>	<i>W. communis</i>	<i>C. margerelii</i>	<i>C. deflandrei</i>	<i>D. lehmani</i>	<i>Stephanolithon</i> spp.	<i>W. britannica</i> large			<i>W. communis</i> large	<i>M. quadratus</i>	<i>L. sigillatus</i>	<i>L. hauffii</i>	<i>F. multicolumnatus</i>	<i>C. mexicana minor</i>	<i>C. mexicana mexicana</i>	<i>P. beckmannii</i>	<i>C. argoensis</i>	
9	E1/2, O1/2	F	F/C	F	R	F	F	F	F	F	F	R	R	R	R	R	F	F/C	F/C	F/C	?	NJT 15b	NJ-20b	
8.05	E2/3, O1	R		R	R	R				R	R													
7.06	E2, O2	R		R	R	R					R													
5.95	E2, O2	R		R	R	R	R																	
5.34	E2, O1/2	R		R	R	R	R						R											
5	E2	R		R			R		F															
2.3	E1, O1	F	F	F	R	F	R		F	R		R	R											
2	E1, O2	F	R	F	F	F	R		C	R		F	C	R										
1.5	E1, O2	F	F	F	F	R	F		C	R		R	F											
0.6	E1, O2/3	C	F	C	F	F			C/A	R	R	R	C/A	R										
0.12	E2/3, O2	F	R	F	F	R	R		R	R	R	R												

### Appendix 3

In this appendix detailed lithostratigraphic descriptions of the studied sections are reported. As pointed out in Figure 2, in this study the Rosso ad Aptici-Maiolica (Lombardian Basin) and Rosso Ammonitico Superiore-Biancone transition intervals are distinguished. The transition interval from Rosso ad Aptici to Maiolica is defined on the basis of the limestones and chert nodules colours: it is the interval between the first light brown-pale grey bed (base) to the last pinkish-reddish bed (top) of Rosso ad Aptici. The transition interval from Rosso Ammonitico Superiore to Biancone is defined with the same criteria and it is the interval between the first whitish bed (base) to the last pinkish bed (top) of Rosso Ammonitico Superiore.

#### Torre de' Busi

Torre de' Busi section (at 45° 46' 34" N, 9° 29' 7" E) is located 3 km north of the village of the same name. It is a 60 m-thick section spanning the upper part of Radiolariti, Rosso ad Aptici and the lowermost part of Maiolica (Figs 1, 4). A detailed lithostratigraphy is following reported, top to bottom:

- 0.00-12.40 m (Maiolica).

Light grey to whitish limestones in 5-10 cm-thick beds with grey cherty nodules 2-10 cm-thick. Meters 7.20 and 4.40 are characterized by two dark grey cherty lists 10-14 cm-thick.

- 12.40-18.65 m (Maiolica).

Light brown to light grey limestones in 10-15 cm-thick beds with grey cherty nodules 2.5 cm-thick. At meter 18, 15.70, 15.20 and 14.10 peculiar grey-brownish cherty lenses crop out, characterized by 8 cm up to 12 cm of thickness.

- 18.65-24.76 m (Maiolica).

Light brown limestones in 10-20 cm-thick beds with grey-reddish cherty nodules 2.5-6 cm-thick.

- 24.76-28.16 m (Rosso ad Aptici-Maiolica transitional interval).

Prevalent light brown to rare pinkish limestones in 15 to 10 cm-thick beds fining upward, with several grey, pinkish cherty nodules 3

cm-thick. The colour of limestones changes upward from pink to light brown.

This lithozone top corresponds to the last pinkish-reddish bed of Rosso ad Aptici.

- 28.16-31.26 m (Rosso ad Aptici-Maiolica transitional interval).

Brown-reddish and light pinkish slightly siliceous limestones in 15-20 cm-thick beds separated by reddish marly or clayey interbeds and condensed in 30-40 cm beds. Rare reddish cherty nodules and lists 1-3 cm-thick crop out. The colour of limestones changes upward from brown-reddish to light pinkish. From meter 28.16 to 29.45 the strata are slightly disturbed by slumps.

- 31.26-36.37 m (Rosso ad Aptici-Maiolica transitional interval).

Prevalent grey-reddish to rare grey-light brown siliceous limestones in 20-15 cm-thick beds fining upward separated by grey-reddish marly or clayey interbeds. Rare grey-greenish cherty nodules and lists 1-2 cm-thick crop out. The colour of limestones changes upward from grey-reddish to grey-light brown.

This lithozone base corresponds to the first light brown-pale grey bed of Rosso ad Aptici.

- 36.37-40.08 m (Rosso ad Aptici).

Brown to reddish siliceous limestones in 10-15 cm-thick beds amalgamated in beds 20-30 cm-thick and subdivides by brownish marly interbeds 1 cm-thick.

- 40.08-46.35 m (Rosso ad Aptici).

Dark brown to dark violet siliceous limestones and marlstones in 10 cm-thick beds with common dark brown to grey-blue cherty nodules and lists 1-3 cm-thick.

- 46.35-51.60 m (Rosso ad Aptici).

Dark brown slightly calcareous chert and strongly siliceous limestones in 10 cm-thick beds separated by dark brown clayey. Strata surfaces often present grey-greenish spots.

- 51.60-61.00 m (Radiolariti).

Dark brown to violet radiolarites in 5-10 cm-thick beds separated by dark brown clayey interbeds few millimetres thick. Rare grey-greenish spots are present on beds surfaces.

### Monte Pernice

Monte Pernice section (at 45° 38' 38" N, 10° 10' 3" E) is located near Monte Pernice, on the secondary road going from Aquilini village to Uccellada Magnoli (Lombardy, North Italy). It is a 22 m-thick section spanning the transitional interval between the Rosso ad Aptici and the lowermost Maiolica (Figs 1, 5). A detailed lithostratigraphy is reported by Erba & Quadrio (1987).

### Colme di Vignola

The Colme di Vignola section (at 45° 45' 58" N, 10° 57' 20" E) lies above the village of Brentonico on the slopes of Monte Vignola, at the western margin of the Trento Plateau (Figs 1, 6). The studied 20 m-thick section spans Calcare Selcifero di Fonzaso, Rosso Ammonitico Superiore, and the lowermost part of Biancone. A detailed lithostratigraphy is following reported, top to bottom:

- 0.00-6.40 m (Biancone).

White slightly nodular limestones in 8-15 cm-thick beds amalgamated in strata 30-40 cm-thick. Thicker strata are separated by grey cherty nodules 0.5-5 cm-thick.

- 6.40-8.60 m (Rosso Ammonitico Superiore-Biancone transition interval).

Pinkish-whitish slightly nodular limestones in 3-5 cm-thick beds amalgamated in strata of 60 cm-thick. Greyish cherty nodules 1-5 cm-thick crop out.

- 8.60-15.00 m (Rosso Ammonitico Superiore).

Dark pink to reddish slightly nodular siliceous limestones in 15-30 cm-thick beds. Red marly interbeds of 1-2 cm-thick characterize the lower part of this lithozone, while numerous red cherty layer or nodules 2-10 cm-thick increase in thickness and frequencies upward.

- 15.00-19.10 m (Rosso Ammonitico Superiore).

Dark pink to reddish very nodular and condensed siliceous limestones. Nodularity and condensation increase downward.

- 19.10-20.00 m (Calcare selcifero di Fonzaso).

Pink to brick red nodular siliceous limestones in 20 cm-thick beds with reddish marly interbeds 1-2 cm-thick.

### Foza

The Foza section (Ogg 1981; Martire 1996; Channell et al. 2010), lies along the road SP 76 (45° 53' 44" N, 11° 36' 3" E) between the villages of Foza and Gallio (east of Asiago village) and provides an exposure of Rosso Ammonitico Inferiore, Calcare Selcifero di Fonzaso, Rosso Ammonitico Superiore, and the lower part of Biancone (Figs 1, 7, 8). The studied 47 m-thick section is complemented by partial exposure of the same section around the next bend in the road towards Gallio village: this second section is designated Foza B, while the primary one is referred to as Foza A. A detailed lithostratigraphy of Foza A is following reported, top to bottom:

- 0.00-14.00 m (Biancone).

White limestones in 8-15 cm-thick beds alternated with rare nodular white limestones in 5-15 cm-thick beds. Light grey cherty nodules 2 cm-thick, rarely up to 5 cm-thick, crop out.

- 14.00-23.00 m (Biancone).

White limestones in 8-15 cm-thick beds amalgamated in strata 30-40 cm-thick and characterized by very rare cherty nodules 1-2 cm-thick. Thicker strata are separated by marly interbeds which display undulate surfaces.

- 23.00-26.10 m (Rosso Ammonitico Superiore-Biancone transition interval).

Whitish and pinkish slightly nodular limestones in 3-5 cm-thick beds with marly interbeds 0.5-1 cm-thick.

- 26.10-33.00 m (Rosso Ammonitico Superiore).

Dark pink to reddish slightly nodular siliceous limestones in 10-20 cm-thick beds separated by red marly interbeds 1-2 cm-thick. The rock colour darkens downward along with an increase of nodularity.

- 33.00-35.40 m (Rosso Ammonitico Superiore).

Dark pink to reddish very nodular and condensed siliceous limestones: stratification is not recognizable due to extreme condensation.

- 36.00-37.10 m (Calcare selcifero di Fonzaso).

Pinkish to reddish very nodular and condensed siliceous marlstones in 2-5 cm-thick beds.

- 37.10-39.10 m (Calcare selcifero di Fonzaso).

Pinkish siliceous marlstones with abundant brick-red cherty nodules 5-10 cm-thick: stratification is not recognizable due to extreme condensation.

- 39.10-42.10 m (Calcare selcifero di Fonzaso).

Pink nodular siliceous limestones in 15-25 cm-thick beds with reddish marly interbeds 1-2 cm-thick.

- 42.10-47.00 m (Rosso Ammonitico Inferiore).

Light pink slightly siliceous limestones in massive 40 m-thick beds amalgamated in 1 m-thick beds. Each massive layer is intercalated with millimetre-thick interbeds.

### Bombatierle

The Bombatierle section is located in an active quarry 1 km south of Monte Kaberlaba, 5 km south of Asiago (at 45° 50' 55" N, 11° 30' 25" E). The studied section spans Rosso Ammonitico Inferiore through Biancone limestones (Figs 1, 9). The following lithozones are partially correlatable to the ones described by Martire et al. (2006) for the Kaberlaba section, which crop out in a private quarry on the North-West slope of Monte Kaberlaba. A detailed lithostratigraphy is following reported, top to bottom:

- (-)2.00-3.00 m (Biancone).

Whitish nodular limestones in 10-30 cm-thick beds separated by marly interbeds 1-3 cm-thick.

- 3.00-4.25 m (Rosso Ammonitico Superiore-Biancone transition interval).

Pale pink nodular limestones in 10-20 cm-thick beds separated by clayey millimetre interbeds.

- 4.25-12.70 m (Rosso Ammonitico Superiore).

Brick red to pinkish nodular limestones in massive 30-80 cm-thick beds.

- 12.70-15.45 m (Rosso Ammonitico Superiore-Calcare Selcifero di Fonzaso transition interval).

Violet-reddish very nodular cherty limestones with violet chert nodules 2-10 cm-thick. The colour of chert nodules becomes lighter upward. At 13.60 m a 20 cm-thick violet, dark red to reddish (upward) bentonite layer crop out: this layer has been previously reported in literature (Bernoulli & Peters 1970, 1974; Martire et al. 2006) and can be followed over long distances.

- 15.45-16.43 m (Calcare Selcifero di Fonzaso).

Brick red calcareous cherts in 3-5 cm-thick planar beds. The carbonate content increases upward. Two 2 cm-thick marly interbeds are present at 15.98 and 15.75 meter.

- 16.43-16.95 m (Calcare selcifero di Fonzaso).

Dark brown to greenish cherts in 3-10 cm-thick beds with millimetre clayey interbeds.

- 16.95-18.80 m (Rosso Ammonitico Inferiore).

Pink-reddish nodular limestones characterized by a bioclastic facies with coarse grains size dominated by skeletal remains and peloids and grain supported texture. A regular network of burrows (*Thalassinoides*, Martire et al. 2006) characterize nodular limestones from meter 18.20 to 18.50.

- 18.80-20.00 m (Rosso Ammonitico Inferiore).

Brown-grey nodular and condensed limestones with no clear stratification. This lithozones is clearly recognizable to the distance because of its darker colour.

- 20.00-22.00 m (Rosso Ammonitico Inferiore).

Brown-reddish nodular limestones with no clear stratification and characterized by pink nodules and brick red matrix.

### Sciapala

The Sciapala section is located in a disused quarry located 7 km SE of Asiago (at 45° 51' 21" N, 11° 34' 42" E). The studied section spans the Rosso Ammonitico to the Rosso Ammonitico Superiore-Biancone transition (Figs 1, 10). A detailed lithostratigraphy is following reported, top to bottom:

- 15.30-19.70 m (Rosso Ammonitico Superiore-Biancone transition interval).

Pink nodular limestones in 10-20 cm-thick beds with rare clayey millimetre interbeds.

- 15.30-4.00 m (Rosso Ammonitico Superiore).

Brick red to pinkish nodular limestones in massive meter-thick beds. In the lowermost part of this lithozone, at 4.80 m, a 5 cm-thick dark red marly layer crop out. No clear stratification is visible in the outcrop and only stilolitic surfaces, underlined by dissolution clays, are visible on the quarry walls.

- 4.00-0.00 m (Rosso Ammonitico Inferiore).

Brown-reddish nodular limestones with no clear stratification and characterized by pink nodules and brick red matrix. From meter 3.70 to meter 3.80 the rock is characterized by a regular network of burrows (*Thalassinoides*, Martire et al., 2006).

### Frisoni

The Frisoni sections are located 5 km east of the village of Foza, along the road SP 76, close to the bridge spanning the Valgadana,

adjacent to the village of Frisoni. A first section (referred to as the Frisoni A section by Channell et al. 2010, at 45° 54' 54" N, 11° 39' 17" E) lies on the SW side of the bridge and spans the Rosso Ammonitico Superiore and its transition to Biancone (Figs 1, 12). A second and shorter section outcrop on the NE side of the bridge (Frisoni B at 45° 55' 1" N, 11° 39' 25" E) and consists in few meter spanning the upper part of Rosso Ammonitico Superiore (Figs 1, 11).

A detailed lithostratigraphy of Frisoni A is following reported, top to bottom:

- 20.0-13.60 m (Biancone).

White limestones in 8-15 cm-thick beds amalgamated in strata 30-40 cm-thick, which are separated by marly interbeds 0.5-5 cm-thick that display undulate surfaces. Very rare cherty nodules 1-2 cm thick crop out.

- 13.60-10.00 m (Rosso Ammonitico Superiore-Biancone transition interval).

Pink slightly nodular limestones in 10-40 cm-thick beds with marly interbeds 0.5-1 cm-thick.

- 10.00-3.60 m (Rosso Ammonitico Superiore).

Brick red to pinkish poorly nodular limestones in 20-25 cm-thick beds intercalated by numerous cm-thick marly and clayey layers.

- 3.60-(-3.00) m (Rosso Ammonitico).

Grey nodular limestones in 10-20 cm-thick beds. Pale brown poorly nodular limestones in two thick strata crop out from -3.00-0.00 and from 2.60-3.60 meter intervals.